ENHANCEMENT OF ACCURACY AND EFFICIENCY OF LASER BASED BENDING AND STRAIGHTENING PROCESSES

A Thesis Submitted in Partial Fulfillment of the Requirements for the Degree of

DOCTOR OF PHILOSOPHY

by

Polash Pratim Dutta

(Roll No. 10610304)

Department of Mechanical Engineering

Indian Institute of Technology Guwahati

Guwahati-781039

INDIA

May 2019

DECLARATION

I declare that,

a. The work contained in this thesis is original and has been done by me under the guidance of my supervisors.
b. The work has not been submitted to any other institute for any degree or diploma.
c. I have followed the guidelines provided by the institute in preparing the thesis.
d. I have confirmed to the norms and guidelines given in the ethical code of conduct of the institute.
e. Whenever I used materials (data, theoretical analysis, figure and text) from other sources I have given the due credit to them by citing them in the text of the thesis and giving their detail in references.

Signature of student
(Polash Pratim Dutta)

Department of Mechanical Engineering,
Indian Institute of Technology Guwahati,
Guwahati-781039,
INDIA

CERTIFICATE

It is certified that the work contained in the thesis entitled "**Enhancement of Accuracy and Efficiency of Laser Based Bending and Straightening Processes**" is submitted by **Mr. Polash Pratim Dutta** to the Indian Institute of Technology Guwahati for the award of the degree of Doctor of Philosophy has been carried out under our supervision in the Department of Mechanical Engineering, Indian Institute of Technology Guwahati. This work has not been submitted elsewhere for the award of any other degree or diploma.

Dr. Uday Shanker Dixit
Professor
Department of Mechanical Engineering,
Indian Institute of Technology Guwahati,
Guwahati-781039, INDIA

Dr. Karuna Kalita
Associate Professor
Department of Mechanical Engineering,
Indian Institute of Technology Guwahati,
Guwahati-781039, INDIA

Date: 06/02/2019

Dedicated to the Almighty, My Parents

Late Horeswar Dutta & Mrs Purnima Neog

and

My Teachers

Acknowledgements

I start this thanking the Almighty for keeping me healthy and giving patience throughout my thesis work. I would like to express my sincere gratitude towards all those who have helped me in various ways directly and indirectly during the tenure of my PhD work at IIT Guwahati. Each step of the PhD work was supported by many people and each one has played important role. I am grateful to express my deep gratitude to all of them.

I would like to acknowledge Tezpur University for giving me the opportunity to conduct my PhD work. I thank Indian Institution of Technology Guwahati for all sorts of infrastructural facilities, Special thanks for Central Workshop, Material Science Laboratory and Advance Manufacturing Laboratory of IITG for providing instruments to carry out the research work. I would also like to thank DST-FIST (2009–2014) scheme of Government of India for providing CO_2 laser facility.

I express my sincere gratitude and appreciation to my supervisor, Prof. U.S. Dixit and Dr. Karuna Kalita, Department of Mechanical Engineering, IIT Guwahati, for their valuable advice, expert guidance, patience and encouragement, and for all the support they have given me from the beginning to the end of the PhD work. Without their support and advice, it would have not been possible for me to carry out this research work. I really feel privileged for having the opportunity to work under them as my PhD supervisors. I shall always be grateful to them.

I would like to thank my doctoral committee members, Prof. A. K. Dass, Prof. A. K. Gogoi and Dr. R. G. Naryanan, for their valuable suggestions and encouragement during the period of my research work. I am also grateful to the former and present heads of the Department of Mechanical Engineering, Prof. D. Chakraborty, Prof. P. Mahanta, Prof. A.K. Dass and Prof. S. K. Dwivedy for extending various facilities during the tenure of my doctoral program.

I wish to express my sincere thanks to Mr. Jiten Basumatary, Mr. Dilip Chetri, Mr. Bijoy Choudhury, Mr. Dipak Deka, Mr. Upen Gohain, Mr. Dhaneswar Khaklary, Mr. Minesh Medhi, Mr. Mrinal Sarma, Mr. Saiffuddin Ahmed and Mr. Sanjib Sarma for helping me during the experimental studies.

I express my sincere thanks to my friends Dr. Besufekad Negesh Fetene, Dr. Vinod Yadav, Mr. Vikash Vanik, Mr. Rajkumar Shufen, Mr. Faladrum Sharma, Mr. Amit Raj and Mr. Nilkamal Mahanta. I shall always be grateful to my IITG and other friends for their great encouragement and wishes.

I express my deep gratitude to my parents late Horeswer Dutta and Mrs Purnima Neog Dutta for their good will and grace, wife Tribeni Phukan Dutta and son Priyanuj Dutta (Joon) for immense support during the course of my PhD program. I shall be grateful to them for sharing every responsibility without my presence during PhD period. I express my deep gratitude to my brother Dr. Partha Pratim Dutta for his affection and guidance during the period and my sister Rupanjita Dutta for her affection and wishes. Last but not the least; I am thankful to all my family members, in-laws, colleagues, relatives and any one related to this work up to any extent in due course of time.

Polash Pratim Dutta
IIT Guwahati

Abstract

Laser based bending process is an advanced process in sheet metal forming in which laser heat source is used to shape a metal sheet. The process has many advantages over conventional forming processes. It is a contact free forming process and is suitable to carry out bending and straightening at areas unachievable by conventional forming. The process is convenient to generate very small and accurate bend angles. The laser bending process can also bend brittle materials in some cases. It is also possible to generate complex shapes by employing a suitable scanning strategy. Basically it is a thermo-mechanical process. Literature contains effects of different laser process parameters, material and workpiece geometry on laser bending. The recent interest in laser bending research and development reflects the industrial potential of the process. Several research groups are currently investigating the fundamentals and applications of laser bending. Several analytical and numerical models have been developed. The forming mechanism of complex sheet geometries has been analyzed using software based on finite element method (FEM). Many studies involved moving laser sources with straight and curve laser beam paths. However, scant attention has been given to the reverse process *i.e.*, laser based straightening. Limited research outputs are available in the literature about straightening. The focus of this thesis is on enhancement of accuracy and efficiency of the laser based bending as well as straightening.

First, in this work the deformation of a sheet, subjected to irradiation, has been studied through a series of experiments where the metal surface was coated with black enamel paint for enhancing the absorptivity of laser and thereby acquiring a higher bend angle. Use of black enamel paint on laser bending resulted in a large increase of bend angle in a mild steel sheet. Later on, a strategy is proposed for choosing the parameters of multi-pass laser line heating for obtaining the accurate bend angle for a prescribed accuracy of prediction. The strategy was verified with experiments for three different materials.

A technique to straighten bent metallic strips with magnetic-force-assisted laser irradiation is also developed. Experiments were conducted for three different types of mechanically-bent mild strips. The first type was bent strips without any heat treatment. The second type was stress-relieved and third type was subcritical-

annealed bent strips. These strips were straightened following different schemes of laser irradiation sequence to understand the performance of straightening. A parametric study was conducted by varying laser power and scanning speed. Micro-hardness and microstructure after straightening were also studied. Different scanning schemes provided different microstructures and mechanical properties. Any serious deterioration in the quality of straightened strips was not noticed.

Later on, electromagnetic-force-assisted laser bending and straightening process is proposed, in which the external force is applied by a controlled force generated by an electromagnet. The process was found suitable for laser assisted bending and straightening. The experiments as well as simulations indicated that a large bend angle can be obtained by controlling the electric current and air gap between electromagnet and workpiece. A good agreement between simulation and experimental result was obtained. Edge effect was very less in case of strips that got attached with the magnet during laser bending. The spring-back effect was very less at high laser power, low scan speed and high current. The laser irradiated region had higher micro-hardness than that of base material. The micro-hardness of laser irradiated region depended on laser power, scan speed and magnetic force of attraction. Straightening of mechanically bent strip was also carried out. Results indicate that the use of an electromagnet with laser irradiation is an effective way to straighten bent strips.

Overall, the efficiency of the bending and straightening processes was improved by adopting the following measures: (1) use of a paint for enhancing the absorption of laser irradiation, (2) use of magnet/electromagnet for assisting the laser bending/straightening. The accuracy of the laser bending process was improved by developing a suitable scheduling strategy for a multi-pass laser bending and bending using an electromagnet. The accuracy of laser straightening was improved by carrying out multi-pass laser straightening with the help of magnetic force and proper heat treatment. Future work should aim on the detailed optimization of the processes for different work materials.

Contents

.

List of Figures

List of Tables

Nomenclature

Roman letters

c_1 and c_2	Constants dependent on materials properties
c_p	Specific heat capacity
d	Distance between two points
$d_{\max}$	Distance between two farthest point
d_s	Scan-line distance
D	Laser beam diameter
D_L	Laser beam diameter before lens
D_t	Thermal diffusivity
E	Young's modulus
E_{m}	Mathematical expectation
f	Focal length
G	Air gap between workpiece and electromagnet
h	Convective heat transfer coefficient
H	Standoff distance
k	Thermal conductivity
k_p	Proportionality constant
l	Length of workpiece
l_h	Half-length of heated zone
M^2	Beam quality factor
N	Number of passes
P	Laser power
p	Probability
q	Thermal heat flux density of laser beam
r	Radius of the laser beam
R^2	Coefficient of determination
t	Thickness of the workpiece
t_h	Thickness of heated volume
T_a	Ambient temperature

T_{max}	Maximum temperature
T_{pred}	Maximum predicted temperature
T_s	Sheet surface temperature
v	Scan speed
w	Width of workpiece
w_o	Laser beam waist

Greek letters

α_a	Actual bend angle achieved in a pass
α_b	Desired bend angle in as pass
α_B	Desired total bend angle
α_{max}	The maximum bend angle in a pass
α_T	Target bend angle in a pass
α_{th}	Coefficient of thermal expansion of the workpiece
δ	Desired % accuracy of bend angle
η	Absorption coefficient
ρ	Density
μ	Poisson's ratio
σ_y	Yield stress
λ	Wave length
ε	Percentage error in prediction
ε_u	Upper bound %error
ε_l	Lower bound %error
ε_{max}	Stand for maximum plastic strain at the heated surface

List of abbreviations

ANN	Artificial Neural Network
BM	Buckling Mechanism
CAO	Coating applied once
CAAP	Coating applied after each pass
CNC	Computer Numerical Control
CO_2	Carbon di-oxide

CW	Continuous Wave
DC	Direct current
DOF	Degree of Freedom
FE	Finite element
FEA	Finite element analysis
FEM	Finite element method
SEM	Scanning Electron Microscopy
HAZ	Heat affected zone
Nd:YAG	Neodymium-doped yttrium aluminum garnet
TGM	Temperature Gradient Mechanism
UM	Upsetting Mechanism
UTM	Universal Testing Machine
UTS	Ultimate tensile strength
WC	Without coating

Chapter 1

Background and Scope

1.1 Introduction

The term ‘LASER’ was first introduced to the public by Gordon Gould in his conference paper “The LASER, Light Amplification by Stimulated Emission of Radiation” (Gould 1959). The first working laser was made by Theodore H. Maiman in 1960. Maiman used a solid-state flash lamp-pumped synthetic ruby crystal to produce red laser light at 694 nanometer wavelength. Since then human beings have been using the laser in various industries and applications like in aerospace, automotive, medical, micro-electronics, material processing shipbuilding etc. (Li and Yao 200a, Shen and Vollertsen 2009, Shi et al. 2012a). There are many types of lasers available for application in different field. Mainly laser is used in research, medical, industrial and commercial purpose. Common way to define any type of lasers is by the kind of lasing medium used as shown in Table 1.1.

Lasers are also characterized by the duration of laser emission. Two popular classes are the continuous wave (CW) laser and the pulsed laser. In the CW laser, the light emission occurs in continuous beam, commonly with less intensity. Gas lasers belong to this category. In case of the pulsed lasers, a powerful burst of light of short duration generates. Q-switched laser, crystals, glass and liquid types of lasers belong to this category. Usually the solid-state lasers operate occasionally, mainly due to the large amount of heat developed in the crystal. Nevertheless, some solid-state lasers can operate in CW mode as well.

In modern manufacturing processes, laser plays significant role. Lasers have been used for different manufacturing process such as, welding, cladding, marking, surface treatment, drilling, and cutting. Laser is widely used in shipbuilding, automobile, steel, aerospace, electronics, and medical industries for accurate and precise production of complex parts. Laser welding is advantageous due to its ability to weld dissimilar metals with high speed. To improve the surface quality, laser

cladding is used for depositing hard material on a weak substrate. Contact free drilling and cutting with lasers are used for better accuracy and precision. Lasers are also used to change the surface properties. It is also used to engrave a metal surface. Laser beam machining is used in the electronic industry for wire stripping and skiving of circuits.

Table 1.1 Type of lasers based on lasing medium

Types	**Lasing Medium**	**Example**	**Merits and Demerits**
Solid state laser	The lasing materials are distributed in a solid matrix. In these lasers, glass or crystalline materials are used	Ruby laser, Nd:YAG laser	No material wastage in active medium, simple and economical construction. Less efficiency, high divergence, power loss due to thermal lasing.
Liquid laser	This kind of laser uses the liquid as a lasing material. In liquid lasers, light supplies energy to the lasing material.	Dye laser (uses an organic dye as a lasing material)	Wide range of wavelengths, very less beam diameter, less beam divergence, high efficiency and power output. High cost, complex tuning of frequency.
Gas lasers	Such lasers use gas as lasing medium,	He-Ne laser, argon ion lasers, CO_2 laser, excimer lasers	Small and compact, generate less heat, simple construction, good coherent property. Moderate output, low gain device, require high voltage, escaping of gas.
Semiconductor lasers	Semiconductor lasers are different from solid-state lasers. In solid-state lasers, light energy is used as the pumping source, whereas in semiconductor lasers, electrical energy is used as the pumping source. Diode lasers fall in this category. It is cheap and compact with low power consumption.	Gallium arsenide (GaAs)	Small size and appearance, less costly simple construction, low power consumption and high efficiency. Low power production, greatly dependent on temperature.

1.2 Laser Forming Process

Sheet metal bending is the process in which a metal plate is subjected to effective stresses above the yield stress to generate deformation beyond elastic range. There are two commonly used ways to achieve bending operation of plates viz. mechanical bending and thermo-mechanical bending. In case of mechanical bending, a suitable die is used to give a flat metal plate to achieve the required shape. Otherwise the flat plate is fed to a set of rolls to produce the plastic deformation to acquire the required shape. Whereas, in thermo-mechanical bending, plastic deformation is produced by proper heating followed by cooling the metal plate. When a plate is heated at one side, keeping the other side open to ambient, the temperature gradient across the thickness occurs. This results difference in expansions across the thickness of the metal plate, and bending occurs. Since the temperature in the region directly under the heat source is high and it result to reach yield stress of the metal, plastic deformation occurs.

1.2.1 Laser bending

Laser bending is a process of bending a workpiece by irradiating with a laser beam and subsequently cooling it. After cooling, thermal residual stresses remain in the workpiece and it gets bent. Usually, the laser beam moves over the bend line with an appropriate scan speed. The process has drawn the attention of the researchers due to certain edge over the conventional bending. The process can be used to achieve very small bend angle. The possibility of producing complex geometries without the requirement of special tooling also makes the process popular in the forming industries. Laser bending process may be with or without assisting force.

Use of laser for bending different metallic and non-metallic components is an emerging and important subject for several researchers for last three decades. In ship building industries, laser based bending can replace flame or roll bending processes in the fabrication of hull, enhancing the accuracy and productivity. In automotive industries, it can be used for forming as well as distortion correction of car body panels and doors. Automotive industries have started using magnesium alloys due to their high specific strength. However, magnesium alloys possess poor formability

during mechanical bending, thus making a strong case in favor of laser based bending. In aerospace industries, laser based forming can be used to fabricate structures made of aluminum and titanium. It can also be used in forming compressor blades. Although there is no comprehensive report in open literature on the existing share of laser forming in manufacturing sector, information obtained in various research papers and a number of funded projects show its growing importance. Figure 1.1 shows a laser bending set up with individual components, scan direction and bend angle produced.

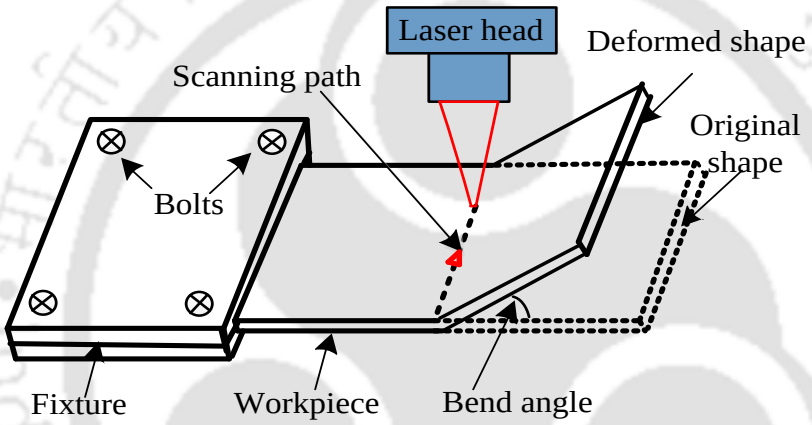

Figure 1.1 Schematic of laser bending process

1.2.2 Laser assisted bending

Different process parameters such as laser power, scan speed, laser beam diameter and number of scans greatly influence the process. Researchers reported different aspects of straight line laser bending and laser-assisted bending processes (Dixit et al. 2015, Fetene et al. 2015, Shichun et al. 2001, Lawrence et al. 2001 and Gautam et al. 2015). The main challenge is to make the process accurate and efficient. Hennige et al. (1997) proposed a methodology to enhance accuracy of bend angle. The process efficiency may be improved in different ways. Enhancing the absorptivity by different coatings is one of the ways (Gautam et al. 2015). Another way is to implement laser assisted bending where assisting load is used to support the deformation process.

Laser assisted bending can be applied to bend brittle materials also (Bammer et al. 2011, Xu et al. 2013). Different ways to perform laser assisted bending are as follows: use of a sapphire die transparent to solid-state and excimer laser beams (Samm et al. 2009), use of a roller to apply mechanical load that moves synchronously with a scanning laser beam (Kant and Joshi 2013) and laser assisted bending with a load applied at the free-end of a cantilevered sheet (Yanjin et al. 2003). The bend angle is enhanced when the direction of the load is consistent with the deformation direction in laser bending. Fetene et al. (2017) applied a load at the free end of cantilevered sheet in the same direction as that of the irradiating beam. Annamaria et al. (2015) performed laser-assisted bending of sharp angles with small fillet radius on stainless steel sheets. Use of mechanical load enhances the bending process considerably. However the contact nature is the common shortcoming for all such processes. Use of non-contact type force may be more convenient in some cases. Recently Fetene et al. (2017) applied magnetic-force using permanent magnet to bend workpiece with CO_2 laser. The schematic diagram of laser assisted bending is shown in Figure 1.2.

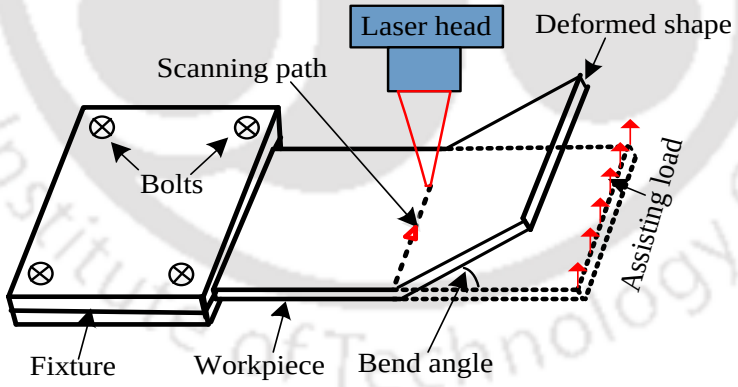

Figure 1.2 Schematic of laser assisted bending

1.2.3 Laser straightening

Compared to laser bending, less amount of work has been done on laser straightening. Dearden et al. (2006) reported experimental investigation to straighten the distorted aluminum sheets and observed that some distortion always remained in

the worksheet. Ueda et al. (2009) tried to flatten the projections in the carbon steel and stainless steel sheets. They developed irradiation strategies based on the numerical computations of plastic strains developed in the workpiece. Ueda et al. (2011) employed lasers for flattening the protrusions induced in a metallic worksheet mechanically and concluded that the convex surface should be exposed to higher temperature to induce larger tensile stresses for obtaining a flat surface. Laser scanning on the convex surface of the protrusion was more efficient in reducing the height of protrusion than that on the concave side. Chakraborty et al. (2015) used temperature gradient mechanism (TGM) dominated laser bending to reduce the bend angle in mechanically bent stainless steel jobs; the change in bend angle was more when laser beam was irradiated on the convex side of the bent worksheet. Garg et al. (2016) suggested that to ensure proper absorption of the laser irradiation during straightening, the workpiece should be kept unclamped in an inverted V-shape. Nevertheless, a large number of scans were needed even for a slightly bent sheet. The schematic diagram of laser straightening of bent sheet is shown in Figure 1.3.

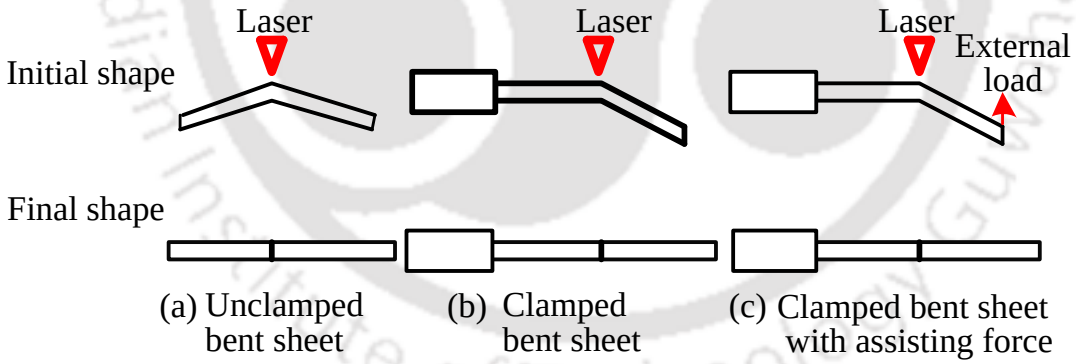

Figure 1.3 Schematic of laser straightening process for a bent plate

1.3 Applications of Laser Bending and Straightening

The unique characteristics of lasers have made them important tools in various applications after the first demonstration of HeNe laser in 1960. Laser bending is used as an accurate and cost effective process to adjust or align the mating parts in welding constructions, ship building industry and straightening the distorted parts, e.g., car body parts (Ueda 2009, Ueda 2011, Hennige 1997, Zhang and Xu 2005a, Qi

and Namba 2011). Laser bending has many applications in the fields of ship building (naval), aerospace, micro-electromechanical system (MEMS), chemical and sensor industries (Zhou et al. 2013, Watkins et al. 2001, Vollertsen et al. 1995, Chen et al. 1998, Tam et al. 2001, Ocana et al. 2007). It can also be used to bend brittle material (Wu et al. 2010a, b, Bammer et al. 2011).

1.4 Advantages and Disadvantages of Laser Bending and Straightening

Laser bending and straightening techniques have considerable advantages over conventional processing methods. Many researchers reported the following advantages of laser based bending (Vollertsen et al. 1995, Chen and Xu 2001, Magee and Vin 2002, Zhang and Xu 2005, Barletta 2006, Casamichel et al. 2007, Shen 2008 and Shidid et al. 2013, Chakraborty et al. 2015):

- Accurate beam control is achievable by fully automatic control system.
- Contact free nature of laser bending leads to elimination of method of separate tooling and die for bending process. Special tooling may be used for laser assisted bending. It is capable of creating large bend angles with accuracy.
- The process is very much convenient for generating very small angle with accuracy which cannot be done by mechanical process.
- Process can be implemented in wide range of parts from micro to macro scale without size constraint in different industries like electronics, aerospace, automobiles etc.
- Due to the elimination of lead-time associated with the design, manufacturing and placement of tools and dies, it is possible to achieve high processing speed.
- Bending of brittle and hard materials e.g., magnesium alloy, titanium alloy, aluminum alloy, nickel alloy and ceramic etc. are also possible by laser heating.
- This process can be suitably coupled to conventional manufacturing processes.

- By using suitable scanning strategy, it is possible to develop complex shapes also.
- Due to fine controlling mechanisms as compared to other heat based bending processes like flame bending, it is high-energy efficient.
- It is possible to carry out laser bending at unachievable areas for mechanical tooling.

Laser bending process has certain limitations. They are as follows:

- The efficiency of the process is highly dependent on radiation absorptivity of material.
- It is suitable for low and moderate thickness but sheet metals of high thickness are not easy to bend.
- Laser bending process is not advisable for mass production as compared to traditional punch and die technique.
- Oxidation during the process is a problem due to which special care needs to be taken to avoid it.
- Initial investment of laser machine is very high.

1.5 Scope of the Present Thesis

The primary objective of the present thesis is to improve the performance of laser based bending and straightening process in terms of accuracy and efficiency. Since laser process parameters play important role, the influence of the laser process parameters, *viz.*, power, scan speed and laser beam as well as material properties including absorptivity have great influence on the accuracy and efficiency of the process. This study is mainly focused on laser and laser assisted bending and straightening of mild steel (AH36). Besides in selected cases aluminum alloy (5052-H32) and stainless steel (SUS304) were also used. The thesis explores efficient and accurate procedures for generation of required bend angle in both bending and straightening. For this purpose, laser assisted straightening; using magnetic force by permanent magnet as well as electromagnet was studied. For bending use of magnetic force by electromagnet was studied. Mechanical tests like tensile test and

impact test were also conducted. Further, microhardness, microstructure and average grain sizes were evaluated as a part of the study.

The workpiece materials used in this thesis have significant utilities in different aspect of industrial application. AH 36 steel is used in the construction of container ships, bulk carriers, commercial ships and different ship components. Aluminum alloy (5052-H32) has low density and excellent thermal conductivity. It is commonly used in sheet, plate and tube form for different applications *viz.* general sheet metal work, heat exchangers. Stainless steel 304 is widely used in different industrial and domestic applications. It is used for high corrosion resistance, good formability and strength.

1.6 Organization of the Thesis

The work performed in the present thesis consists of eight chapters. The content of each chapter has been briefly given as follows.

Chapter 1 presents an introduction of laser bending and scope of the thesis.

Chapter 2 presents a literature review on the laser bending and straightening process and a detailed summary on the techniques used to predict the quality of the laser bend. It discusses a number of processes of laser bending, effect of process parameters on laser bending, mechanisms of laser bending, materials processed by laser forming process, edge effect in laser bending process and process modelling of laser forming processes.

Chapter 3 describes the detailed plan regarding experiments and simulations of laser bending and straightening. The experimental set up, testing machine and details of numerical simulation have been explained.

Chapter 4 describes improvement of the bend angle by using black enamel spray thereby improving the results. Comparison of numerical simulation with experimental results has been presented.

Chapter 5 presents development of methodology to estimate bend angle with accuracy. The methodology was implemented in shop floor to achieve desired bend angle with predefined accuracy. Further this methodology has been verified with three different materials in shop floor.

Chapter 6 describes experimental study on multi-pass laser straightening of bent AH36 steel strips. Three types of specimen namely as-formed, stress relieved and annealed have been used. The effect of laser power, scan speed, number of laser pass, and thickness of workpiece are discussed. Further microhardness and microstructure study with tensile and impact test have been performed. Possibility for numerical simulation has been also investigated.

Chapter 7 present laser bending and straightening of AH36 steel strips with electromagnetic force. Effect of process parameters and microhardness test has also been studied. The process of laser assisted bending with electromagnet has been modeled numerically and a good agreement with experimental results has been achieved.

Conclusions and scope for future work are presented in Chapter 8 followed by references and appendices.

Chapter 2

Literature Survey and Detailed Objectives

2.1 Introduction

Laser bending is a process of bending a job by irradiating with a laser beam and subsequently cooling it. After cooling, residual stresses remain in the job and it gets bent. Usually, the laser beam moves over the bend line with an appropriate scan speed. The process has drawn the attention of the researchers due to certain edge over the conventional bending. A detailed review of the process is presented by two important papers viz. Shen and Vollertsen (2009) and Dixit et al. (2015). These two papers have been used to gather numbers of information in this chapter. A detailed review of literature for laser based bending and straightening have been presented in this chapter.

2.2 Laser Bending Mechanism

The laser bending mechanism is categorized into different mechanism based on the direction of bending. The workpiece geometries i.e. thickness, length and width of the workpiece play the key role to decide the direction of bending. Similarly laser parameters (laser scan speed, power and laser beam spot diameter) and properties of the material also have significant effect on laser bending. It is possible to achieve the required bend direction and bending by proper selection of workpiece geometries, laser parameter and material properties (Vollertsen and Rodle, 1994).

The three fundamental mechanism for laser bending process was reported by Geiger and Vollertsen (1993); Shen and Vollertsen (2009) and Vollertsen and Roodle (1994). The workpiece and laser process parameters have significant role over these mechanisms. The three mechanisms are

1. Temperature gradient mechanism (TGM),
2. Buckling mechanism (BM),

3. Upsetting mechanism (UM).

Guan et al. (2005) mentioned as a result of temperature difference between upper and lower face of the workpiece across the thickness direction the bending of the sheet material occurs. The temperature difference induces stress owing to the variable expansion of neighbouring layers.

2.2.1 Temperature gradient mechanism (TGM)

TGM is the most frequently appeared mechanism in most of the cases of sheet metal bending. Hu et al. (2002), Kant and Joshi (2012a), Merklein et al. (2001), and Vollertsen and Rodle (1994) reported that the direction of bending is influenced by the laser beam diameter, scan speed and thickness of the workpiece. TGM occurs when workpiece thickness is of the order of laser beam diameter. The scan speed should be fast enough to create a sharp temperature gradient (Li and Yao, 2001a).

TGM operates in two stages, heating of the workpiece followed by natural cooling. During heating, reverse side bending occurs because of thermal expansion of heated area. The thermal gradient produces expansion which is resisted by neighbouring materials causing compressive stresses in the heated region. On achieving flow stress, near the top surface plastic deformation is produced. However, in the vicinity of bottom surface due to low temperature plastic deformation is not produced. The bending direction is towards the laser beam during cooling, as a result of contraction and shortening of the material at the upper layers. Hence the final bend occurred towards laser beam.

Lawrence et al. (2001) reported that for single pass laser bending, bend angle in the range of 0.1º to 3º was achieved. Wang et al. (2016) studied thickening behaviour of stainless steel/carbon steel laminated plate (SCLP) in laser bending zone. SCLP comprised the matrix layer of carbon steel cladded on both side by stainless steel plates. Researchers concluded that due to both thermal and plastic deformation effect, thickening initiated.

2.2.2 Buckling mechanism (BM)

BM is generated when laser beam diameter is higher than the thickness of the sheet, in the range of 10 times of the thickness of the sheet (Hu et al. 2002). It occurs due to generation of minor temperature gradient through thickness (Li and Yao 2001b; Hu et al. 2002 and Shi et al. 2006b). Also for a thin sheet with greater thermal conductivity, it may occur when the sheet is scanned using a larger laser spot diameter and gentle scan speed. This results a higher strain (thermo-elastic) (Vollertsen et al., 1995 and Dearden and Edwardson, 2003). For deforming thin metal sheets, BM is used .The bend angle produced in BM lies in the range of 1°–15° for single laser pass and it significantly higher than in TGM (Lawrence et al., 2001).

The bending procedure in BM operates in two stages, heating stage and cooling stage. In heating stage due to laser application, thermal expansion of the material occurs and compressive stresses got generated in the heated region. The sheet develops swelling with increase in compressive stresses and decrease in flow stress of the heated region. Further reduction in flow stress, the sheet bends plastically in the locality. In cooling stage due to reduction in temperature relative increase in the flow stress in heated region occurs. Hence elastic bending of the sheet happens.

The bend direction in BM is not well acquainted. It can produce the bending in both direction (towards and away) from laser source. Number of factors influence bending direction in BM (Edwardson et al. 2001; Hennige et al. 1997; Shi et al. 2006a and Jamil et al. 2011a). The key factors are workpiece geometry, laser parameters, internal and external stresses including gravitation forces. Pre-bending orientation of the sheet and residual stresses are responsible for the bending direction. Nevertheless, by using BM, it is possible to bend a sheet metal in a predefined way suitably.

Chakraborty et al. (2016) accomplished experimental investigation and simulations (Finite Element) to form a surface having bowl shape using a stationary laser beam. The irradiation was done at the centre of flat circular sheet whose diameter was 25 with 1 mm thick and the material was AISI 304 stainless steel sheet. They used a 2 kW Yb fibre laser. Irradiation time was taken from 1 to 4 s,

with variable laser spot diameter from 6 to 12 mm and power as 300 W. It was reported that with constant laser beam diameter and laser power, for higher irradiation time more bending occurred. BM was produced while using a beam diameter around 10 times of sheet thickness.

2.2.3 Upsetting mechanism (UM)

Upsetting mechanism (UM) initiates for laser beam diameter significantly smaller than the thickness of sheet. Furthermore, high thermal conductivity of the workpiece material assists UM (Pretorius, 2009). In UM, the workpiece gets shortened in length and it becomes thicker in thickness direction near to laser irradiation. Therefore, it is also termed as shortening mechanism (Shen 2008). Shi et al. (2012) reported that the UM appears due to irradiation on thick sheet accompanied by gentle scanning speed of laser and smaller laser spot diameter. The process parameters in UM are similar to BM with the exception that heated area is considerably smaller as compared to sheet thickness; thus the buckling is not permitted by the workpiece. The slow speed produces almost consistent heating of the sheet across the thickness. There is a decrease in flow stress and approaching of thermal strain toward elastic strain at yield stress in the heated area. Further heating results a plastic compression on heated material due to restriction for free expansion by surrounding bulk material. Consequently, the bulky thermal expansion gets converted into plastic compression. It results compression of the sheet with an almost constant strain along the thickness. Finally it leads to a decrease in length with increase in thickness for the sheet (Li and Yao 2001a; Lawrence et al. 2001; Hu et al. 2002 and Shi et al. 2006b). The mechanisms for laser bending are shown in Fig. 2.1.

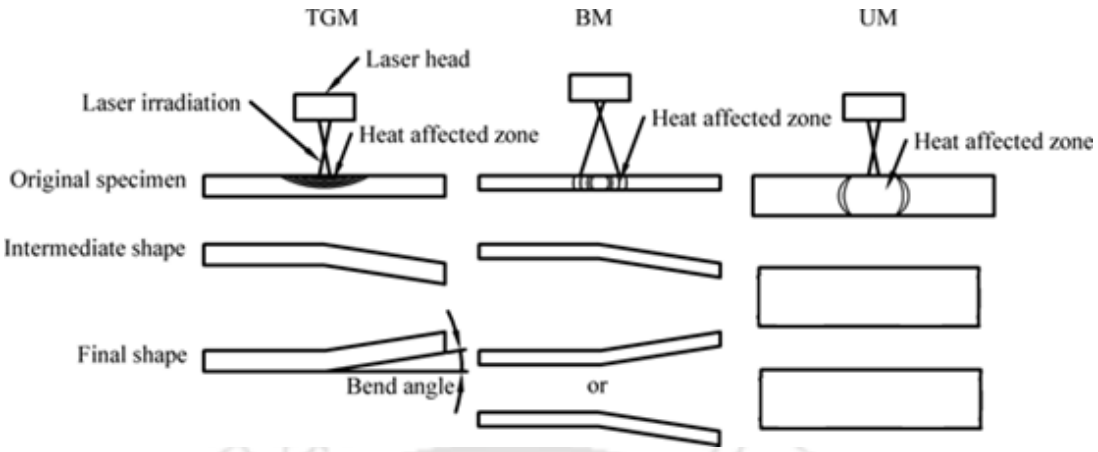

Figure 2.1 Schematic representation of laser forming: (a) temperature gradient mechanism, (b) buckling Mechanism and (c) upsetting mechanism

2.3 Experimental study on Laser Based Bending and Straightening

Considerable research papers are available about experimental study on laser based bending and straightening. Researchers discussed about different aspect of experimental studies, such as various process parameters and factors which have significant control on the laser bending process, different material processed by laser forming process, mechanical and metallographic properties, edge effect and laser bending and straightening.

2.3.1 Effect of Process Parameters and material property in Laser Bending and Straightening

The different parameters involved can be classified as laser process parameters, workpiece geometry parameters, material properties parameter and external constraint parameters. These are listed in Table 2.1. The detail about significance and influence of process parameters has been discussed in the succeeding paragraphs.

Table 2.1 Different process parameters in laser forming

Category	**Example**
Laser process parameters	Laser scan speed, laser power, number of laser passes, laser beam diameter.
Workpiece geometry parameters	Workpiece size, length, width and thickness.
Material properties parameters	Thermal properties, mechanical properties and absorptivity.
External constraint parameters	Mechanical load and clamps, force cooling, external load.

Effect of laser power

Laser power maintains a proportionate relationship with density of heat flux. The laser power should be not maximum but optimum to achieve the maximum laser bend angle. The literature says that bend angle increases with increase in laser power (Chen and Xu, 2001; Shichun and Jinsong, 2001 and Hsieh and Lin, 2004b), nevertheless it is important to cite that after reaching certain definite value, the bend angle reduces with increase in power (Lawrence et al. 2001). This occurs either due to the workpiece melting instead of plastically deforming high laser power (Paunoiu et al. 2008) or reduction in the temperature deviation between the top and bottom surfaces as a result of higher laser power (Kant et al. 2013b). Laser bending is also not possible at laser power below certain level (Lawrence et al. 2002) due to the shortage of threshold energy. Vasquez-Ojeda and Ramos-Grez (2009) used proper scanning patterns and generated larger bend angles at low laser (*viz.*, zig-zag, squared and step) providing spatial modulation of energy.

Effect of scan speed

The scan speed has a significant role in the laser based heating process. Vollertsen and Rodle (1994) described that scan speed is responsible for controlling per unit length heat input and the temperature variation between the bottom and top surfaces across thickness. The heat input per unit length also maintains an inversely

proportional relationship to the scan speed. As the scanning speed increases, the contact time between sheet surface and laser beam gets reduced. This results in decrease in maximum temperature and temperature gradient across thickness of sheet. Hence amount of plastic deformation decreases resulting reduction bend angle produced (Ji and Wu, 1998 and Kyrsanidi et al. 1999). Li and Yao (2000) considered diverse groupings of laser power and scan speed and also maintained the top surface peak temperature constant. There was a 30% decrease in the bend when the scanning speed was doubled. Hu et al. (2001) investigated different combinations of laser power and laser scan speed with fixed energy input. They reported that larger bend angle was observed due to high temperature gradient and power at fast laser scan.

In case of magnesium alloy M1A the final bend angle initially increased slightly and then got reduced with increasing scan speed (Chen and Xu, 2001). The bend angle increases with the increase in scan speed at higher power because of the high temperature gradient produced (Barletta et al. 2006). The temperature gradient increases with scan speed and results in an increased bend angle. With an increase in the scan speed, the bottom surface plastic deformation gets reduced (Kant and Joshi, 2015).

Effect of laser beam diameter and geometry

The beam geometry of laser is a significant parameter for controlling heat flux. Laser beam geometry signifies laser beam shape with total spot area. Different types of laser beam shapes are available like circular, rectangular, line, star, triangular, D-shape, donut, cross, etc. The circular shaped laser beam is the mostly common one. The laser flux density increases with decrease in laser beam diameter.

Safdar et al. (2007b) examined both experimentally and by finite element model the effect of different beam shapes, viz. circular, rectangular, triangular, and donut respectively on laser tube bending by continuous wave (CW) laser. They reported that the donut beam provided the least lateral bending and circular laser beam provided highest bending. Mazhukin et al. (2007) studied laser pulse shape effect variation on temperature distribution under different operating condition. Sheikh and Li (2010) reported that the laser beam shape is useful for the control of

temperature gradients, temperature distribution, heating and cooling rates. The beam geometry in TGM dominated process considerably controlled the bend angle, bending the edge radius and edge effect (Jamil et al. 2011b). The temperature gradient between laser irradiated and opposite surface in a sheet rises with the reduction in the laser beam diameter. The bending angle decreases with growth in laser beam diameter. Converse result may be produced by reduced beam diameter and increased beam diameter for temperature gradient and bend angle in case of BM (Chen and Xu, 2001 and Kant and Joshi, 2015).

Effects of number of laser passes

Multi scan laser bending is used to attain large bend angle, by repeated scan. With increase in number of laser of passes, bend angle increases (Lawrence et al. 2001 and Edwardson et al. 2010a). However, a reduction occurs in the bend angle after each pass. Wu et al. (2010a) also observed the same. He took silicon sheets of 0.1 mm, 0.2 mm and 0.3 mm respectively. Surface absorptivity to laser irradiation, variation in sheet thickness, laser beam geometry variation as a result of bending and strain hardening play important role in reducing the increment in bend angle per pass. At repeated scanning of laser, surface coatings get removed or burnt off resulting in a decrease of the bending angle at each pass. Proper choice of cooling condition and process parameters is significant for better result in multi pass laser bending. Selection of proper combination of process parameters and cooling condition is essential in multi pass laser bending process. Due to temperature rise after each laser pass, melting may occur on workpiece surface (Edwardson et al. 2010b). Griffiths et al. (2010) stated that geometrical effects and absorptivity become dominant with the increase in number of laser passes. During laser bending of magnesium M1A alloy sheet the temperature difference between top and bottom surfaces of worksheet decreases with increase in number of laser pass. It happens as a result of inadequate cooling time among two successive laser passes (Kant and Joshi 2016)

Effect of workpiece geometry

Geometrical parameters, *viz.*, length, width and thickness of workpiece affect the bend angle produced. Workpiece thickness significantly controls the temperature difference between two surfaces of sheet. The bending angle maintains inverse relation to the square of the thickness of workpiece (Geiger and Vollertsen, 1993 and Lee and Lin, 2002). The bending mechanisms are also reliant on thickness. The bending mechanism transforms from BM to TGM with the increase in the thickness of the workpiece. Thickness has significant effect on edge effects. Edge effect increases with the increase in workpiece thickness (Zahrani and Marasi, 2013a). The length of the sheet (perpendicular to the scanning line) does not have significant effect on laser bend angle (Shichun and Jinsong, 2001 and Chen et al. 2004a). Different researchers reported about different factors and their influence on bend angle in laser bending process (Hu et al. 2001; Cheng et al. 2006 and Dixit et al. 2015).

Experimental, numerical and analytical studies on effect of size on laser forming for low-carbon steel sheet revealed that with an increase in sheet width, the bending angle increased along the scanning direction when sheet length was fixed (Cheng et al. 2005b). Similar observations were reported by Shichun and Jinsong (2001), Chen et al. (2004a) and Shi et al. (2011).

The effect of absorptivity on laser bending

Material absorptivity to laser irradiation plays a key role in bending by laser. With increase in absorptivity, increase in input energy to the workpiece also occurs. When material surface is of higher reflective, considerable amount of power loss happens. Absorptivity can be enhanced by different manner. Wavelength has significant effect on absorptivity. With decrease in wavelength of laser irradiation absorptivity increases (Chen et al. 1999). The absorptivity of diode laser is efficient than CO_2 laser owing to small wavelength (Lawrence 2002). Due to application of suitable coating over the vicinity of scanning path, improvement in bending occurs (Barletta et al, 2006). The graphite coating has higher absorptivity (60%–80%), low cost, high melting point and can be applied easily (Edwardson et al. 2006, Carey et al. 2007). The requirement of number of laser passes decreases significantly with increase in absorptivity (Edwardson et al. 2007). Graphite coating enhances

absorptivity for pulsed laser irradiation (Chehrghani et al. 2012). The hydrated lime coating poses superior absorptivity compared to graphite coating in CO_2 laser bending (Singh et al. (2013b). The cement coating was better than hydrated lime coating (Gautam et al. 2015). Fetene et al. (2017) conducted laser bending for friction stir processed as well as cement-coated sheets.

Effect of thermal properties

Temperature distribution is governed by thermal properties in the workpiece. With decrease of thermal conductivity both peak temperature and temperature gradient increases. It happens because of low heat dissipation in case of material with low conductivity (Li and Yao, 2001a and Hu et al. 2002). With variation in thermal conductivity the temperature gradient and peak temperature also vary (Bejan and Kraus, 2003). Yanjin et al. (2003) reported that the bend angle maintains proportional relationship with the coefficient of thermal expansion while inversely proportional relationship to density, specific heat capacity and thermal conductivity of any material. The peak temperature increases with the reduction in thermal conductivity, specific heat capacity and density (Guan et al. 2005).

Effect of mechanical properties

The mechanical properties such as modules of elasticity, coefficient of thermal expansion, Poisson's ratio and yield strength has important effect in the laser forming process. Because of strain hardening, bend angle gets reduced with the increment of yield strength (temperature dependent). (Yanjin et al. 2003 and Guan et al. 2005). The strain hardening and Poisson's ratio do not have considerable effect in the bending process. An increase in thermal expansion coefficient leads to increasing bend angle (Vásquez-Ojeda and Ramos-Grez, 2009). The Poisson's ratio is significant factor to govern the coagulating of the heated region. Thickening increases with the increase in Poisson's ratio. Usually, increasing elastic modulus leads to the decrease in bend angle.

Effect of forced cooling

Forced cooling is used to facilitate efficient and effective laser bending process. By using force cooling, substantial saving in idle time among consecutive laser passes can be incorporated (Cheng and Yao, 2001). Forced cooling helps in reducing adverse effects on microstructure and mechanical properties.

Lambiase et al. (2013) performed study on passive water-cooling by partly immersing the workpiece in water throughout the process. They reported considerable lessening of the time of cooling among successive passes. Also rapid reduction in temperature prevents from undue oxidation and melting of workpiece surface. Kant and Joshi (2013a) performed FEM simulations and reported that forced cooling contribute to increased bend angle.

Shen et al. (2014) performed laser forming of stainless steel 304 with workpiece of 100 mm × 50 mm × 1 mm size by using underwater pulsed fibre laser. They reported that maximum bend angle was attained by keeping top surface exposed and immersing the bottom surface in water. When the job was fully immersed, no surface oxidation occurred resulting in improved surface quality. There was an optimum depth for minimization of the HAZ.

Effect of external load

Use of external load enhanced the bend angle produced during laser irradiation. To differentiate from conventional process, the technique is termed as laser-assisted bending (Kratky, 2007). This method is suitable to produce larger bend angles with a single laser scan. For hard material with very less ductility, this method is very effective (Dearden and Edwardson, 2003 and Roohi et al. 2012). Laser assisted bending has numerous applications such as in ship building (naval), automobile, medical, aerospace and microelectronics industries. Bammer et al. (2011) performed laser-assisted bending of Al alloys, Mg alloys (AZ31, ZE10), Ti alloys (Titan grade 2, WL 3.7164), (7075, Titanal) and steels (M85, St 52, Hardox). They reported that Ti alloy sheet upto 12.7-mm-thick was bent successfully.

Samm et al. (2009) used a method in which the laser beam was passed through a transparent sapphire tool, and material heating was done at tool contact point only. Kant et al. (2013b) used a setup for parallel and synchronous movement

of mechanical load along with the laser beam. Another suitable way was proposed by Yanjin et al. (2003) where a preload was applied in a cantilevered way at the free end of sheet. It enhanced the bend angle considerably. Gisario et al. (2011) performed V-bending mechanically followed by the laser heating.

Bammer et al. (2011) used laser assisted bending successfully to bend brittle materials. Mueller et al. (2013) invented Laser Origami technique. Mueller et al. (2013) performed forming of three-dimensional objects by folding a sheet by softening it at bend lines with the help of a defocused laser beam. Gisario et al. (2016) bent Grade 2 CP titanium and AA 7075 T6 aluminium sheets by external-force (pneumatic tool) and local and selective heating by laser irradiation. They used a high power diode laser with external assisting force to improve the bending.

Effects of clamp

The clamping provides a mechanical constraint to hold the workpiece during laser irradiation. The clamping reduces the edge effect along scanning direction because of the stress distribution into the sheet. Clamping technique affect bend angle and edge effect.

Birnbaum et al. (2007) carried out experiments in two conditions on a squared sheet with side of 80 mm and 0.89 mm thickness. In first condition, the sheet was clamped in a cantilevered manner other condition while in second condition sheet was simply put on a platform without clamping. Both types of specimens were scanned at distances of 40 mm, 25 mm, and 10 mm from the clamp edge. It was observed that the greatest bend angle was achieved when scanning was carried out at 25 mm distance from the clamp edge and the lowest bend angle was achieved when the scanning was carried out at a distance of 10 mm from the clamp edge. Except for 10 mm distance case, the bend angles for the clamped sheet were greater than those for the unclamped sheet.

Kant and Joshi (2012b) used four different ways to clamp workpiece– sheet clamped at one side completely, sheet clamped at mid-point of the side, sheet clamped at two corners of the side and unclamped sheet. They reported that

maximum and minimum edge effect was obtained for the unclamped sheet and for clamping the sheet completely at one side, respectively. When the sheet was clamped at one edge of the workpiece and also clamped at the end points of laser scan, the edge effect was the least (Hu et al. 2013).

2.3.2 Material Processed by Laser Forming Process

Laser bending has been investigated for different types of materials. A detailed study about different materials has been useful for the manufacturing industries. The process of laser bending has been applied to various industrial materials. A brief description is provided systematically for different materials.

Carbon steel

Dearden and Edwardson (2003) used mild steel sheet to generate a 3-D complex shape by using Nd:YAG, Q-switched laser. Chen et al. (2008) used cold-rolled grade 1008-1012 carbon steel to study the bending in laser forming by use of continuous wave fibre laser. Both TGM and BM laser bending were studied for the multi-path and multi-scan irradiations. Shen and Yao (2009) performed a detailed study on the mechanical properties of low carbon steel sheets after laser bending. They reported an enhancement in the fatigue life due to the compressive strains induced by the process. Safari and Farzin (2013) used tailor-machined blanks of mild steel to study laser bending characteristics with the use of continuous wave CO_2 laser having the maximum power of 2 kW.

Stainless steel

Chen et al. (1999) implemented pulsed laser having line shape to bend workpiece of 301 stainless steel. Gollo et al. (2011) evaluated the process parameter's effect on bend angle in laser bending by the use of Taguchi experimental design. They used pulsed Nd:YAG lasers and working material was 304 alloy steel and St12 sheets. Lambiase et al. (2013) reported the effect of the passive water-cooling using a diode laser with the maximum power of 1.055 kW. Maji et al. (2014a) produced dome shapes from AISI 304 sheet using continuous wave fibre laser. Shen et al. (2014) performed underwater pulsed laser bending of

the stainless steel. Chakraborty et al. (2015a) investigated laser forming of stainless steel sheet to form a deep pillow shaped surfaces.

Aluminum and aluminum alloys

Chan and Liang (2000a) studied the deformation behavior of Al6013/SiCp aluminum alloy composite sheet. They used parallel and transverse scanning to the rolling direction. Results showed larger bend angle in the case of transverse scanning along rolling direction. Similar result was achieved by Chan and Liang (2000b). They used two specimens of metal matrix composites (Al2009/20 vol. % SiCw and Al2009/20 vol. % SiCp) of aluminium. (Here, w and p stand for whiskers and particles respectively). Labeas (2008) investigated on laser bending of aluminum sheets and proposed a model. Fetene et al. (2016) proposed a finite element modelling of laser bending of friction stir welded aluminium 5052-H32 sheets

Aluminium foam

Quadrini et al. (2010) conducted laser bending on open-cell foam panels (rectangular specimens, AlSi7Mg, size 100 mm × 35 mm × 10 mm). They used diode laser (940 nm wavelength) and attained a bend angle of 50° after 150 scans. Compared to high-density foam, considerably larger bend angle was obtained for low-density foam. Guglielmotti et al. (2009) conducted laser bending of aluminium foam sandwich panels.

Nickel alloy

Yau et al. (1998) reported that with increasing number of laser pass, the bend angle for thin A42 nickel alloy steel sheet increases. In their study on laser bending of pre-stressed thin-walled nickel micro-tubes, Jamil et al. (2015) observed that effectiveness of short pulses with high power laser beam is more.

Brittle materials

Forming of low formability materials like single and mono crystal silicon, borosilicate glass, aluminum oxide Al_2O_3 and ceramics is a challenging task. By

using mechanical bending operation with conventional tools and dies, it is challenging to deform due to the formation of crack on the worksheet. Laser and laser assisted bending have been magnificently working to bend brittle materials. The laser bending mechanism of the silicon sheet was studied by Xu et al. (2013) and they noted the permanent bending of the workpiece due to the plastic deformation. The brittle-ductile transition threshold was crossed by the working temperature. By using Nd:YAG laser, laser bending of a single-crystal silicon sheet was described by Wang et al. (2011). The silicon sheet was set in the dimensions of 10 mm × 5 mm × 0.2 mm. BM and TGM together composed the pulsed laser bending instrument of thin silicon-sheet. A bend angle of up to 6.5° was attained for the silicon sheets after six laser passes. Wu et al. (2010b) studied laser bending of borosilicate glass and Al_2O_3 ceramic by CO_2 laser and mono-crystalline silicon using Nd:YAG pulsed laser respectively. They concluded that for mono-crystalline silicon and Al_2O_3 ceramic, the bending occurred towards the laser beam direction. For borosilicate glass workpiece, both toward and away direction were achieved. The bend angles increased with increase in the width. Considerable bend up to 40° was achieved with multiple laser passes on the same location. The laser bending of Al_2O_3 ceramic was found highly sensitive to process parameters; still, bend angles of 2° could be obtained.

Titanium alloys are very difficult to bend due to their brittle nature. Gisario et al. (2017) conducted laser-assisted bending on titanium Grade-2 sheets and achieved sharp bend angles (>140°) having small fillet radii. Gisario et al. (2016) improved springback effect by using external force in laser bending of titanium alloys. Some researchers reported the laser bending of titanium (Walczyk et al. 2000; Bartkowiak et al. 2004 and Fan et al. 2005).

Magnesium and magnesium alloys

Chen and Xu (2001) investigated the effect of scan speed on the bend angle for magnesium alloy M1A and observed an initial increase of the bend angle followed by a decrease with the increase in scan speed. Due to high scan speed reduction in heat energy occurs which results fall in peak temperature generated. Hence, the temperature gradient decreases along the thickness, resulting the

reduction in bend angle (Shichun and Jinsong 2001). Kant and Joshi (2016) conducted finite element method (FEM) simulation and experimental investigation for multi-pass laser bending of magnesium M1A alloy sheets.

Plastics

Okamoto et al. (2000) conducted precision laser forming for plastic with Nd:YAG laser. They observed that after laser irradiation bend angle increased speedily during cooling process. The biggest bend angle was attained under a certain energy density. Okamoto et al. (2004) studied deformation behaviour of high density polyethylene with Nd:YAG laser forming. Due to viscoelastic nature of the material, large amount of bend angle was achieved. Davim et al. (2008a) worked on evaluation of cutting quality of polymethyl methacrylate (PMMA) using CO_2 lasers. PMMA is a versatile thermoplastic that is suitable for engineering and many common applications. Further Davim et al. (2008b) performed experimental studies on CO_2 laser cutting quality of polymeric materials and evaluate the effect of the process parameters (laser power and cutting speed) during laser cutting for some polymeric materials.

2.3.3 Effect of Laser Forming on Mechanical and Microstructural Properties

The mechanical and microstructural properties of a material are considerably affected by laser forming. During laser scanning due to rise in temperature, localized deformation occurs in the heated region. The vicinity of laser scan line undergoes strain hardening, dynamic recrystallization and phase transformation. This leads to significant changes in mechanical and microstructural properties of the heated region. Researchers studied different aspects of mechanical and microstructural changes on workpiece due to laser process parameters.

Effect of laser forming on microstructural properties

Cheng and Yao (2002) carried out microstructure integrated modelling of multi-scan laser forming of low carbon steel. Fan et al. (2007) investigated the effect of microstructure changes on the flow stress to elaborate the effect of phase transformations on mechanical behaviour of AISI 1010 steel during laser bending.

The boundary of the HAZ is clearly observed. They observed clear boundary of the Heat Effected Zone (HAZ). They also conclude that the refined grains in the HAZ are much smaller than in the base material due to high cooling rate.

Cheng et al. (2007) studied possibility of a hybrid forming which combines the advantages of laser shock peening and metal forming process, having an ultra-high strain rate forming utilizing laser shock waves. The microstructure of the formed copper foils was characterized quantitatively with electron backscatter diffraction (EBSD) techniques after laser forming. The effects of initial grain size were investigated.

Liu et al. (2011) used two different laser beam scanning paths, i.e. single direction raster scanning (SDRS) and cross direction raster scanning (CDRS) respectively, by using same laser solid forming (LSF) processing parameters to study the effect of laser scanning path on microstructures of laser solid formed nickel-base super-alloy Inconel 718. After recrystallization they observed non-uniform grain size in SDRS samples compared to CDRS samples. After heat treatment, grains of both the samples refined due to recrystallization. The grains of the CDRS sample were finer than the grains of the SDRS sample.

Singh et al. (2013a) conducted study on the microstructure after multi-scan laser bending of mild steel. They summarized as, the average grain size progressively increased from the top to the bottom surface along the thickness direction. On the vicinity of the scanning surface due to higher temperature at the top surface of the workpiece, fine grains were observed. Palani et al. (2015) studied microstructure analysis of the deformed region and the heat affected zone of FE-410 plate. They reported that the bainite formation occurred in the irradiated region and in the heat affected region grain coarsening occurs compared to unaffected region.

Effect of laser forming on mechanical properties

Due to laser bending process compressive and tensile strains, residual stresses and hardening in the scanning region have been developed. These factors affect different mechanical properties like tensile strength, fatigue strength, hardness and ductility of material. As result of laser pass, difference in hardness occurred between the base material and the laser bent workpiece. Merklein et al. (2001)

reported that the hardness of AA1050 increased with increase in number of laser pass. Hardness is not uniform due to dislocation density, temperature and relevant stress or strain material. Thomson and Pridham (2001) studied change in material property associated with laser forming of mild steel. Due to laser forming the yield strength of the material increases locally.

Majumdar et al. (2004) studied laser bending of AISI 304 stainless steel with 2 kW continuous wave CO_2 laser and reported that microhardness of the laser-irradiated zone was increased by 1.5 to 2 times as compared to the base material. It happens due to grain refinement as a result of quenching during laser bending. McGrath and Hughes (2007) studied fatigue performance of laser-formed high-strength low-alloy (HSLA) steel plate after laser scanning. They used a 5 kW continuous wave CO_2 laser and draw the conclusion about increase in endurance limit after laser forming.

Shen and Yao (2009) investigated mechanical properties after laser forming of low carbon steel specimens. The observed enhancement in the tensile strength and yield strength after laser forming, while the percentage elongation was reduced. Laser forming improves the fatigue life of low carbon steel. With increase in laser power the hardness of laser formed workpiece increases (Singh et al. 2013a).

2.3.4 Edge Effect in Laser Bending Process

Shi et al. (2013) performed different heating methods for reduction of the edge effect during multiple laser irradiations. Shi et al. (2016) proposed to reduce edge effect under the action of two unequal concentrated forces and reported that significant reduction in edge effect occurred. Zahrani and Marasi, (2013b) reported that with increase in number of laser passes, the edge effect decreased.

Hu et al. (2013) suggested that proper clamping reduced the edge effect. Zahrani and Marasi (2013a) studied the relative variation of the bend angle (RBAV) and concave depth of longitudinal distortion (CDLD) during laser bending. With increased laser power, scan speed and thickness of the workpiece produce reduction of RBAV and CDLD. With increase in laser beam diameter, both RBAV and CDLD reduce. With increasing number of passes, the RBAV decreased considerably but

CDLD increased. CDLD decreased with decrease in heating-position from the free edge, however RBAV remained unaffected. Edge effect decreases with increase in scan speed.

2.3.5 Curvilinear Laser Bending Process

Chen et al. (2002) reported that during laser bending of titanium alloy sheets in a curvilinear profile, bend angle decreased with the increase in scan path curvature. Zhang et al. (2009) performed the curved laser irradiation in ring shaped sheet metal. They reported that a constant variation of bending because of the rigid ends-effect which caused warping of sheet edge. With increase in the spot diameter, the warped curvature also got increased.

Kant and Joshi (2014) in their work on experimental and numerical study on curvilinear laser bending of magnesium alloy M1A sheet reported the difference in deformation behaviour between curvilinear and straight laser bending process. They observed decreases in bend offset with the increases in laser power and decrease in laser beam diameter. Less edge effect was observed for the curvilinear laser bending process compared to straight line bending process. However, with increase in arc height the edge effect got increased.

Safari and Farzin (2015) carried out experiments on laser bending of a saddle shape of mild steel having size of 100 mm × 100 mm × 0.85 mm with spiral laser irradiating pattern with a continuous CO_2 laser. They reported that for producing saddle shapes, spiral irradiating scheme is suitable. The curvature of saddle shape increased with increase in the number of spiral paths.

2.3.6 Laser Straightening

Compared to bending with the help of lasers, the reverse process, i.e., straightening, has been investigated very sparsely. From the limited literature, it is noted that straightening process is not as simple as it appears. Dearden et al. (2006) conducted experiments to straighten the distorted aluminum sheets and observed that some distortion always remained in the worksheet. Ueda et al. (2009) attempted to flatten the projections in the carbon steel and stainless steel sheets and developed irradiation strategies based on the numerical computations of plastic strain in the

worksheet. Ueda et al. (2011) employed lasers for flattening the protrusions induced in a metallic worksheet mechanically. They observed that laser scanning on the convex surface of the protrusion was more efficient in reducing the height of protrusion as compared to laser scanning on the concave side. Thus, the convex surface should be exposed to higher temperature to induce larger tensile stresses for obtaining a flat surface. Chakraborty et al. (2015b) used temperature gradient mechanism (TGM) dominated laser bending to reduce the bend angle in mechanically bent stainless steel jobs. The change in bend angle was more when laser beam was irradiated on the convex side of the bent worksheet. Garg et al. (2016) suggested that the workpiece should be kept unclamped in an inverted V-shape to ensure proper absorption of the laser irradiation during straightening.

2.4 Modelling of Laser Forming Process

Modelling for a complex process like laser forming is very much important aspect. Significant information related to process, the physics of the process, process parameters etc. may be evaluated by modelling. Significant research works are reported in literature till date about modelling of laser forming process. Modelling of laser forming process can be classified into four categories namely— analytical model, numerical simulation model, soft computing model and inverse model. All four types are discussed in following subsections.

2.4.1 Analytical models on laser bending

The researchers established various analytical models for better understanding of the physics of the process. Analytical models are suitable for predicting stress, bend angle, temperature distribution and other related parameters in a workpiece subjected to laser forming. A brief assessment of different analytical model of the laser bending process has been presented in this section.

The initial and simple model for laser bending was provided by Vollertsen (1994). As said by Vollertsen model, the bend angle is directly proportional to laser power and inversely proportional to the laser scan speed and square of the worksheet thickness. This model excludes the yield strength and elastic modulus of the processed material. The analytical relation is given by

$$\alpha_b = \frac{3\alpha_{th} P\eta}{\rho c_p v t^2}, \tag{2.1}$$

where α_b is the bend angle, α_{th} is the coefficient of thermal expansion, P is the laser power, η is the absorptivity to laser irradiation, ρ is the material density, c_p is the specific heat capacity, v is the laser scan speed and t is the sheet thickness.

Vollertsen's model does not have inclusion of yield strength and Young's modules of material. It is difficult to understand change in material properties after laser bending. Yau et al. (1998) developed new relation including them in their model. The bend angle is given by

$$\alpha_b = \frac{21\alpha_{th} P\eta}{2\rho c_p v t^2} - \frac{36 l_h \sigma_y}{tE}, \tag{2.2}$$

where E is the Young's modulus, σ_y is the yield stress and l_h is the half length of heated zone.

The model of Yau et al. (1998) includes the role of yield strength and elastic modulus, but it is not appropriate for high laser power application when the bend angle maintain a nonlinear relation to laser power. Kyrsanidi et al. (2000) proposed non-uniform temperature distribution across the thickness of the sheet. This model is computationally efficient, requires programming for iterative steps.

Cheng et al. (2006) proposed a model which can predict the bend angle for a varying thickness plate. They considered that due to variation of the heat sink and the variable bending rigidity, the primary bending occurred. The bend angle at the location with $t(x)$ thickness is given by

$$\alpha_b = b(1-\mu^2)\varepsilon_{\max}\left(\frac{3f(x)\pi}{2t^2(x)} - \frac{4f^2(x)}{t^3(x)}\right), \tag{2.3}$$

where

$$b = c_1\sqrt{P/v}, \tag{2.4}$$

and

$$f = c_2 P/(vt), \tag{2.5}$$

where c_1 and c_2 are constants dependent on materials properties, t is the sheet thickness and μ is the Poisson's ratio. In Eq. (2.3), $\varepsilon_{\max}$ stands for maximum plastic strain at the heated surface. It is given by

$$\varepsilon_{\max} = \alpha_{th} T_{\max} - \sigma_y / E, \tag{2.6}$$

where T_{max} is the maximum temperature increase and σ_y is the yield stress.

Based on the postulation that the plastic deformation happens only during heating Shen et al. (2006) developed an analytical model. This model says that during cooling plate undergoes only elastic deformation. The model is effective for both TGM and BM.

By assuming elastic-bending theory, Lambiase (2012) formulated an analytical expression for the bend angle in which plastic deformation during heating and cooling phases was not considered. It is a two-layer model where the effective temperature distribution along the sheet thickness governs heated layer thickness. To evaluate the accuracy of the model, the main process parameters, i.e. laser power, scanning speed and sheet thickness were changed among numerous levels. The bend angle is given by

$$\alpha_b = \frac{3\eta P(t - t_h)\alpha_{th}}{\rho v c_p t(t^2 - 3tt_h + 3t_h)}, \tag{2.7}$$

where t and t_h represent sheet thickness and heated volume thickness, respectively, which has been estimated empirically. Lambiase and Ilio (2013) developed a complex analytical model for prediction of the thin sheets deformation.

Shi et al. (2007a) developed a model that estimate the bend angle in plane axis which is perpendicular to the laser irradiation path. During thermal expansion due to laser heating, top surface undergoes greater expansion than bottom surface. During cooling phase, the top layer materials are under contraction. Therefore a local shortening of this layer results bending about the perpendicular axis to the scanning direction. The bending angle is given by

$$\alpha_b = \frac{6.92\eta P \alpha_{th} w r^{1/2}}{\pi^{3/2} l^2 t(\rho c_p k v)^{1/2}}, \tag{2.8}$$

where *w* is width of workpiece, *l* is length of workpiece and *k* is thermal conductivity.

Vollertsen et al. (1995) proposed an analytical model to estimate bend angle for a thin sheets as a function of laser power, laser scan speed, thickness, modulus of elasticity and flow stress. This model can estimate the bend angle in BM. The strain in vicinity of the laser beam is plastic while strain in other portion of the beam is considered elastic. The model provides bend angle as

$$\alpha_b = \left[36 \frac{\alpha_{th}\sigma_y}{c_p \rho E} \frac{\eta P}{v} \frac{1}{t^2} \right]. \tag{2.9}$$

Kraus (1997) formulated a closed–form relation for estimating the bend angle during upsetting mechanism. Kyrsanidi et al. (2000) established a mathematical model to predict the bend angle in laser forming. Ueda et al. (2005) formulated an empirical expression to find out bend angle based on the surface temperature measurement. Gollo et al. (2011) developed a formula that includes laser process parameters viz. number of laser passes, material properties and thickness of the workpiece to estimate bend angle. Lambiase (2012) proposed a model on basis of the elastic-bending theory. Generally, these models can predict bend angle with high amount of error. Lambiase and Ilio (2013) proposed a relatively accurate thermal model capable of predicting the laser bending of thin sheets. Eideh et al. (2015) developed a model for laser bending that works on elastic-plastic bending theory. These recent models showed the overall reasonable prediction barring some cases with more than 25% error. In general, the accuracy of the prediction for analytical expressions ranges from about 10% to 50% to estimate the bend angle (Dixit et al., 2015).

Temperature distribution has important role for laser bending process. Hence, continuous research was there to establish several analytical models capable of estimating the temperature distribution. Woo and Cho (1999) developed an analytical model that can predict transient temperature distribution for a finite thickness plate in laser surface hardening. Convection boundary condition was applied on surfaces of the workpiece. Cheng and Lin (2000a) developed an analytical model in laser forming to elaborate the 3D temperature field for the finite thickness. The laser beam having Gaussian profile was considered as a constant

velocity moving source. Shen et al. (2001) developed an analytical model for laser heating and melting by suggestion of a simple temperature profile and described the temperature profile before and after melting. Cheng et al. (2005a) suggested an analytical model in laser forming which can attain the temperature distribution over a finite size sheet. They performed experimental, numerical and analytical study on laser-induced deformation and variation along length and width. Shi et al. (2007b) established an analytical model for the estimation of the temperature field during laser forming by use of convection and radiation boundary conditions. They used a one-dimensional heat conduction model to estimate the temperature during laser forming and assumed variation of temperature only in thickness direction. Van Elsen et al. (2007) presented an analytical model for a uniform moving heat source suitable for any type of use in laser materials processing. Solution of an instantaneous point heat source has been implemented where the heat source is considered as the semi-ellipsoidal. Belghazi et al. (2010) suggested an analytical model subjected to Gaussian laser beam and having transient heat conduction in two-layered material of finite depth. Chen et al. (2010) formulated an analytical model for the estimation of the temperature distribution based on temperature distribution similarity for varying thickness.

Recently, Kumar and Dixit (2018a) developed an empirical relationship for predicting the peak temperature attained during laser bending process. The empirical model is given as

$$T_{\text{pred}} = 0.954 \frac{\eta P}{D_t^{0.72} c_p^{1.0372} v^{0.4} D^{1.15} t^{0.1}} + T_{\text{a}}, \tag{2.10}$$

where η is absorptivity to laser irradiation, P is laser power , D_t is thermal diffusivity, c_p is specific heat capacity, v is laser scan speed, D is laser beam diameter, t is thickness and T_{a} is ambient temperature. Optimization of process parameters *viz.*, power, scan speed and laser beam diameter were also accomplished to achieve prescribed laser bend angle with high production rate, less energy consumption and small tensile residual stress. The parameters were, laser power: 50W, 100W and 200W, scan speed: 10 mm/s, 20 mm/s and 30 mm/s, beam

diameter: 1 mm, 2 mm and 3 mm, heat capacity: 0.002.50 J/mm^3.°C, 0.00308 J/mm^3.°C and 0.00453J/mm^3.°C, thermal diffusivity: 4.25 mm^2/s, 8.50 mm^2/s, 17 mm^2/s, and workpiece thickness: 1 mm, 2 mm and 4 mm. A model was developed for the estimation of hardness of the laser bent parts by incorporating the effects of phase fraction, cooling rate and strain hardening by Kumar and Dixit (2018b). The model was accomplished by using microstructure integrated FEM simulation.

2.4.2 Numerical models on laser bending

A continuous study has been going on numerical models since early 1990s. Finite element method (FEM) and Finite difference method (FDM) based model significantly contribute to achieve the temperature variation and bend angle (Vollertsen et al. 1993). Ji and Wu (1998) conducted transient temperature field simulation using FEM of laser bending. Chen et al. (1999) compared the experimental and FEM result for bend angle obtained. Kyrsanidi et al. (1999) established a 3D FE algorithm having coupled thermal–structural analysis. Hu et al. (2001) developed a 3D-FEM simulation system which includes a nonlinear transient indirect coupled thermal-structural analysis. The models considered the temperature-dependent mechanical and thermal properties of materials. From the numerical simulation temperature distribution, residual stress, bend angle etc. were achieved. Hsieh and Lin (2004a) studied laser-induced vibration in thin sheet metal during pulsed laser forming. Zhang and Xu (2005b) developed a FE model for pulsed laser bending. The simulation represents melting and solidification by the use of uncoupled thermal and thermo-mechanical theory. Assumption was made that the pulsed laser beam is uniform across the width. Thus, a 2D thermal-stress model having less computational time can be applied. Safdar et al. (2007a) applied FEM to explore the effects of scanning schemes on laser bending.

Use of commercial FEM packages, *viz.*, ANSYS®, ABAQUS® COMSOL® etc. was also performed in many application of laser bending process. Holzer et al. (1994) accomplished the FEM simulation by ABAQUS® to analyse BM. Chen and Xu (2001) developed a 3D-FEM model for simulation of the laser bending process (continuous wave) operated by the TGM. Nonlinear FE solver, ABAQUS® has been implemented to inspect both the mechanical and the thermal properties. Labeas

(2008) established an ANSYS® model for simulation of aluminium workpiece bending by laser and also validated their results experimentally. Venkadeshwaran et al. (2012) used ANSYS® package for modelling of the laser bending of stainless steel sheets. Edwardson et al. (2010a) simulate the multi-pass laser bending of mild steel, Ti-6Al-4V and AA5251 by CO_2 laser by using COMSOL® MultiPhysics. Pitz et al. (2010) conducted moving mesh simulation of the laser forming by COMSOL package. Yilbas and Akhtar (2014) used ABAQUS® FEM package to predict residual stress, temperature, metallurgical and morphological deviations. It was reported that the microstructure transformed into martensite from ferritic–pearlitic as a result of high cooling rates.

FEM models provide fair predictions; however, high computational time requirement is significant point in every simulation. Numerous efforts have been made for decreasing the time of computation. Appropriate mesh refinement and time-increment are vital for gaining result accuracy in rational time of computation. Yu et al. (2001) established a FE model and implemented region wise division technique for reduction of the time of simulation considerably. They studied influence of the refinement of mesh size on final distortion and temperature distribution. Zhang et al. (2002) proposed 3D FE model for pulsed laser bending to establish an efficient method that reduced computational time meaningfully. Zhang et al. (2004) developed FEA models to establish least spatial and temporal necessities for discretization and mesh density on angular distortion. The main objective was the reduction in the time of computational for modeling the laser forming. They suggested that the temporal discretization is suitable in case of at least four time-increments while moving a distance equal to laser beam radius. The spatial discretization required at least three and two elements in the thickness direction and in a beam radius respectively.

Pitz et al. (2010) established an efficient method for bulky workpiece. They presented a concept of moving mesh for saving the computational time considerably. The mesh in the vicinity of laser scan line was fine meshed and the rest part was coarse meshed accordingly. With the laser beam the mesh kept on moving.

Hu et al. (2012) proposed a strong, simple and accurate method of modeling

by use of shell elements having multi-layered. The workpiece was distributed into three zones, heating, diffusion and cooling constraint zone. Under TGM, the heating zone was steep. However the temperature gradient for other two zones was nearly equal to zero. Three types of models, *viz.*, solid, solid-shell and multilayered shell were implemented. The efficiency for simulation of the solid-shell and multi-layered shell models enhanced significantly as a result of the reduced nodes and elements.

Eideh (2014) suggested a method to improve speed of computation speed by strategy of accelerated cooling. The convective heat transfer coefficient was taken as 10 $W/m^2.K$ and 1,000 $W/m^2.K$ during heating phase and cooling phase respectively. The highest temperatures of the workpiece are same in both cases i.e. forced and conventional cooling. Both the cases predicted almost the identical bend angle, but the significant reduction in computational time occurred for speeded cooling case. The model was accurate appropriate for the simulation of large workpiece. Dixit and Fetene (2016) performed laser bending of friction stir welded 2-mm thick 5052-H32 aluminium alloy sheets. They also developed FEM model using ABAQUS® for the prediction of bend angle. Fetene et al. (2017) conducted numerical and experimental studies for laser assisted bending by magnetic force. Detailed study on numerical and experimental analysis on multi-pass laser bending of AH36 steel strips were carried out by Fetene et al. (2018).

2.4.3 Soft computing models

Soft computing refers to the use of self-learning methods such as artificial neural network, uncertainty problem solving by fuzzy set theory and evolutionary optimization techniques such as genetic algorithms. Dragos et al. (2000) developed ANN model to predict bend angles in laser bending by use of experimental data. Cheng et al. (2000b) further presented three supervised learning methods by use of neural network to predict bend angle in laser bending. The feed-forward back-propagation multilayer perceptron (MLP) neural network was used. They used hyperbolic tangent activation function, logistic transfer function and radial basis function (RBF) neural network. The best performance was attained using an RBF neural network. Casalino et al. (2002) proposed a feed-forward MLP ANN model with back propagation where the numbers of hidden layer neurons were varied from

6 to 20 in an iterative manner. Barletta et al. (2009) carried out a comparative study of numerous neural network models of a hybrid forming (mechanical bending along with laser scanning to reduce springback) by use of RBF, generalized feed forward (GFF), and MLP. Maji et al. (2013) applied neural network for predicting the bend angles and carried out inverse analysis for laser forming. Similar work was carried out for pulsed laser forming by Maji et al. (2014a). Further they conducted laser forming on a dome-shaped surface (Maji et al. 2014b). Palani et al. (2015) proposed an ANN model for parametric investigation in laser forming and bend angles prediction by use of experiment data. Experiments were conducted for the laser bending of FE-410 steel sheets of 100 × 50 × 8 mm^3 size using CO_2 laser. During parametric study, laser power was varied from 2 to 3 kW in step size of 250 W, scan speed was varied in the range 0.6–1.2 m/min in step size of 0.3 m/min, laser beam diameter was varied in the range 9–13 mm in step size of 2 mm and laser passes was varied from 1 to 210. The measurements were taken after every 10 passes. Kant et al. (2015) used an integrated FEM-ANN method for prediction of bend angles as a function of beam diameter, power, and scanning speed and result was verified using experimental data. Lambiase et al. (2015) optimized multi-pass laser bending by means of soft computing techniques. They conducted a set of experimental tests on thin AISI 304 stainless steel sheet. An ANN model was fitted that was used in the optimization.

The training and testing of data in all the above-mentioned workings were grouped on an arbitrary basis. The majority of the experimental data of the work presented by Dragos et al. (2000) were grouped into two halves each for training and testing. The complete data is grouped into 60 % training, 15% cross-validation, and 25% testing data by Barletta et al. (2009). Maji et al. (2013, 2014a, 2014b), grouped 1000 data into two subgroups of identical size at random. For training and testing of the ANN, one subgroup was used, while they used the other subgroup for validation purpose. They exchanged the training and testing data to confirm the contribution of both the data in the training. Among 1000 data, some of them were experimental and the left over data were produced by a regression model. The total number of

experimental data in Maji et al. (2013); Maji et al. (2014a), and Maji et al. (2014b) were 129, 45 and 75 respectively.

To guess the extreme surface temperature of the workpiece at a specific sampling time from the input constraints— laser beam power and the temperature from the previous sampling time, Pérez et al. (2010) used an adaptive neuro-fuzzy inference system(ANFIS) model for laser surface heat treatment method. They used MATLAB to develop the model. For the bending and thickening estimation of the shaped surface, Jovic et al. (2017) used an adaptive neuro-fuzzy inference system (ANFIS) model to select the most governing aspects.

To produce a preferred shape, Cheng and Yao (2004) evaluated the optimum values of diverse process parameters for laser forming method established on genetic algorithm (GA). The different control factors, namely laser scan speed, laser power and width (along scan line) and type of fitness utility have major effects on GA outcomes. The decision variables were, number of scan lines, laser powers at different scans, laser scan speed at different scans and distances between any two successive scan lines. The decision variables amount was near by 30; though, to reach the convergence values, it took a huge number of generations. The algorithm control parameters and the fitness function type have significant effects on the GA synthesis results. The proper selection of fitness function is vital for balancing among competing objectives, such as forming time, geometric accuracy and energy consumption. Du et al. (2010) improved the accuracy of bend angle prediction by improve in back-propagation network (BPN) based on the Double Chains Quantum Genetic Algorithm (DCQGA). The BPN-DCQGA network was trained and verified through the sample experimental data. This proposed network improved the rate of convergence by obtaining higher training efficiency. Maji et al. (2013a) used both genetic-neural network (GA-NN) and genetic adaptive neuro-fuzzy inference system (GA-ANFIS) for experimental data of laser bending process. They took laser power, scan speed, spot diameter, scan position and number of scans as inputs and the bend angle as the output. They summarized that GA-NN approach was better than the GA-ANFIS approach in predicting the bend angle, while the predictions using inverse analysis were comparable in both the approaches. Recently Fetene et al.

conducted (2016) FEM-based neural network modelling of laser-assisted bending with less number of experimental data.

2.4.4 Inverse modelling

Romer and Maijer (2000) used inverse analysis to derive the power density profile of the laser beam by. Kim and Oh (2001) evaluated heat transfer coefficient by using inverse heat transfer formulation in a 2D finite element model. Rouquett et al. (2007) in an electron beam welding, predicted the parameter of Gaussian heat source using Levenberg-Marquardt method. Yang et al. (2007) implemented inverse analysis by conjugate gradient method machining with laser. Woodfield et al. (2007) established a method to decide the thermal diffusivity of a solid by use of an analytical inverse solution.

Shidfar et al. (2012) used conjugate gradient method (CGM) to estimate the pulse parameter of a laser pulse which varies exponentially with time to achieve temperature at the material. Mishra and Dixit (2013) used inverse heat conduction method to determined absorptivity, thermal diffusivity and laser beam diameter. Temperature was measured at the centre of the workpiece. Dissimilar time interval was used and estimated thermal properties by the use of measured temperature. Eideh and Dixit (2013) used a heuristic methods based inverse estimation by measuring the temperature at two locations. Their objective was the minimization of the combined error between predicted and measured temperatures at two locations. Xu et al. (2013) implemented combine approach of experimental and simulation results to estimate absorptivity of the workpiece. Maji et al. (2013) model and optimize the pulse laser bending process by using the response surface methodology. Kumar et al. (2019) developed an inverse method to estimate the thermal conductivity, absorptivity and heat transfer coefficient for a laser irradiated sheet based on the measurement of temperature.

2.5 Optimization of Laser Forming Process

Cheng et al. (2000b) applied artificial neural network (ANN) for prediction of bend angle by developing regression models. Liu and Yao (2002) carried out

response surface methodology to determine a group of parameters for a given sheet metal shape. Ciurana et al. (2009) performed artificial neural network modeling and particle swarm optimization (PSO) of process parameters in pulsed laser micromachining of hardened AISI H13 steel. Gollo et al. (2011) and Maji et al. (2013) implemented Taguchi experimental design method to select specific parameters that can considerably affect bending process by laser. Teixidor et al. (2013) accomplished process parameters optimization for pulsed laser milling of micro-channels on AISI H13 tool steel. Akinlabi et al. (2015) applied L27 orthogonal array design for studying the effect of process parameters on laser bending. They reported that the contributions in percentage are: laser power: 21%, 32% scan speed: 27%, cooling effect: 2% and beam diameter: 18%. Das and Biswas (2015) developed the design of experiment by using L-16 orthogonal array and reported effect of operating parameters on mild steel plate bending. Number of passes is the most inducing parameter to achieve good results, followed by thickness of sheet, laser power and scan speed. Roohi et al. (2015) evaluated relative density, mean cell size and sheet thickness on bending by fixing laser process parameter (power P=210 W, scan speed v= 800 mm/min and laser beam diameter D= 5 mm). They conducted 27 numerical simulations for full factorial design of experiments. The bend angle decreased with increase in density, sheet thickness and mean cell size. The bend angle decreased by 70.9%, 61.7% and 12.3%, for increase in density by 40%, sheet thickness by 100% and mean cell size by 66.6%, respectively. Arısoy et al. (2017) worked on influence of scan strategy and process parameters on microstructure and its optimization in additively manufactured nickel alloy 625 via laser powder bed fusion. Criales et al. (2017) developed a predictive model and optimize multi-track processing process for laser powder bed fusion of nickel alloy 625. Kumar and Dixit (2018a) conducted multi-objective optimization of single pass laser bending by use of a fuzzy set based method.

2.6 Major Gaps in the Literature

The published literature gives numerous information. From a detailed study the published literature reveals definite research gaps and possibilities persist for further examination. The gaps found from the literature are summarized as follows:

1. For accurate numerical simulation proper mesh refinement and time increment analysis is required. It is an essential aspect of the simulation which was not elaborately discussed.
2. For microstructure study and change or refinement in grain after laser pass, scant literatures are available till date.
3. The absorption of the material to laser irradiation plays a significant role. The absorption quality of sheet metal can be enhanced by using different coating (graphite, black colour, cement coated, etc.) and by roughing the surface. Although a lot of work has been done, there is a need to carry out further research to gain better absorption.
4. Very less amount of literature is available on enhancement of accuracy of bend angle produced. Increase in accuracy in bend angle is very much important aspect for real life application in industrial requirement.
5. The single laser scan generates a small bend angle. Edge effect also creates non-uniform bend angle along width. However, in real life application, large bend angles are required from an efficient and cost effective way in less number of laser passes. There is a need for further improvement of bending process and eliminate edge effect.
6. Laser assisted bending was successfully used by a method in which the laser beam was passed through a transparent sapphire tool, and material heating was done at tool contact point only. Also use of a setup for parallel and synchronous movement of mechanical load along with the laser beam or preload has been applied in cantilevered way at the free end of sheet. All these methods use the contacts of mechanical load with the sheet. Scant literature is available on non-contact laser assisted bending. No research work is available on non-contact laser assisted bending with controlled assisting force.
7. Very less literature is available for laser straightening process. Use of assisting force with laser irradiation for straightening was not performed. No research work is available on both contact and non-contact laser assisted bending with assisting force. A controlled assisting force was also not used for this process.

8. There is no literature available about accurately controlled assisting force set up. Research work mainly shows use of assisting force which is not suitably controlled. Use of accurately controlled assisting force with standard setup is not available. An accurately controlled assisting force may generate accuracy in bending.

2.7 Objectives of the Present Thesis

Based on the literature survey, the following objectives are decided:

1. **Enhancing the efficiency of laser bending of mild steel by coating with black enamel Paint**

   The first objective of the present thesis is to improve the bend angle by the use of black enamel spray thereby improving the results. Selection of proper strategy of coating in multipass laser bending for enhancing result has been also investigated. Comparison of numerical simulation with experimental results has been explained.

2. **A strategy for achieving accurate bending by multi-pass laser line heating**

   The second objective of this work is development of methodology to estimate and generate bend angle with accuracy. Further this methodology has been verified with three different materials in shop floor.

3. **Laser assisted straightening by permanent magnet**

   The third objective of this work is experimental study on multi-pass laser straightening of bent AH36 steel strips. Three types of specimen namely as-formed, stress relieved and annealed have been used. The effect of laser power, scan speed, number of laser pass, and thickness of workpiece are discussed. Further microhardness and microstructure study with tensile and impact test have been performed. Possibility for numerical simulation has been investigated also.

4. **Laser assisted bending and straightening by electromagnetic force**

   The fourth objective of this work is laser bending and straightening of AH36 steel strips with electromagnetic force. Effect of parameters, microhardness evaluation has been also performed. The process of laser assisted bending

with electromagnet has been modeled numerically and good agreement with experimental results has been achieved.

The flow chart displaying the research plan is presented in Fig. 2.2.

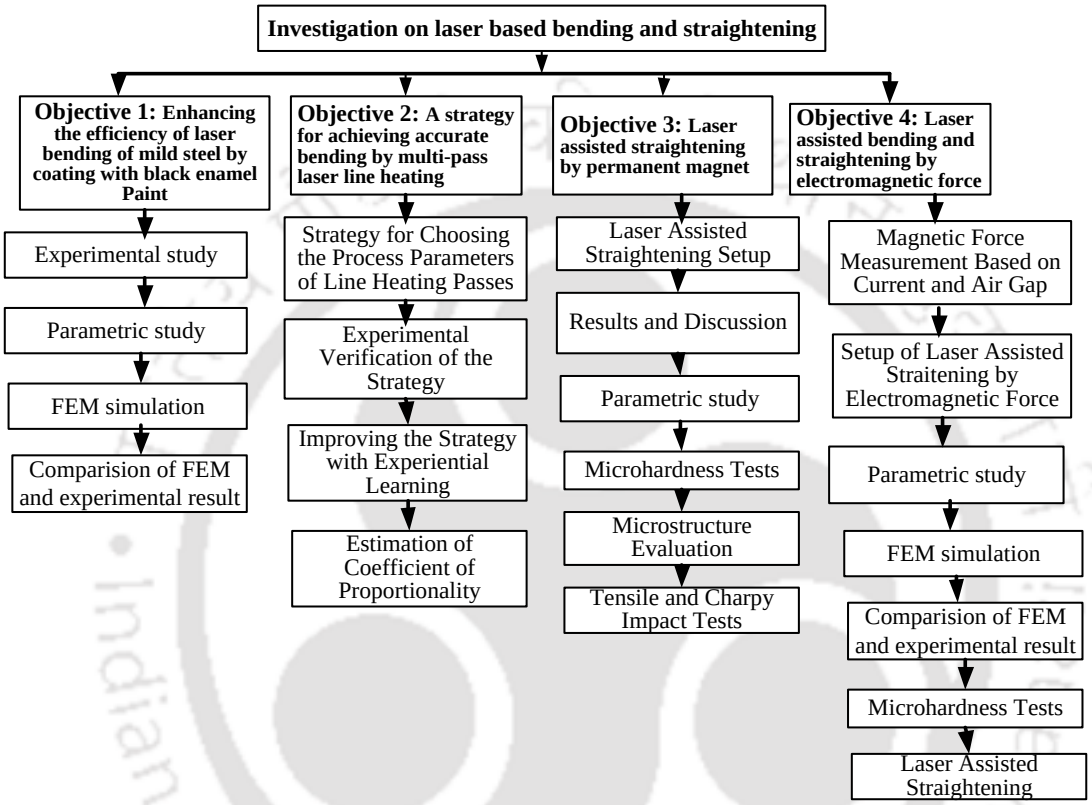

Figure 2. 2 flow chart of research plan

Chapter 3

Details of Experimental and Simulation Procedures

3.1 Introduction

This chapter discusses all experimental setups and equipment used for experimental work (laser bending and straightening) as well as its modelling by finite element method (FEM). Details of the experimental setup, working procedure and methods, workpiece types and dimensions, laser parameters, type of working material have been discussed. In most of the cases besides experimental results work, FEM simulations were also conducted. Mesh sensitivity analysis has been also discussed to select optimum mesh size in the models. This chapter mainly focuses on methodology of the work; the research outcomes have been reported in the subsequent chapters in details. Some of the setup details are also available in the thesis of Fetene (2018).

3.2 Experimental Study on Laser Machine and other Instruments

A CO_2 laser machine was used for experimental work for laser bending and straightening operation in all cases. During experimental work, the temperature of laser irradiated workpiece was kept below its melting temperature by adjusting laser parameters. After bending and straightening the final bend angle was measured by a Profile Projector. Detailed discussion has been provided in the following subsections.

3.2.1 CO_2 Laser machine

The laser machine is a CNC controlled 2.5 kW continuous wave (CW) mode CO_2 laser (Make: LVD, Model: Orion 3015) machine. It has been used to perform laser-based bending and straightening of different samples. The cutting head moves along Y-axis and work table moves along X-axis to define route to irradiation. The laser beam travels along Z-direction. For laser beam generation, helium (He),

nitrogen (N_2) and carbon dioxide (CO_2) with a composition of 60%, 35% and 5%, are used respectively. Nitrogen is the exciting medium which transfers energy to carbon dioxide, helium is used for cooling and carbon dioxide gas is used for laser production by lasing action. Figure 3.1 shows the photograph of the laser machine system. The specifications of the laser machine have been given in Appendix A.

For laser bending, laser assisted straightening by permanent magnet, laser assisted bending and straightening electromagnet, separate experimental setups have been used. Details have been discussed in Chapter 4, Chapter 5, Chapter 6 and Chapter 7, respectively.

Figure 3.1 Orion 3015 2.5 kW CO_2 laser machine with the laser head

3.2.2 Optical profile projector

The bend angle was measured on an optical profile projector (Model: PP400 TE, make: Optomech) equipped with a10× lens and a vernier scale with a least count of 0.01° (i.e., 36″). Every specimen was measured from both the edges and the average bend angle was recorded. After bending or straightening of all samples, they

are measured. Figure 3.2 shows photograph of optical profile projector while its specifications are listed in Appendix B.

Figure 3.2 Optical profile projector (Model: PP400 TE, make: Optomech)

3.2.3 Dial Indicator with magnetic base (Plunger type)

For measurement of edge effect, it is required to measure bend angles at different locations including the edges along the width (laser scan direction). For this purpose a dial indicator (Make: Mitutoyo; Model: 2109S) has been used. The touch probe can be moved along *x*, *y*, and *z*-axis for collecting the data points on either side of scan line. Figure 3.3(a) shows a photograph of dial indicator while its specifications are listed in Appendix C. As shown in Figure 3.3 (b), the data points are recorded for the value of L_{12}, L_{34}, d_{12} and d_{34}. The bend angle was computed for any of the positions as

$$\alpha = \alpha_1 + \alpha_2 = \tan^{-1}\left(\frac{d_1 - d_2}{L_{12}}\right) + \tan^{-1}\left(\frac{d_4 - d_3}{L_{34}}\right) \tag{3.1}$$

(a)

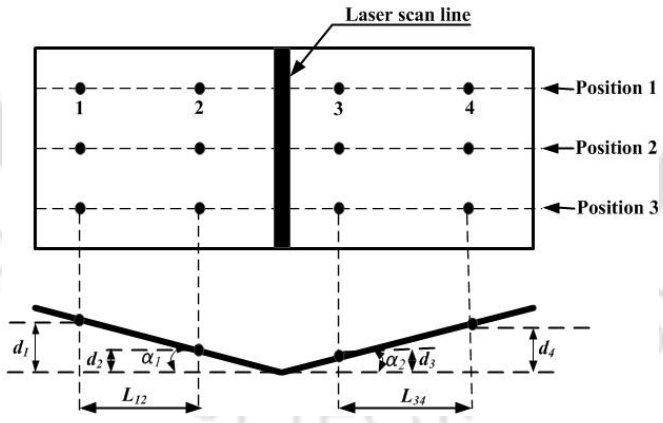

(b)

Figure 3.3 Measurement by dial indicator: **(a)** Dial indicator (Plunger type with magnetic base) and **(b)** a schematic of bend angle measurement

3.2.4 Sample preparation

To carry out the laser bending operations, samples were first cut into required dimension. Sample sizes were different for different experiments. The workpiece surfaces were cleaned by acetone to remove wax, oil or dusts. Before the laser

irradiation, the laser path on the metal surface was coated with black spray paint. After coating, the samples were dried for one day.

3.3 Studies on Mechanical Properties of Workpiece

The tensile and Charpy impact tests were carried out on raw and straightened strips. In each scheme of straightening as depicted in chapter 6, the best straightened samples were chosen. The results of the ultimate tensile strength (UTS) and the maximum percentage elongation and Charpy impact values are reported in Chapter 6.

The maximum elongation in the tensile test and impact energy in Charpy test provide an idea about the ductility. Tensile tests were carried out in an INSTRON 8801 machine (100 kN capacity) at room temperature with a constant cross-head speed of 1 mm/min. The strain rate was lesser than 1×10^{-3} s^{-1}. Charpy test was carried out with guidelines provided by ASTM E23-16b standard.

3.3.1 Universal testing machine (UTM)

In order to measure the mechanical properties of parent materials (AH36), uniaxial tensile tests were carried out according to ASTM E8M standard. All the samples were tested at room temperature in universal testing machine (UTM) (Make: INSTRON, Model: 8801J4051) as shown in Figure 3.4. Three replicates were used in each case. The average properties were taken for analysis. The load extension data from the machine was converted into engineering stress-strain behavior and the mechanical properties such as yield strength, ultimate tensile strength and total elongation were evaluated for mild steel (AH36). The important specifications of the UTM are given in Appendix D.

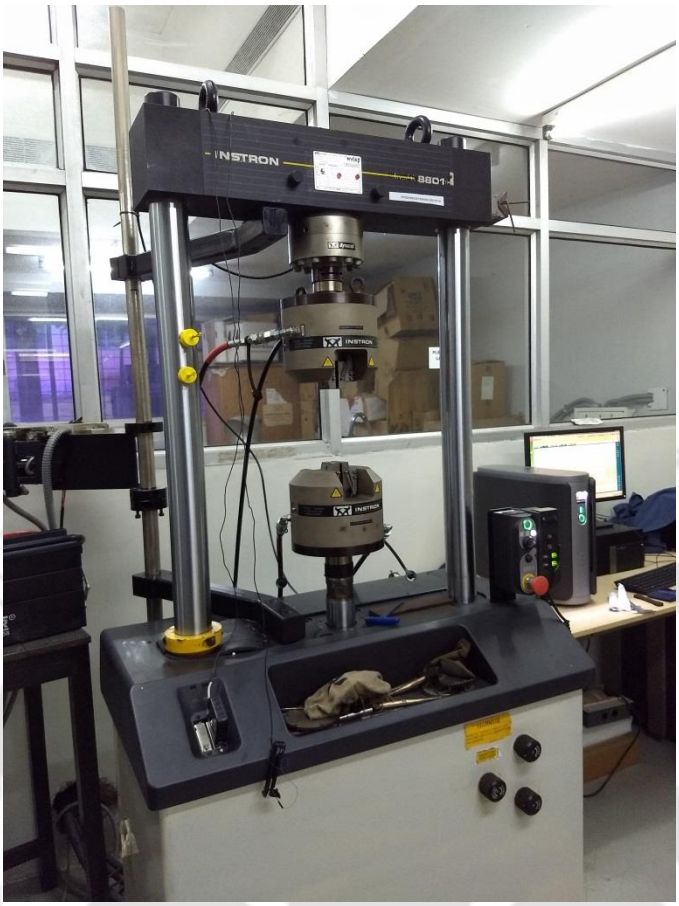

Figure 3.4 Universal testing machines for tensile test

3.3.2 Impact testing machine

Charpy test was carried out with guidelines provided by ASTM E23-16b standard on Impact Tester, make: FUEL INSTRUMENT AND ENGINEERING PVT. LTD. The Pendulum is mounted on antifriction bearings. The impact wedge has two positions to keep for releasing for impact, the upper one for Charpy. On release of the pendulum it swings down to brake the specimen and the energy absorbed in doing so is measured as the difference between the heights of drop before rupture of the test specimen and is read from the maximum pointer position on the dial scale. The Charpy test piece rests on alloy steel support anvils, fitted on the base of the machine rigidly held in position by Allen screws. End stopper is provided for quickly and accurately locating the test piece centrally between the supports. Figure 3.5 shows the Impact Tester, IT-30. The important specifications of the impact testing machine are given in Appendix E.

Figure 3.5 Impact testing machine

3.4 Study on Metallographic Sample Preparation and Examination

Figure 3.6 shows the basic steps followed for the preparation of samples for finding microstructure and microhardness. Different instruments were used in the whole operation (metallographic sample preparation and examination). They are explained in the following subsections. The detailed results for microhardness and microstructure have been discussed in Chapter 6 and Chapter 7.

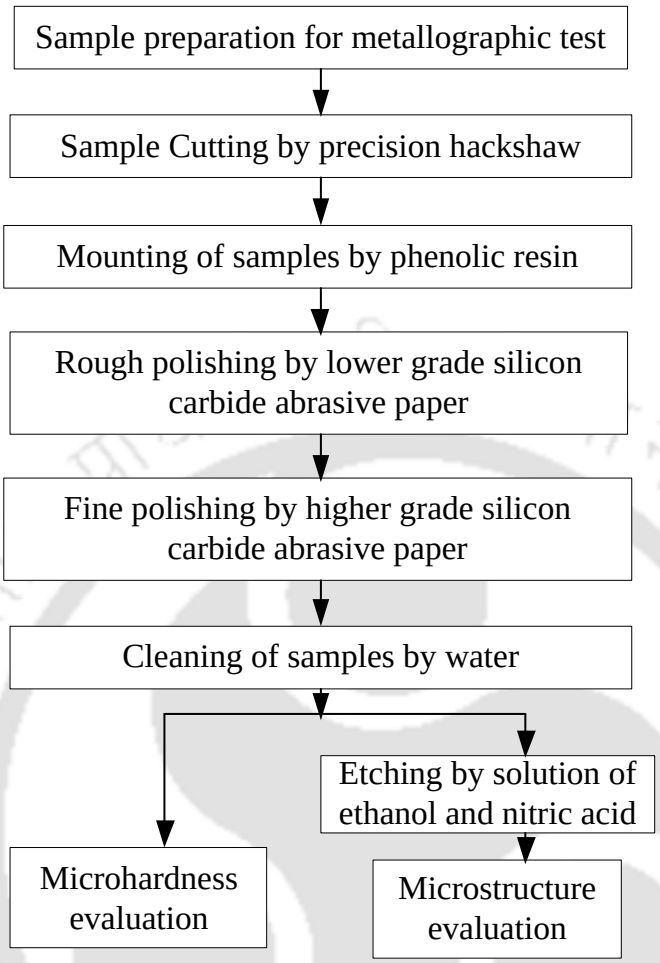

Figure 3.6 Basic steps for microhardness and microstructure evaluation

3.4.1 Precision saw

Precision cutting saw has been used for precise and deformation-free cutting. Figure 3.7 shows precision hacksaw that generates less heat with less cutting time due to integrated flood coolant delivery system from both sides of the blade. It produces very less depth of damage with minimum material loss. All the samples have been cut in precision hacksaw (Make: BUEHLER; Model: Isomet® 4000) for microstructure and microhardness study.

Figure 3.7 Precision saw

3.4.2 Sample molding press machine

After cutting of the specimen, sample mounting has to be done. The purpose is to handle samples and to protect properly. Mounting facilitates specimens easier to handle for further process. Figure 3.8 shows the molding machine where phenolic plastic based encapsulation for the sample was created by using proper heat and pressure in the mounting press. All samples for microstructure and microhardness were prepared by this molding press machine accordingly (Make: BUEHLER; Model: Simpliment® 2).

Figure 3.8 Molding machine

3.4.3 Polishing machine

All samples for microhardness and microstructure evaluation were polished by using double disc polishing machine (Make: B.S. Pyrometic India (P) LTD.); (Model: BSPIL–MET–01008A) (8A)) as shown in Figure 3.9. It has smooth speed variation of the grinding wheel with soft start and stop. Polishing machine was used to avoid surface effect in microhardness and microstructure testing. The sample holder was held by operator and desired grinding depth was also managed by operator manually. All samples were polished by silicon carbide abrasive paper having 400–2000 grit size (35±1.5 micron to 10.3±0.8 micron) sequentially and were finally polished on velvet cloth using MicroPolish alumina particles of size 1 μm.

Figure 3.9 Double disc polishing machine

3.4.4 Optical microscope

After polishing and etching, samples were inspected using an optical microscope (Make: Carl ZEISS; Model: Axiotech-100HD) as shown in Figure 3.10. The samples were carefully examined at different magnifications, *viz.*, 5×, 10×, 20×, 50×, and 100×. The laser irradiated and base regions are mainly focused for relevant metallographic. For finding out the grain size, the image analysis method using AxioVision SE64 Rel.4.9.1 software and the line intercept methods were used. The average sizes of grain have been reported. The specification of the microscope is given in Appendix F.

Figure 3.10 Optical microscope

3.4.5 Scanning Electron Microscopy (SEM)

Scanning electron microscopy (SEM) has been employed for high-resolution imaging of surfaces to achieve higher magnification and greater depth of field than that attainable by optical microscopy. The SEM setup used is, Model : Jeol JSM 6390 LV and make: Jeol. The electrons interact with atoms of the specimens to produce various signals. Such signals contain information about the surface topography, morphology and compositions. Figure 3.11 represents photograph of Scanning electron microscope. The specifications of the microscope are given in Appendix G.

Figure 3.11 Scanning electron microscope

3.4.6 Microhardness testing

To measure hardness of laser irradiated sample (both bent and straightened sample) and base material, Microhardness test has been performed. Figure 3.12 shows the microhardness tester (Make: BUEHLER; Model: Micromet-2101 with diamond indenter) used for this work. In the microhardness testing machine, the loads of 1, 10, 50, 100, 300, 500 and 2000 gf can be applied smoothly (without impact), forcing the indenter into the test workpiece by using different indentation time. The proper indentation force varies from material to material. The microhardness is measured at three positions along and across thickness direction by using 500 gf for mild steel specimens. Microhardness tester specifications are listed in Appendix H.

Figure 3.12 Microhardness tester

3.4.7 Electric high temperature furnaces

To produce stress relieved and sub-critically annealed specimens, systematic heat treatments were performed. Figure 3.13 shows the Electric high temperature furnace (Meta Therm TTC, SL no. 887 and rating 18kW) with maximum achievable temperature of 1400°C. One group of 27 specimens of AH36 steel was kept in furnace at 500 °C for one hour and then cooled in air for stress relieving. Another group of AH36 steel was kept in furnace at 700 °C for one hour and was furnace cooled for 24 hours. This caused subcritical annealing of the specimens. Further details are provided in Chapter 6.

Figure 3.13 Electric high temperature furnaces (Meta Therm TTC)

3.5 FEM Modeling of Laser Bending and straightening

For simulation purpose, FEM package ABAQUS® was used to model the laser bending and straightening process. 3D coupled thermo-mechanical analysis has been used. In the modelling process, the modules are as follows:

- Part module: For generating a part, the part module tools are used. For laser bending and straightening process, relevant 3D parts were created.
- Property module: In this module relevant temperature dependent material properties have been assigned.
- Assembly module: Assembly module placed the part in a global coordinate system.
- Step module: Fixed time step increments were chosen in this module. It is required for coupled temperature-displacement analysis.
- Interaction module: For laser bending process, type of interaction like surface to surface contact interaction was selected. A film condition

interaction property was defined with film coefficient as a function of temperature and field variables.

- Load module: In this module load and type, boundary condition, and predefined field to view and manipulate the stepwise history of prescribed conditions have been implemented. It can also use the step list located in the context bar to specify the steps in which new loads, boundary conditions, and predefined fields become active by default for the system. To specify time dependencies, amplitude toolset in the load module was used. For laser bending and straightening process, thermal load was applied in the form of heat flux assuming laser beam to be circular with Gaussian distribution of heat flux.
- Mesh module: For mesh generation the mesh module has been used. It contains variety of tools that allow specifying different mesh characteristics, such as mesh density, element shape and element type. To divide geometric regions into smaller regions required for assigning different mesh sizes (fine and coarse), the partition toolset was used. The workpiece was discretized with three-dimensional linear hexahedron eight-node elements (C3D8T). The heated region due to laser irradiation was discretized with fine mesh while coarse mesh was used in other regions to minimize the simulation time. Various details of the mesh sensitivity analysis are given in Section 3.5.3.
- Job module: After finishing all of the tasks involved in defining a model it was submitted for analysis. After the analysis, temperature, stress-strain, bend angle, edge effects were recorded.

Due to nonlinear nature of the process, it is required to consider certain assumptions. The following assumptions were considered in the simulation:

1. The material is isotropic.
2. The CO_2 laser has Gaussian distribution of heat flux inside the spot diameter.
3. The material yields as per von Mises criterion (suitable for ductile materials).
4. The workpiece is flat, weight-less and free of residual stresses.
5. Heat transfer is only through conduction and convention. The radiation transfer is very small and negligible.

3.5.1 Thermal and mechanical properties of the materials

The thermo-mechanical analysis requires temperature-dependent mechanical and thermal properties of the materials. Due to temperature dependent property they vary with change in temperature during the process. These values plays important role in result of the simulation process.The temperature dependent material properties of mild steel were taken from Zhang et al. (2004).

3.5.2 Thermal and mechanical analysis

Since the process is a thermomechanical process, both thermal and mechanical aspect of the process have to be considered. Thermal stresses developed due to heat flux model act on the vicinity of laser scan line. The thermal stress generated which in turn work as load for mechanical deformation. Heat flux model and boundary conditions are discussed in detail. Basically this numerical simulation has been accomplished with three-dimensional thermo-mechanical analysis.

A) Heat flux model

The laser beam was assumed to be circular in shape and exhibit Gaussian distribution of heat flux. By varying the standoff distance between the tip of the nozzle and the top surface of the workpiece, the beam diameter was controlled. The laser beam radius r was calculated as reported (Sun, 1998)

$$r = w_0 \left\{ 1 + \left(\frac{M^2 \lambda H}{\pi w_0^2} \right)^2 \right\}^{1/2}, \tag{3.2}$$

$$w_0 = \frac{2M^2 f \lambda}{\pi D_L}, \tag{3.3}$$

where w_o is the laser beam waist, M^2 is a beam quality factor. For perfect Gaussian beam, M^2 is 1, but in actual practice M^2 is more than 1; here M^2 = 1.4. H is standoff distance, λ is the wave length (10.6 μm for CO_2 laser), f is the focal length (127 mm for the machine used), D_L is laser beam diameter before lens (24 mm for all experiments). During the simulation, thermal load was given in the form of heat flux that obeys the normal Gaussian distribution given by

$$q(x,y)=\frac{2\eta P}{\pi r^2}\exp\left\{-2\frac{\left(x^2+y^2\right)}{r^2}\right\}, \tag{3.4}$$

where q is the heat flux density of laser beam, η is the absorptivity of the sheet material, P is the power of the laser and r is the radius of the laser beam.

B) Boundary conditions

To avoid the rigid body movement, clamped side of the workpiece was fully constrained in mechanical analysis (zero displacement and rotation). All the other sides were free from mechanical boundary condition in the case of laser bending; however, for laser assisted bending with permanent magnet the mechanical load of 5.5 N was applied on the free side. The magnetic force was determined experimentally by Fetene (2018). In case of electromagnet, as discussed in section 7.2.2, magnetic force of attraction was measured and equivalent load has been applied on magnet end side. After the laser beam irradiation, the sheet metal was cooled down in the air. Heat convection took place between the sheet metal and the surroundings. Convective heat transfer occurred between the workpiece and the surroundings after the laser beam irradiation. The convection boundary conditions can be expressed by Newton's law of cooling as

$$q=h\left(T_s-T_a\right), \tag{3.5}$$

where q is the heat flux, h is the heat transfer coefficient, taken as 10 W/m^2.°C during the heating time. T_s is the specimen surface temperature and T_a is the ambient temperature (25 °C).

3.5.3 Mesh sensitivity and time increment analysis

Numerical simulation of laser bending process has been carried out to determine bend angle, and edge effect. A sequential thermo-mechanical process was conducted to simulate the laser assisted bending process by developing a moving heat source along scanning line. The laser scan was conducted at the middle along the length of the workpiece. Appropriate mesh refinement and time-increment is essential for obtaining the accurate results within rational computational time. Zhang

et al. (2004) used a 20-node brick element and also suggested 4 elements in a beam diameter and 3 elements in thickness direction as suitable for the better result. The mesh size depends upon the size of workpiece thickness and laser beam diameter. Mesh refinement was carried out accordingly.

Preliminary simulation results show that simulation time increased as the laser power increased due to increase in temperature at high power which causes high thermal gradient. Zhang et al. (2004) reported that temporal discretization requires at least four time increments per radius. The scan speed was chosen during experimental work as in a manner that the time increment should be less than $t_1/4$. Where t_1 is the duration of laser beam irradiation equal to the ratio of laser beam diameter to scan speed. Hence simulations were carried out with time-increments of 0.01 and 0.005 second and it was observed that at these two conditions, almost the same predictions were obtained. Hence, 0.01 second time-increment was selected as appropriate.

FEM simulations were carried out with eight-node thermally coupled brick element (C3D8T) using ABAQUS package. The entire domain was divided in three regions. In each region, the mesh size was uniform. The mesh was the finest in the region containing the laser irradiation path. Region between laser irradiated line and free side also region from fixed end to laser irradiated line were made of larger elements. Fine mesh size was used in the laser irradiated zone and coarse biased mesh was used at rest of the places. Fetene et al. (2017) observed that during laser assisted bending; mostly the deformation took place between the scan line and point of the application of the load. The zone between the clamped side and laser irradiated zone, the mesh sensitivity was low and it was considered few divisions along the length in this zone as good enough. A relatively finer mesh was used in the zone between laser scan line and free edge. As a compromise between computational time and accuracy, the mesh sizes were selected in a suitable manner. Mesh sensitivity was performed in a systematic manner for laser bending, laser assisted bending by electromagnetic force and laser assisted straightening by permanent magnetic force as follows.

A) Mesh sensitivity for laser bending

For laser bending 60 mm × 40 mm × 2 mm workpiece size was used. As shown in Figure 3.14 the meshing has been made in a systematic manner. For specimen of dimension 60 mm×40 mm× 2 mm, three clear divisions can be observed as explained previously. The laser irradiated region has been meshed with fine element while the other two regions are meshed with coarse element. Table 3.1 shows that in case of laser irradiated region element size of 0.5 × 0.5 × 0.5 are suitable considering accuracy in result and computational time. While region along clamp has 2 element and region along free end has 4 elements as shown. The results for this simulation have been discussed in chapter 4.

Table 3.1 Effect of fine mesh element size on bend angle for laser power of 900 W and scan speed of 800 mm/min

Element size in refined zone (mm^3)	Bend angle (Degree)	Screen time (s)
2 × 2 × 0.5	4.17°	2124
1 × 1 × 0.5	7.42°	5011
0.5 × 1 × 0.5	11.71°	8019
0.5 × 0.5 × 0.5	14.8°	14437
0.25 × 0.25 × 0.25	15.09°	25121

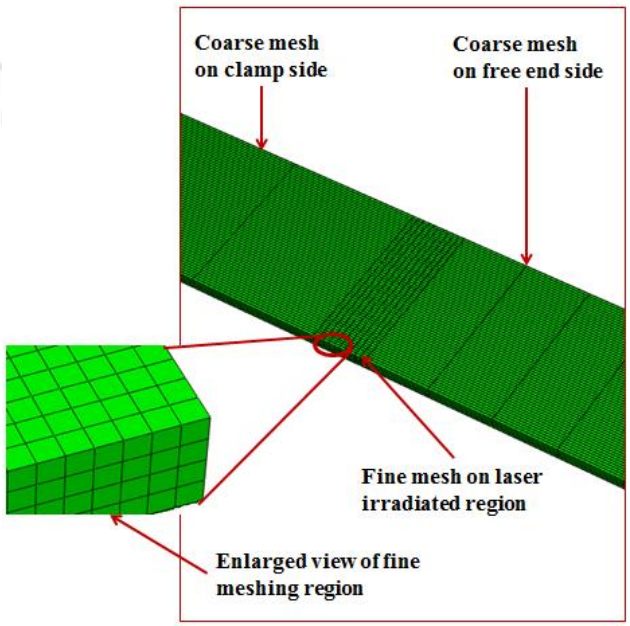

Figure 3.14 Coarse and fine meshing for this simulation in laser bending

B) Mesh sensitivity for laser assisted bending

For laser assisted bending 100 mm × 30 mm × 2 mm workpiece size was used. As shown in Figure 3.15 in the zone between the clamped side and laser irradiated zone, the mesh sensitivity was low and it was considered sufficient to have 4 divisions along the length. A relatively finer mesh was used in the zone between laser scan line and free edge and was decided to use 8 divisions along length in this zone. Table 3.3 presents the scheme for selection of proper element size in refined zone. It was observed that accuracy of the predicted bend angle increases with refined element size and high computational time. As shown in Table 3.3 as a compromise between computational time and accuracy, an element size 0.5 mm × 0.5 mm × 0.5 mm was found appropriate. The results for this simulation have been discussed in Chapter 7.

Table 3.2 Effect of element size on bend angle for laser power of 900 W, laser beam diameter 3.87 mm, scan speed 800 mm/min and current 5A

Element size in refined zone (mm^3)	Bend angle (Degree)	Screen time (s)
2 × 2 × 0.5	2.43	5317
1 × 1 × 0.5	3.67	7441
0.5 × 1 × 0.5	4.03	15376
0.5 ×0.5 ×0.5	4.68	22567
0.25 × 0.25 × 0.5	4.71	37796

C) Mesh sensitivity for laser assisted straightening

For laser assisted straighten 100 mm × 30 mm × 2 mm workpiece size was used. As shown in Table 3.3, considering computational time and accuracy, an element size of 0.5 mm × 0.5 mm × 0.5 mm was taken in the heated region. On the magnet side, a coarse biased mesh comprising 20 elements was used. On the clamping side, mesh consisted of 5 elements. The largest element in the biased mesh was 5 times bigger than the smallest element in length direction. The size was same throughout the strip in the thickness and width directions. Figure 3.16 shows the coarse and fine meshing for this simulation. The results for this simulation have been discussed in chapter 6.

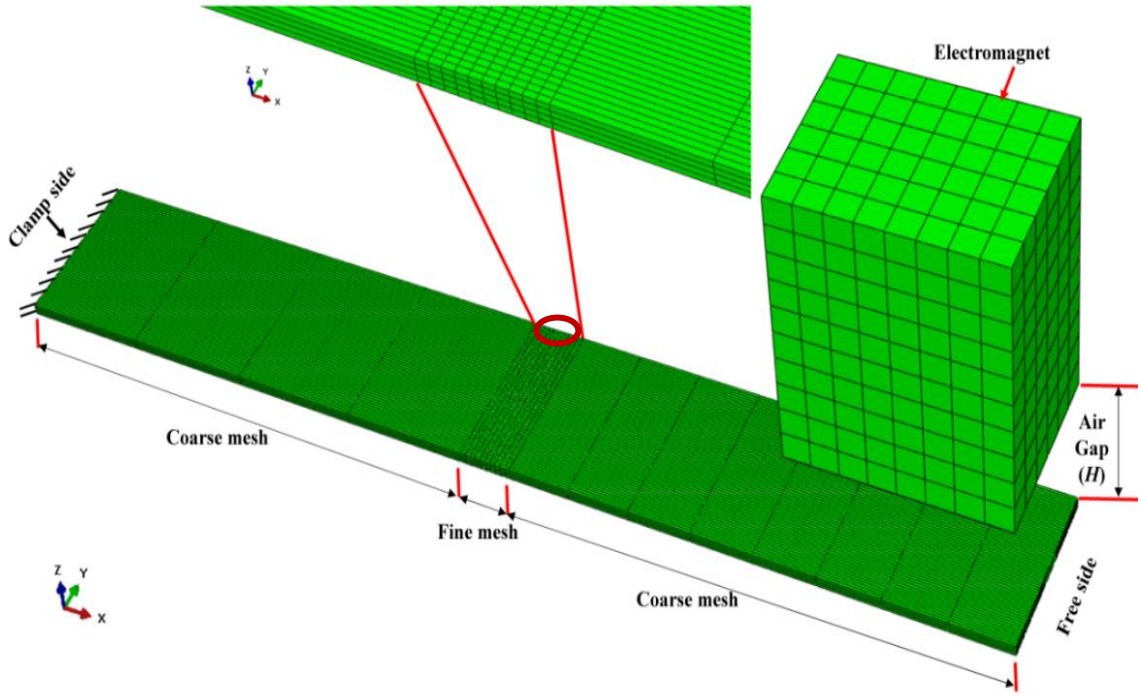

Figure 3.15 FEM simulations with coarse and fine meshing for the simulation and magnified view

Table 3.3 Effect of fine mesh element size on bend angle for laser power of 1000 W and scan speed of 800 mm/min

Element size in refined zone (mm^3)	Bend angle (Degree)	Screen time (s)
2 × 2 × 0.5	0.67°	6105
1 × 1 × 0.5	0.72°	8020
0.5 × 1 × 0.5	13.3°	16906
0.5 × 0.5 × 0.5	12.8°	25460
0.25 × 0.25 × 0.25	13.0°	40906

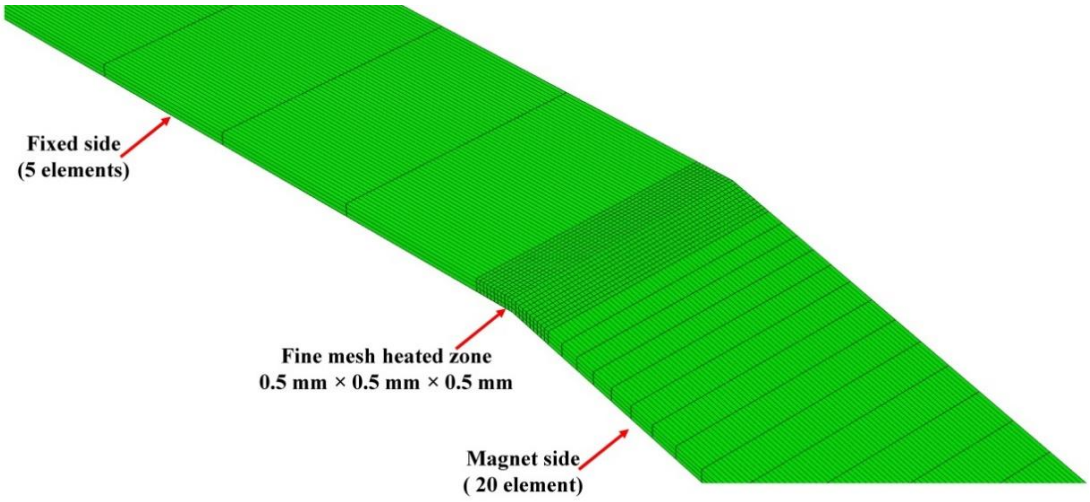

Figure 3.16 Coarse and fine meshing for this simulation in laser assisted straightening by permanent magnet

In mechanical analysis, necessary constraints are added according to the experimental fixture used in real experiments. The boundary conditions are zero translation and rotation at one side of the work specimen, which is fully constrained. The thermal load was given in the form of heat flux generated by the laser beam. It was applied only on the top surface of the sheet metal

3.6 Conclusion

This chapter explains the details of planning regarding experiments and simulations. The following point may be summarized.

- The experimental setup, use of different machines and instruments, types of work material and sizes of workpiece has been explained.
- The commercial FEM package ABAQUS® was used to model the laser bending process.
- Numerical simulation of the laser bending process was accomplished using the 3D non-linear coupled thermo-mechanical analysis.
- Heat flux of Gaussian distribution was applied on the workpiece surface.
- The temperature-dependent material properties were used.

- Mesh sensitivity analysis was carried out for precise prediction in a rational time.
- The screen time is reported, which is also not much different from CPU time in this case.

Chapter 4

Enhancing the Efficiency of Laser Bending of Mild Steel by Coating with Black Enamel Paint

4.1 Introduction

In this work, a series of experiments was performed to get a better insight about the process and process parameters. The main objective of this work was to enhance the bend angle produced due to laser bending. The laser irradiated surface was coated with black enamel paint. A commercially available black spray paint (EZMatch, Aerosol paint black.) was used on the workpiece surface before subjecting to laser irradiation. The black spray paint is three times cheaper as compared to commonly used graphite spray. It can be applied easily to workpiece surface and also dries quickly. Thereafter effect of laser power, number of scan, scanning velocity was discussed. The black spray paint gave the advantages of rapid increase in bend angle due to high absorption. A comparative study on bend angle was carried out considering three different way of specimen preparation. Multi pass laser irradiation was performed for coating applied once (CAO), coating applied after each pass (CAAP) and without coating (WC) specimens. Considering two levels of laser power and two levels of scan speed, experiments were conducted as low power low speed, low power high speed, high power low speed and high power high speed combinations respectively.

4.2 Experimental Plan

The CO_2 laser cutting machine used in this work was Orion 3015, 2.5 kW industrial LVD-make CNC operated machine which is used for all operations (Figure 3.1). The material of work piece was AH36 steel. The specimens were cut into standard size of 60 mm × 40 mm × 2 mm dimension. Before the laser

irradiation, the laser path on the metal surface was coated with black spray paint. The average thickness of coating was 26 micron. The thickness was measured with an optical microscope. The sheet metal samples were fixed as cantilevers. Then the samples are subjected to the maximum of 10 passes in selected cases. After completing the laser scanning of the specimens the deformations obtained by the laser irradiation were measured using an optical profile projector (Figure 3.2). FEM simulation was conducted to make a comparison with the experimental work. All details about FEM simulation were discussed in Section 3.5.3.

4.3 Results and Discussion

Laser bending of mild steel (AH36) was conducted with different sets of laser power, scanning speed, coating strategies and number of laser passes. Three types of coating strategy were applied. In the first type, the sheet was left uncoated. In the second case, the sheet was coated once along the laser scanning path and in the third type, it was coated after every pass. Four cases of experiments have been conducted. The four cases are termed as high power-low speed (1000 W, 900 mm/min), high power-high speed (1000 W, 1300 mm/min), low power-high speed (500 W, 1300 mm/min) and low power-low speed (500 W, 900 mm/min). The entire procedure with four cases was described in the following subsections. Total 120 specimens were taken and further divided into group of 30 specimens each for the four cases as mentioned. Mild steel plate of dimension 60 mm × 40 mm × 2 mm are considered in all cases. Each sample was subjected to different number of laser passes. First sample was subjected to one pass, second sample to two passes, and third sample to three passes and so on. The process was continued till ten passes on tenth sample. This process was repeated for CAO, CAAP and WC samples.

4.3.1 High laser power and low scan speed (Case 1)

The specimens were subjected to laser irradiation with to a power of 1000 W and scan speed of 900 mm/min. Laser irradiation was performed upto maximum of 10 passes and bend angle after each pass was measured carefully. All three types of samples with or without coating were taken for laser bending. The observations are as follows.

Effect of number of pass: As shown in Figure 4.1 with increase in number of pass bend angle is also increasing though it is not following a linear pattern. For CAO and CAAP specimens close bend angle produced upto 5^{th} pass having maximum variation of 0.65°. Thereafter the bend angle in both the cases varied. CAPP specimen generates higher bend angle then CAO specimen after 10^{th} pass. To obtain a desired value of bend angle the number of laser pass can be calculated from average bend angle per pass from experimental results keeping power and speed constant.

Effect of coating: Figure 4.1 shows a rapid increase in bend angle with application of black spray paint due to the fact that it increases surface absorptivity, keep the surface safe at high power and make the process more efficient. The final angle for WC, CAO and CAAP specimens are 2.90°, 14.01° and 17.79°, respectively after 10 passes. Hence by applying proper coating strategies desired bend angle can be obtained even with low power to make the process efficient and cost effective.

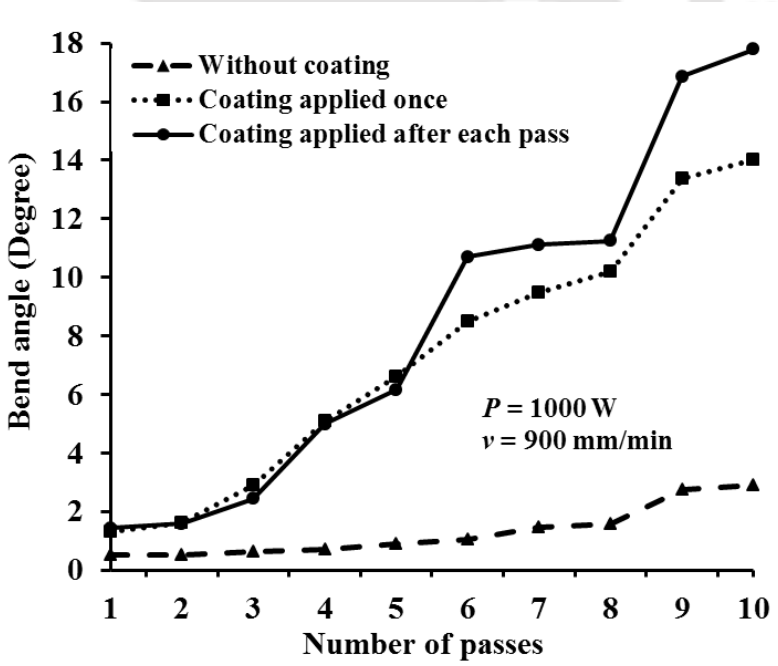

Figure 4.1 Variation of bend angle with number of passes for high power-low speed (1000W, 900 mm/min)

4.3.2 High laser power and high scan speed (Case 2)

The specimens are subjected laser irradiation with to a power of 1000 W and scan speed of 1300 mm/min. Laser irradiation was performed upto the maximum of 10 passes and bend angle after each pass was measured carefully. All three types of samples with or without coating were taken for laser bending. The observations are as follows.

Effect of number of pass: As shown in Figure 4.2 with increase of number of pass bend angle also increases. It can be observed that upto 5th pass bend angle in case of coated once and coated after each pass remain similar. The differences between the two are 0.49°.

Effect of coating: Results shows a rapid increase in bend angle with application of black spray paint due to the fact that it increases surface absorptivity. It can be observed that after 5th pass coating applied after each pass specimen become dominant. The final angle for WC, CAO and CAAP specimens are 1.37°, 23.29° and 25.13°, respectively after 10 passes. A significant increase of 21.92° was observed for CAO specimen over WC specimen after 10th pass.

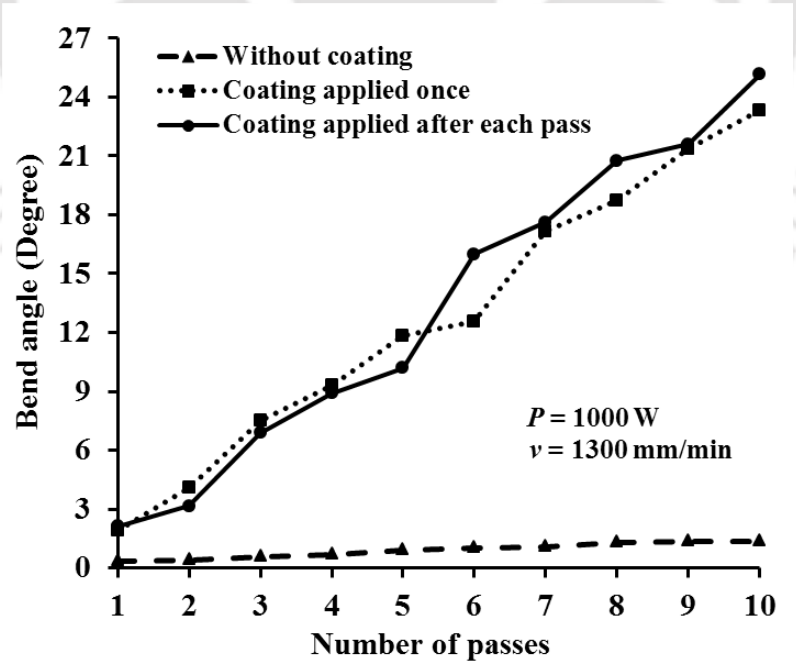

Figure 4.2 Variation of bend angle with number of passes for high power-high speed (1000 W, 1300 mm/min)

4.3.3 Low laser power and high scan speed (Case 3)

The specimens are subjected to laser irradiation with a power of 500 W and scan speed of 1300 mm/min. Laser irradiation was performed upto maximum of 10 passes and bend angle after each pass was measured carefully. All three types of samples with or without coating were taken for laser bending. The observations are as follows.

***Effect of number of pass*:** As shown in the Figure 4.3 with the increase of number of pass bend angle also increases in a non-liner trend. It can be observed that upto 4th pass bend angle in case of coated once and coated after each pass remain similar. The differences between the two are 0.46°. But after that variation in bend angle occurs.

***Effect of coating*:** Results show a rapid increase in bend angle with application of black spray paint in case of samples coated after each pass due increases surface absorptivity. The difference between bend angle in coated and uncoated samples shows a difference of about 6.70°– 8.9°. The final angle for uncoated, coated once and coated after each pass samples are 0°, 6.7° and 8.9°, respectively after 10th pass.

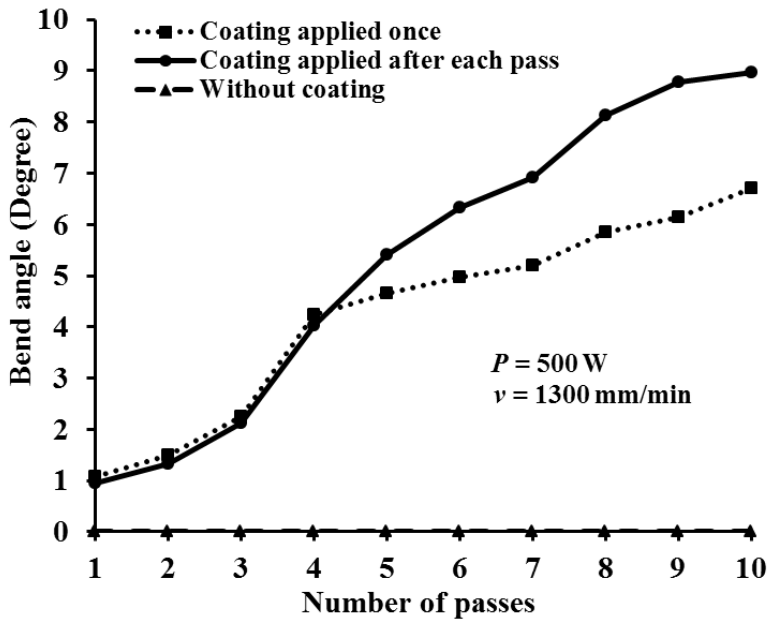

Figure 4.3 Variation of bend angle with number of passes for low power-high speed (500W, 1300 mm/min)

4.3.4 Low laser power and low scan speed (case 4)

The specimens are subjected laser irradiation with to a power of 500 W and scan speed of 900 mm/min. Laser irradiation was performed upto the maximum of 10 passes and bend angle after each pass were measured carefully. All three types of samples with or without coating were taken for laser bending. The observations are as follows.

Effect of number of pass: As shown in Figure 4.4 with the increase of number of pass bend angle is also increasing though it is not following a non-linear pattern. It can be observed that upto 2nd pass bend angle in case of coated once and coated after each pass remain similar. The difference in bend angle between CAO and CAAP is 0.43° after 2nd pass. But after that the variation in bend angle occurs.

Effect of coating: Results show a rapid increase in bend angle with application of black spray paint in case of samples coated after each pass due to increase in surface absorptivity. The final angle for uncoated, coated once and coated after each pass samples are 1.07°, 20.05° and 20.65° respectively after 10 passes. Therefore by applying proper coating strategies desired bend angle can be obtained even at low power to make the process efficient and cost effective.

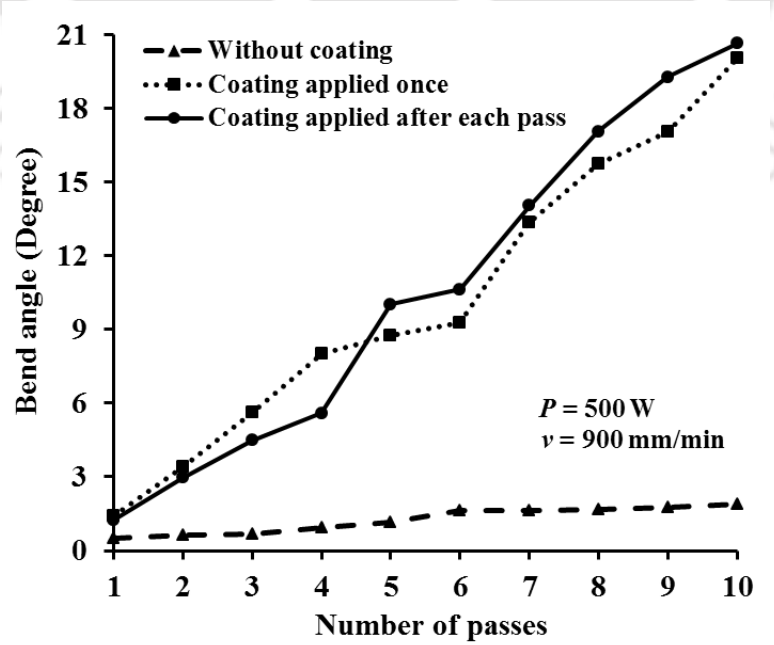

Figure 4.4 Variation of bend angle with number of passes for low power-low speed (500 W, 900 mm/min)

4.4 Comparative study on the effect of coating for all cases

It can be observed that after the maximum of four passes the bend angle is higher in CAO specimens compared to CAAP specimens as shown in Figure 4.5 (a). This is due to an increase in temperature during continuous laser passes that leads to increase in bend angle produced. However, after 4th pass, the CAAP specimen produced higher angle. This was due to increase in continuous passes removed the black spray coating partially resulting in decrease in surface absorptivity to laser. Finally the bend angle produced decreased in CAO specimens. Figure 4.5 (b) shows that after 4th pass CAAP specimen results higher bend angle than CAO specimen upto 10th pass in all four cases.

In all the cases laser scan speed also played a significant role. For all the cases, with increase in laser scan speed the bend angle decreased and with decrease in scan speed bend angle increased. To achieve higher bend angle scan speed should be reduced. However, scan speed should be selected in a judicious manner. Too high scan speed might not produce any deformation and too low scan speed might melt the workpiece surface.

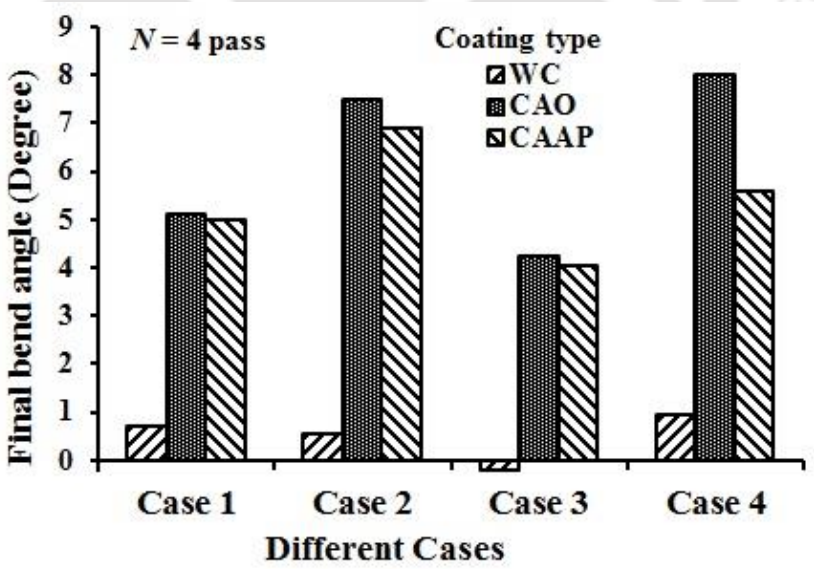

(a)

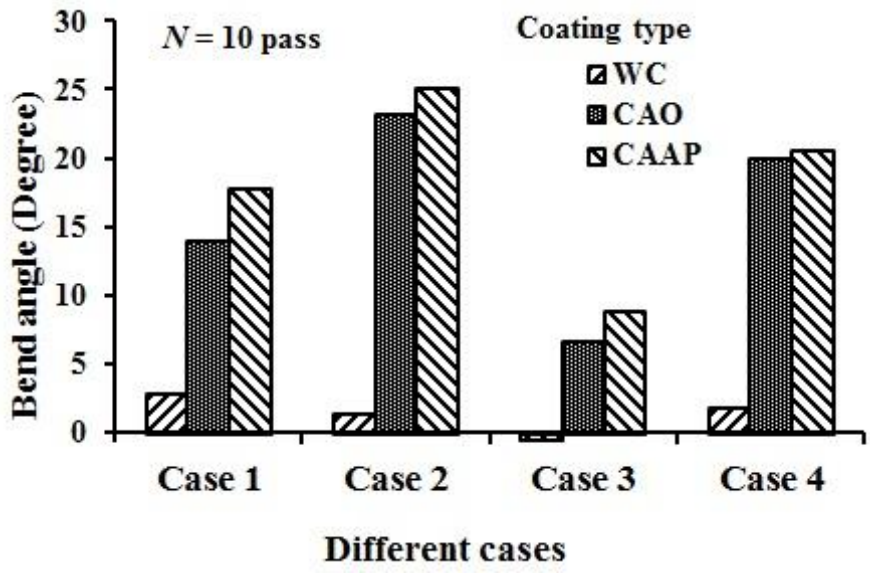

(b)

Figure 4.5 Effect of coating for different scheme (a) after 4 passes and (b) after 10 passes

4.5 Comparison of experimental results with FEM results

FEM simulations were performed for selected cases for AH36 steel used in experiment. As change in absorptivity was unpredictable in case of multipass operation with coating, only specimens without coating were considered for simulation. The temperature dependent thermo-mechanical properties of material were taken from Zhang et al. (2004). The simulation results for bend angle and comparison with experimental can be seen in Figure 4.6, Figure 4.7 and Figure 4.8. The comparison shows a similar increase in bend angle along with number of laser pass for all passes upto 10. Figure 4.6 shows similarities between experimental and simulation results as similar at beginning and then little variation but finally come closer. The maximum variation was 21.29%. Similarly in Figure 4.7 and Figure 4.8 similarities between experimental and simulation can be seen with 19.47% and 14.12% maximum variation on bend angle result. Low power and high speed (500W, 1300 mm/min) scheme was not presented as due to low power and high speed no bend angle occurred.

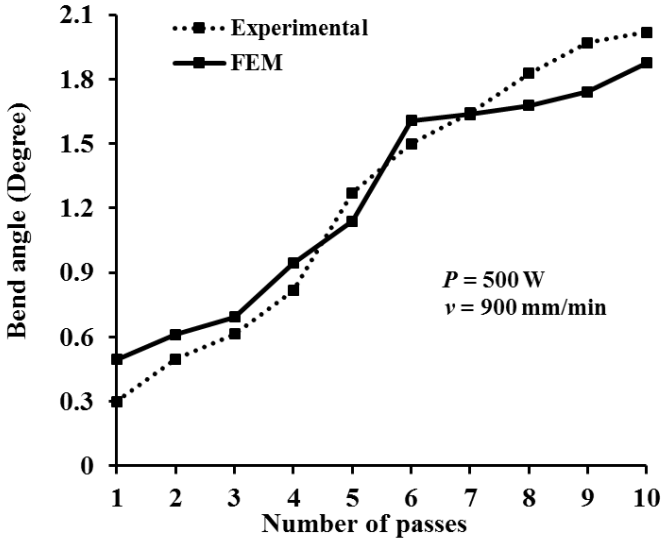

Figure 4.6 Comparison of experimental result for bend angle with FEM simulation results for low power and low speed (500 W, 900 mm/min)

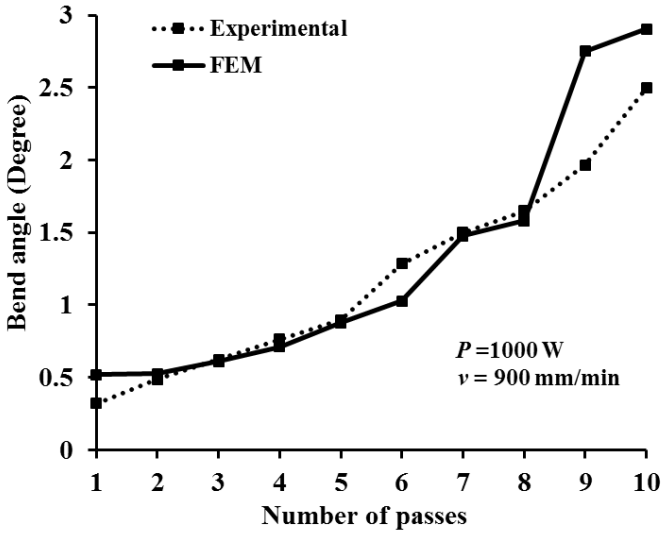

Figure 4.7 Comparison of experimental result for bend angle with FEM simulation results for high power and low speed (1000 W, 900 mm/min)

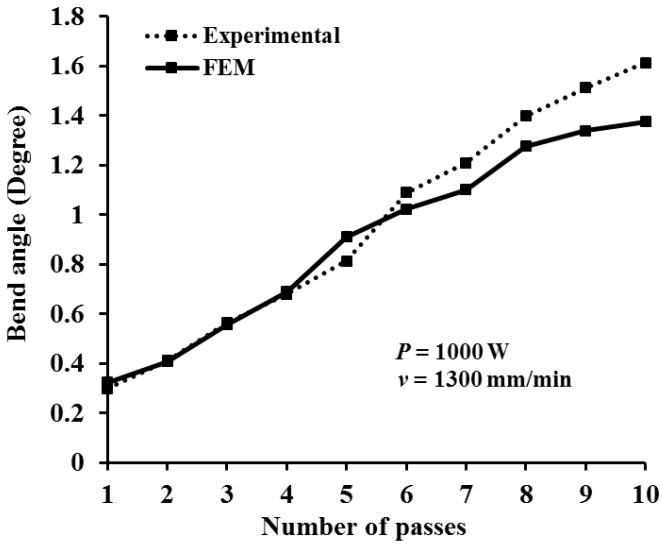

Figure 4.8 Comparison of experimental result for bend angle with FEM simulation results for high power and low speed (1000 W, 1300 mm/min)

4.6 Conclusion

This work presents a preliminary study on selection of proper coating scheme using commercially available Aerosol Paint Black coating for enhancing the bend angle produced. Following findings may be presented from this work:

- It is observed that the coating improves the performance of the laser bending significantly and thus power can be saved by applying coating on the surface of the workpiece.
- It is also noted that the coating can be applied only once in the beginning of the bending processes as there is no significant difference in bend angle for CAAP upto 4^{th} pass. Thereafter CAAP specimen produced higher bend angle. Applying coating after each pass gives best results. Nevertheless, CAAP took much more time comparison to CAO.
- It was observed that only in case of low power-high speed case, the application of coating after each pass produces significantly higher bend angle compared to other cases. Hence it can be summarized that CAAP is the best case in terms of results but CAO may be the best choice considering all aspect as it saves time considerably. The FEM results show good agreement with the experimental results.

Chapter 5

A Strategy for Achieving Accurate Bending by Multipass Laser Line Heating

5.1 Introduction

Laser bending is a process of bending a job by irradiating with a laser beam followed by cooling. After cooling, residual stresses remain in the job and it gets bent. Usually, the laser beam moves over the bend line with an appropriate scan speed. The process has drawn the attention of the researchers due to certain edge over the conventional bending. It can be used to achieve very small bend angle. The possibility of producing complex geometries and rapid prototyping also make the process popular to the forming industries. It is a non-contact process and final bend angle is achieved by adjusting the laser process parameters. Hence, there is no issue of spring-back. The major difficulty in the application of laser bending is the poor predictability of the process. In an excellent review paper on the modelling of laser forming, Shen and Vollertsen (2009) observed that the best model till date had the model prediction error more than 20%. In some cases, the error was as high as 60%. Some early models on the laser forming have a model error of more than 100%. Recent analytical models by Lambiase and Di Ilio (2013) and Eideh et al. (2015) also predict more than 25% error in some cases. Moreover, these models have been tested against the bending of some particular materials. It is not known what the error will be in the case of other materials. The analytical models are not able to consider temperature-dependent material properties. Hence, high prediction accuracy cannot be expected from these models. In the recent years, several finite element method (FEM) based models have been developed by different researchers (Shen et al., 2009; Pitz et al., 2010; Hu et al., 2012). These models are capable of

incorporating temperature dependent material properties. However, due to the requirement of very high computational time, the models are not suitable for online prediction.

Although a number of analytical and numerical models have been developed for laser bending process, very scant attention has been paid to the realistic selection of process parameters for laser bending considering the model accuracy. Hennige et al. (1997) proposed a closed loop control strategy to study the accuracy of the bend obtained by laser bending process. They conducted closed-loop bending experiments to verify their strategy and achieved an accuracy of 0.2° for a bend angle of 10° in case of mild steel. Kumar and Dixit (2008) proposed a strategy for online learning of laser bending. In their approach, initially a number of trials are required for achieving the desired bend angle, where all the data during the trial is saved in a computer. This helps in training a neural network in an incremental manner. After the sufficient amount of learning, very high prediction accuracy can be obtained. In spite of it, the error can never be made zero.

In the present work, a strategy is developed to achieve the desired accuracy in a multipass laser bending process based on the concept proposed in Hennige et al. (1997). In multipass bending, the number of passes depend on the amount of bend angle, desired accuracy and the accuracy of the predictive model used. If the desired accuracy in the bend angle is high and the model error is large, then the accuracy in the bend angle is achieved by increasing the number of passes. In each pass, the target bend angle is chosen accounting for the uncertainty in prediction. The melting point of different materials is different and therefore to achieve the target bend angle the input process parameters need to be suitably chosen. Also, the highest bend angle achievable per pass is different for different materials. The strategy proposed in this paper provides flexibility in its application for different materials. The main aim of this strategy is to make it robust enough to take care of the uncertainties associated with the materials. The novelty of this work lies in developing an easily-implementable strategy and validating it for three materials.

5.2 Problem Definition

It is desired to achieve a bend angle α_B with a prescribed accuracy of $\pm\delta$%. The bend angle α_B can be estimated for the given process parameters and mechanical properties of the sheet using an available mathematical model. Consider that the mathematical model predicts the bend angle with an accuracy of $\pm\varepsilon$ %. If ε is less than δ, then the desired bend angle can be achieved in one laser pass provided that α_B is less than or equal to the maximum achievable bend angle in a single pass (α_{max}). If α_B is more than α_{max}, more than one laser pass are required and the maximum number of passes will be α_B/α_{max}, rounded to its upper integer value. However, if ε is more than δ, the desired bend angle may not be achieved in a single pass even when $\alpha_B \leq \alpha_{max}$. In that case, a strategy can be devised to obtain the desired bend angle in a number of passes. At each pass, the target bend angle α_T needs to be different than the desired bend angle to account for the model uncertainty. After each pass, the achieved bend angle α_a can be measured and the target bend angle for the next pass α_T can be decided. The strategy should be able to give results for any desired α_B with corresponding percentage accuracy value of δ. The objective of the present work is to propose such strategy. The challenge is in developing a strategy that is optimum. The definition of optimum may vary from case to case. Common goals are the minimum production time, minimum consumption of the energy, maximization of the product quality and minimum cost. In most of the cases, the optimization requires that the number of passes should be minimized, which is the main focus of the proposed strategy.

5.3 Strategy for Choosing the Process Parameters of Line Heating Passes

Following strategy can be adopted for choosing the process parameters of the model. If the desired percentage accuracy value (δ) is more than the percentage error in prediction (ε), then target the total bend angle (α_B) in a single pass. If $\alpha_B \leq \alpha_{max}$, it should be possible to obtain the desired total bend angle in a single pass by proper selection of the process parameters by the model. Assuming that the laser beam diameter is fixed, the two process parameters are laser power (P) and scan

speed (v) are considered. There may be several combinations of P and v providing the same bend angle. The best combination is chosen for optimizing certain goal. For example, if the goal is the maximum production rate, the combination giving the highest scan speed should be chosen. If $\alpha_B > \alpha_{max}$, at the first pass the target bend angle becomes α_{max}. The achieved bend angle (α_a) is likely to be different than the target bend angle. In the next pass, the target bend angle becomes either ($\alpha_B - \alpha_a$) or α_{max}, whichever is lower. This procedure is repeated till the total desired bend angle is achieved with prescribed accuracy.

If the desired percentage accuracy value (δ) is less than the percentage error in prediction (ε), the procedure differs. In this case, the target bend angle in each pass α_T is given by Eq. 5.1

$$\alpha_T = \frac{\alpha_b\left(1+\frac{\delta}{100}\right)}{\left(1+\frac{\varepsilon}{100}\right)}, \qquad 5.1$$

where α_b is the remaining bend angle to be achieved at the beginning of the corresponding laser pass. At the beginning of the first pass, it is equal to α_B. If $\alpha_T \leq \alpha_{max}$, the model provides the appropriate process parameter to achieve the bend angle equal to α_T. Otherwise the process parameters are chosen to get the maximum possible bend angle (α_{max}) in that pass. Let the achieved bend angle in the pass be α_a. If $(\alpha_b - \alpha_a)$ is less or equal to ($\alpha_B \delta/100$), the process is completed. Otherwise α_b is set equal to $(\alpha_b - \alpha_a)$ and procedure is repeated to execute the next laser pass.

The entire procedure is depicted by a flowchart (Figure 5.1). It considers two cases — desired accuracy value less than model error and desired accuracy value more than model error. Apart from the procedure described in the preceding two paragraphs, it also highlights the situation in which actual bend angle has more than expected deviation from the planned bend angle. In that situation, there may be a need to change the estimate of model error. In some rare cases, due to under-prediction of the model, the job may get scraped. Although it is possible to carry out reverse bending for rectifying the scrapped job, it requires separate setup and more number of laser passes to do so.

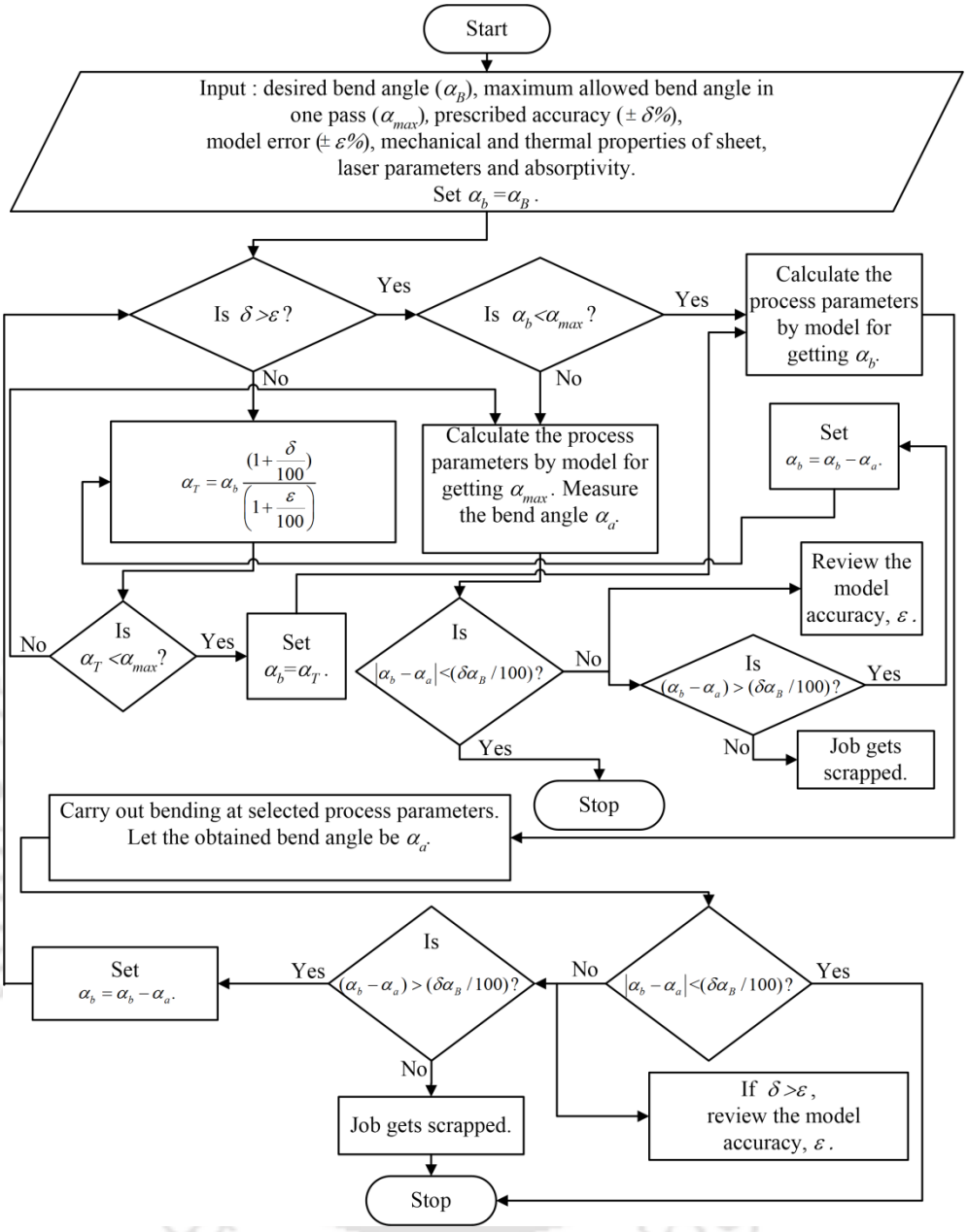

Figure 5.1 A flowchart illustrating the strategy of laser bending

5.4. Experimental Verification of the Strategy

To obtain the bend angle α_b in a laser bending process, the following expression given by Vollertsen (Shen and Vollertsen, 2009) is used:

$$\alpha_b = \frac{3\alpha_{th} P\eta}{\rho c_p v t^2}, \qquad 5.2$$

where α_{th} is the coefficient of thermal expansion, P is the laser power, η is the absorptivity of the surface, ρ is the density of the sheet metal, c_p is the specific heat capacity, v is the laser scan speed and t is the thickness of the sheet. This model does not incorporate the effect of modulus of elasticity and yield strength of material. This results into inaccuracy in the prediction of bend angle. Eq. 5.2 indicates that the bend angle is directly proportional to P/v, which implies that for a desired bend angle; the power can be kept as low as possible by decreasing velocity (v). However, in practice, it is not possible to choose any low value of power at decreased velocity (v). This is due to the fact that at low temperature, bending may not be achieved. On the other hand, high temperature may cause melting or deterioration of mechanical properties.

In the present work, the prediction error ε is initially taken as ±40% based on the results reported by Shen and Vollertsen (2009) and in-house experiments. Later on, observing the accuracy of the bend angle given by Eq. 5.2 with a number of experiments, some experiments were conducted assuming the prediction error of ±20%. In the following subsections, the verification of the proposed strategy for mild steel (AH36), aluminium alloy (5052-H32) and stainless steel (304) is discussed.

5.4.1 Mild steel sheet (AH36)

Initially, a number of experiments were conducted on the bending of 2 mm thick cold rolled mild steel (AH36) sheet. The material properties of mild steel (AH36) are as follows: $\alpha_{th}=1.2\times10^{-5}$ /°C, $\rho=7.8\times10^{3}$ kg/m^3, $c_p=4.295\times10^{2}$ J/kgK (Zhang et al., 2004). The laser beam diameter was 3.87 mm. The absorptivity η was found in an inverse manner based on 10 experiments in a range of process parameters. Similar method was used for 10 each experiment for both aluminium alloy and stainless steel. The inverse procedure minimized the error between the predicted and the experimental bend angle. The value of absorptivity 0.25 was produced very close bend angle by Vollertsen equation while compared with experimental result for all cases of material used. Taking the power and scan speed as the dependent variables, the different experimental data points representing bend angles are shown as a surface plot in Figure 5.2 along with error bars. After each

experiment, the surface was visually examined for checking the melting. A surface was drawn to demarcate the acceptable temperature zone (no melting) and high temperature zone for different combinations of power and scan speed. The points falling on the demarcation surface and acceptable temperature zone are safe. Two sets of replicates were conducted at each point. The repeatability was very good; the maximum range was found to be 0.15°. By carrying out the experiments for different combinations of safe power and scan speed, it has been found that the maximum achievable bend angle is 2.56° in a single pass.

a) Application of the strategy for ±0.1° accuracy

Table 5.1 provides the list of combinations of process parameter that were used in a laser pass for obtaining a target bend angle. These laser process parameters were obtained using Vollersen's formula. It is to be mentioned that strict adherence to the maximum possible scan speed was not observed as the objective of this work was not the maximization of production rate, but merely the assessment of the strategy.

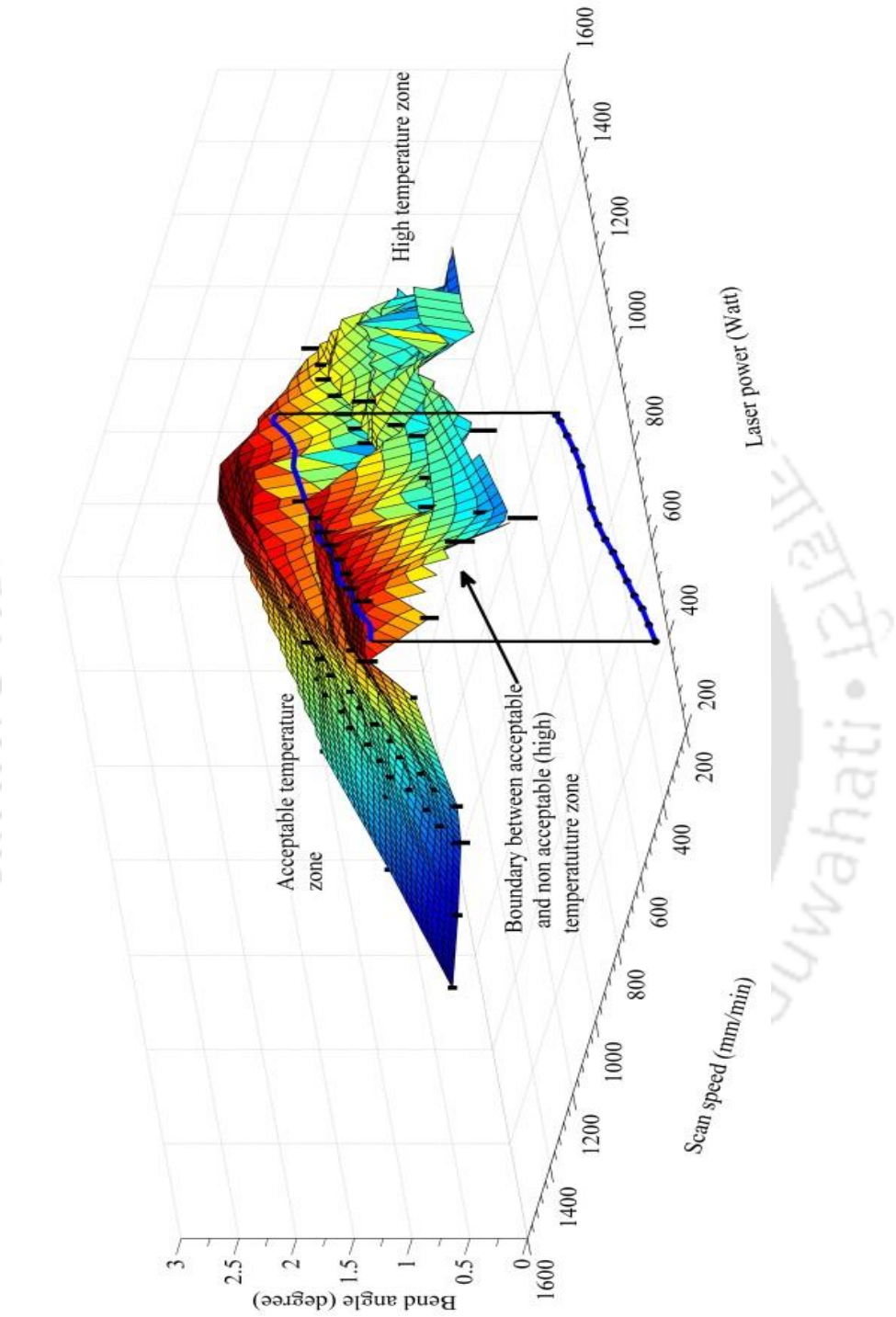

Figure 5.2 Safe and unsafe zone in laser bending for various combinations of laser power and scan speed

Table 5.1 Process parameters for various targeted bend angles for mild steel (AH36)

Bend angle (Degree)	Laser power (W)	Scan speed (mm/min)	Bend angle (Degree)	Laser power (W)	Scan speed (mm/min)	Bend angle (Degree)	Laser power (W)	Scan speed (mm/min)
0.05	200	9235	0.46	575	2886	1.15	525	1054
0.07	200	6597	0.48	500	2405	1.19	675	1310
0.08	200	5772	0.5	700	3232	1.2	525	1010
0.1	200	4618	0.53	700	3049	1.22	725	1372
0.12	250	4810	0.54	600	2565	1.26	775	1420
0.14	300	4948	0.63	600	2199	1.27	675	1227
0.15	250	3848	0.64	600	2165	1.33	750	1302
0.16	375	5411	0.67	500	1723	1.36	650	1104
0.18	375	4810	0.68	625	2122	1.5	500	770
0.19	350	4253	0.69	575	1924	1.68	675	928
0.2	400	4618	0.71	625	2032	1.75	550	726
0.21	300	3298	0.73	650	2056	2	800	924
0.21	450	4948	0.74	500	1560	2.01	700	804
0.22	300	3148	0.76	650	1975	2.02	750	857
0.23	400	4015	0.78	650	1924	2.27	800	814
0.26	200	1776	0.81	600	1710	2.31	750	750
0.27	400	3421	0.83	600	1669	2.32	800	796
0.28	275	2268	0.84	600	1649	2.36	750	734
0.29	400	3185	0.88	600	1574	2.38	750	728
0.31	450	3352	0.89	600	1557	2.39	850	821
0.33	475	3323	0.91	600	1517	2.41	750	719
0.36	525	3367	0.92	750	1882	2.43	850	808
0.38	525	3190	0.96	650	1563	2.46	850	798
0.4	475	2742	0.99	600	1399	2.47	750	701
0.43	559	3002	1.02	625	1415	2.48	750	698
0.44	550	2886	1.1	625	1312	2.52	750	687
0.45	600	3079	1.13	725	1481	2.56	900	812
0.46	500	2510	1.14	525	1063			

Following the strategy discussed in Section 5.3, various bend angles were achieved on the mild steel (AH36) sheets. Table 5.2 shows the pass schedules for bend angles of 2°, 5°, 8°, 10°, 12° and 15°. The target for bend angle accuracy was ±0.1°. In each case, fresh experiments were conducted on three replicates to check the repeatability. The bend angles of 2° can be achieved in 3 passes. The bend angles of 5°and 8° were achieved in 4 passes, while 10° and 12° bend angles were achieved in 6 passes. The bend angle of 15° was achieved in 7 passes. The

requirement of more number of passes for higher bend angle is mainly due to the limitation of the maximum bend angle of 2.56° in a single pass. The repeatability of the results is very good and the maximum range is 0.06°.

Table 5.2 Pass schedule in multipass laser bending for mild steel (AH36) (assumed model error =±40% and desired accuracy =±0.1°)

Desired bend angle	Pass 1 bend angle		Pass 2 bend angle		Pass 3 bend angle		Pass 4 bend angle		Pass 5 bend angle		Pass 6 bend angle		Pass 7 bend angle		Final bend angle
	T.	A.	T.	A.	T.	A.	T.	A.	T.	A.	T.	A.	T.	A.	
2	1.5	1.43	0.48	0.37	0.21	0.12	-	-	-	-	-	-	-	-	1.92
2	1.5	1.45	0.46	0.32	0.23	0.12	-	-	-	-	-	-	-	-	1.89
2	1.5	1.45	0.46	0.37	0.20	0.11	-	-	-	-	-	-	-	-	1.93
5	2.56	2.29	2.01	1.79	0.73	0.63	0.29	0.36	-	-	-	-	-	-	5.07
5	2.56	2.30	2.00	1.74	0.74	0.65	0.29	0.34	-	-	-	-	-	-	5.03
5	2.56	2.28	2.02	1.88	0.67	0.64	0.22	0.26	-	-	-	-	-	-	5.06
8	2.56	2.25	2.56	2.27	2.56	2.24	0.91	1.20	-	-	-	-	-	-	7.96
8	2.56	2.24	2.56	2.25	2.56	2.25	0.89	1.19	-	-	-	-	-	-	7.93
8	2.56	2.23	2.56	2.29	2.56	2.24	0.88	1.18			-	-	-	-	7.94
10	2.56	2.22	2.56	2.21	2.56	2.25	2.56	2.24	0.96	1.01	0.20	0.16	-	-	10.09
10	2.56	2.24	2.56	2.25	2.56	2.29	2.56	2.23	0.78	0.86	0.16	0.21	-	-	10.08
10	2.56	2.26	2.56	2.22	2.56	2.26	2.56	2.25	0.76	0.85	0.15	0.19	-	-	10.03
12	2.56	2.25	2.56	2.29	2.56	2.27	2.56	2.28	2.56	2.24	0.54	0.71	-	-	12.04
12	2.56	2.25	2.56	2.26	2.56	2.25	2.56	2.24	2.56	2.21	0.64	0.82	-	-	12.03
12	2.56	2.24	2.56	2.28	2.56	2.24	2.56	2.21	2.56	2.23	0.65	0.81	-	-	12.01
15	2.56	2.23	2.56	2.25	2.56	2.27	2.56	2.21	2.56	2.23	2.56	2.21	1.20	1.49	14.89
15	2.56	2.25	2.56	2.26	2.56	2.25	2.56	2.27	2.56	2.24	2.56	2.22	1.15	1.43	14.92
15	2.56	2.24	2.56	2.28	2.56	2.24	2.56	2.25	2.56	2.24	2.56	2.26	1.14	1.42	14.93

T. =Target (Equation), A. =Actual (Experimental). All bend angles are in degree.

Table 5.2 shows that Vollertsen's simple formula provides less than 10% error between the target and actual bend angles in first pass. The error increases with the increase in the number of passes. For example, for 15° bend angle, the error between the target and actual bend angle in the 7^{th} pass is around 25%. This is due to change in the surface characteristics after laser irradiation that changes the absorptivity. In most of the cases, the Vollertsen's formula over-predicts the bend angle due to reduction in the absorptivity. This helps in avoiding the scrap due to over-bending.

Under-bending is not a serious problem as it is easier to increase the bend angle compared to reducing it.

Next, the model prediction error was taken as ±20%. In addition to the pass schedules for bend angles considered in Table 5.3, pass schedules for small bend angles of 0.5°, 1° and 1.5° are also shown in Table 5.3. It is observed that for small bend angles, the target bend angle is achieved only in two passes with an accuracy of ±0.1°. To achieve the bend angle of 5°, 3 passes were required. Thus, the saving in production time is not apparent. However, if the tolerance in the desired bend angle is widened, it may be possible to carry out the operation in two passes only. The repeatability is very good. In the case of 10° desired bend angle, the range of 3 replicates is 0.12°, whilst in all other cases the ranges vary from 0.01° to 0.05°. A comparison of Table 5.2 and Table 5.3 shows that for a desired bend angle of 5°, assuming ±40% model error could achieve the bend angles in the range of 4.04°-4.16° in two passes, whilst assuming ±20% model error could achieve the bend angles in the range of 4.21°-4.28° in two passes, indicating an increase in the production rate.

It is to be noted that for the same target bend angle, the actual bend angle increases upto 3rd pass, then decreases. This is due to the decrease in absorptivity of the coated surface after 3 passes as well as increase in the surface hardness resulting less deformation. The results presented in Table 5.2 and Table 5.3 show that for assumed ±20% model error, the strategy provides lesser number of laser passes for achieving 2° and 5° bend angle as compared to assumed ±40% model error. The strategy has worked well in the present case and an accuracy of ±0.1° is achieved for target bend angles up to 15°. The present strategy provides better accuracy as compared to the closed-loop control strategy of Hennige et al., (1997), which shows an achievement of only ±0.2° accuracy for the bend angle of 10°.

Table 5.3 Pass schedule in multipass laser bending for mild steel (AH36) (assumed model error =±20% and desired accuracy =±0.1)

Desired bend angle	Pass 1 bend angle		Pass 2 bend angle		Pass 3 bend angle		Pass 4 bend angle		Pass 5 bend angle		Pass 6 bend angle		Pass 7 bend angle		Final bend angle
	T.	A.	T.	A.	T.	A.	T.	A.	T.	A.	T.	A.	T.	A.	
0.5	0.50	0.41	0.16	0.11	-	-	-	-	-	-	-	-	-	-	0.52
0.5	0.50	0.39	0.18	0.14	-	-	-	-	-	-	-	-	-	-	0.53
0.5	0.50	0.43	0.14	0.10	-	-	-	-	-	-	-	-	-	-	0.53
1	0.92	0.75	0.29	0.23	-	-	-	-	-	-	-	-	-	-	0.98
1	0.84	0.77	0.20	0.17	-	-	-	-	-	-	-	-	-	-	0.94
1	0.92	0.71	0.33	0.27	-	-	-	-	-	-	-	-	-	-	0.98
1.5	1.33	1.12	0.40	0.34	-	-	-	-	-	-	-	-	-	-	1.46
1.5	1.33	1.14	0.38	0.31	-	-	-	-	-	-	-	-	-	-	1.45
1.5	1.33	1.17	0.36	0.29	-	-	-	-	-	-	-	-	-	-	1.46
2	1.75	1.59	0.43	0.36	-	-	-	-	-	-	-	-	-	-	1.95
2	1.75	1.57	0.44	0.37	-	-	-	-	-	-	-	-	-	-	1.94
2	1.75	1.55	0.47	0.39	-	-	-	-	-	-	-	-	-	-	1.93
5	2.56	2.25	2.38	1.96	0.76	0.85	-	-	-	-	-	-	-	-	5.06
5	2.56	2.27	2.36	1.98	0.71	0.80	-	-	-	-	-	-	-	-	5.05
5	2.56	2.21	2.41	2.07	0.68	0.76	-	-	-	-	-	-	-	-	5.04
8	2.56	2.23	2.56	2.28	2.56	2.29	1.10	1.14	-	-	-	-	-	-	7.94
8	2.56	2.22	2.56	2.26	2.56	2.29	1.10	1.16	-	-	-	-	-	-	7.93
8	2.56	2.27	2.56	2.29	2.56	2.32	1.02	1.10	-	-	-	-	-	-	7.98
10	2.56	2.26	2.56	2.29	2.56	2.34	2.56	2.24	0.84	0.79	-	-	-	-	9.92
10	2.56	2.24	2.56	2.28	2.56	2.32	2.56	2.26	0.83	0.94	-	-	-	-	10.04
10	2.56	2.27	2.56	2.29	2.56	2.34	2.56	2.26	0.81	0.78	-	-	-	-	9.94
12	2.56	2.26	2.56	2.29	2.56	2.34	2.56	2.24	2.48	2.12	0.71	0.82	-	-	12.07
12	2.56	2.24	2.56	2.27	2.56	2.31	2.56	2.26	2.52	2.21	0.68	0.76	-	-	12.05
12	2.56	2.27	2.56	2.30	2.56	2.32	2.56	2.26	2.47	2.19	0.64	0.73	-	-	12.07
15	2.56	2.21	2.56	2.26	2.56	2.3	2.56	2.25	2.56	2.24	2.56	2.21	1.36	1.56	15.03
15	2.56	2.26	2.56	2.28	2.56	2.34	2.56	2.26	2.56	2.29	2.56	2.24	1.19	1.38	15.05
15	2.56	2.24	2.56	2.29	2.56	2.32	2.56	2.23	2.56	2.24	2.56	2.26	1.27	1.45	15.03

T. =Target (Equation), A. =Actual (Experimental). All bend angles are in degree.

b) Application of the strategy for ±0.01° accuracy

In this section, the desired accuracy in the bend angles is ±0.01° for the bend angles presented in Table 5.4. The present strategy fails to provide an accuracy value less than ±0.01°. The smallest bend angle that can be generated with good repeatability was ±0.1°. Moreover, the range of 3 replicates for 10° bend angle was 0.07°. Thus, accuracy of ±0.01° cannot be achieved. Only in one replicate of 10° bend angle, an accuracy of 0.01° could be achieved. It indicates that one can achieve an accuracy of ±0.01° also by carrying out a large number of experimental trials as the error is random in nature. However, this procedure will generate a number of scrap parts.

Table 5.4 Pass schedule in multipass laser bending for mild steel (AH36) (model error =±20% and desired (but unachieved) accuracy =±0.01°)

Desired bend angle	Pass 1 bend angle		Pass 2 bend angle		Pass 3 bend angle		Pass 4 bend angle		Pass 5 bend angle		Pass 6 bend angle		Pass 7 bend angle		Final bend angle
	T.	A.	T.	A.	T.	A.	T.	A.	T.	A.	T.	A.	T.	A.	
0.5	0.43	0.39	0.10	0.14	-	-	-	-	-	-	-	-	-	-	0.53
0.5	0.43	0.41	0.08	0.12	-	-	-	-	-	-	-	-	-	-	0.53
0.5	0.43	0.39	0.10	0.15	-	-	-	-	-	-	-	-	-	-	0.54
1	0.84	0.74	0.23	0.18	0.08	0.12	-	-	-	-	-	-	-	-	1.04
1	0.84	0.77	0.20	0.17	0.05	0.10	-	-	-	-	-	-	-	-	1.04
1	0.84	0.79	0.18	0.16	0.05	0.12	-	-	-	-	-	-	-	-	1.07
1.5	1.26	1.19	0.27	0.23	0.07	0.10	-	-	-	-	-	-	-	-	1.52
1.5	1.26	1.17	0.28	0.25	0.08	0.11	-	-	-	-	-	-	-	-	1.53
1.5	1.26	1.20	0.26	0.22	0.08	0.13	-	-	-	-	-	-	-	-	1.55
2	1.68	1.56	0.44	0.31	0.12	0.09	-	-	-	-	-	-	-	-	1.96
2	1.68	1.52	0.48	0.34	0.14	0.10	-	-	-	-	-	-	-	-	1.96
2	1.68	1.55	0.45	0.32	0.12	0.08	-	-	-	-	-	-	-	-	1.95
5	2.56	2.24	2.31	1.93	0.73	0.52	0.31	0.29	-	-	-	-	-	-	4.98
5	2.56	2.23	2.32	1.96	0.68	0.57	0.21	0.22	-	-	-	-	-	-	4.98
5	2.56	2.27	2.27	1.99	0.63	0.52	0.19	0.24	-	-	-	-	-	-	5.02
8	2.56	2.27	2.56	2.29	2.56	2.26	0.99	1.12	-	-	-	-	-	-	7.94
8	2.56	2.23	2.56	2.27	2.56	2.29	1.02	1.14	-	-	-	-	-	-	7.93
8	2.56	2.24	2.56	2.28	2.56	2.34	0.96	1.09	-	-	-	-	-	-	7.95
10	2.56	2.26	2.56	2.29	2.56	2.34	2.56	2.24	0.73	0.79	-	-	-	-	9.92
10	2.56	2.29	2.56	2.26	2.56	2.35	2.56	2.28	0.69	0.81	-	-	-	-	9.99
10	2.56	2.28	2.56	2.25	2.56	2.34	2.56	2.29	0.71	0.79	-	-	-	-	9.95
12	2.56	2.27	2.56	2.29	2.56	2.34	2.56	2.24	2.39	2.23	0.53	0.59	-	-	11.96
12	2.56	2.22	2.56	2.27	2.56	2.36	2.56	2.25	2.43	2.31	0.50	0.56	-	-	11.97
12	2.56	2.21	2.56	2.28	2.56	2.33	2.56	2.24	2.46	2.37	0.48	0.53	-	-	11.96
15	2.56	2.29	2.56	2.27	2.56	2.37	2.56	2.23	2.56	2.29	2.56	2.23	1.1	1.23	14.91
15	2.56	2.25	2.56	2.26	2.56	2.36	2.56	2.24	2.56	2.27	2.56	2.28	1.13	1.28	14.94
15	2.56	2.23	2.56	2.27	2.56	2.31	2.56	2.23	2.56	2.25	2.56	2.26	1.22	1.38	14.93

T. =Target (Equation), A. =Actual (Experiment). All bend angles are in degree.

In general, the present strategy provides higher accuracy at the cost of increased production time. Thus, high accuracy in shop floor may be achieved by increasing the number of passes. If the shop floor requires high rate of production, then this can be achieved by reducing the number of passes at the cost of reducing accuracy. The strategy is flexible and can be used for any materials.

5.3.2 Aluminum alloy (5052-H32) sheet

Multipass experiments were carried out on aluminum alloy (5052-H32) sheets to achieve bend angles of 0.5°, 1° , 1.5°, 2°, 5° and 8°. The material properties of aluminium alloy (5052-H32) are as follows: $\alpha_{th}=2.38\times10^{-5}$ /°C, $\rho=2.68\times10^{3}$ kg/m^3, $c_p=8.80\times10^{2}$ J/kg.K (Fetene et al.,2017). The pass schedules are shown in Table 5.6. An accuracy of ±0.1° in bend angles was achieved by assuming a model error of ±40%. However, compared to mild steel (AH36), in some cases the repeatability is poorer. The range is 0.13° for the desired bend angles of 0.5° and 8°.

Table 5.5 Process parameters for various targeted bend angles for Aluminium alloy (5052-H32)

Bend angle (Degree)	Laser power (W)	Scan speed (mm/min)	Bend angle (Degree)	Laser power (W)	Scan speed (mm/min)
0.15	130	4994	0.45	184	2662
0.16	130	4987	0.47	260	3598
0.17	130	4974	0.5	228	2902
0.19	239	8159	0.51	228	2902
0.2	195	6341	0.56	217	2517
0.22	174	5125	0.57	217	2517
0.23	250	7047	0.59	141	1553
0.24	260	6264	0.59	141	1553
0.27	260	6264	0.6	152	1644
0.29	250	5589	0.68	141	1347
0.3	130	2819	0.69	163	1532
0.32	174	3523	0.79	174	1427
0.33	174	3523	0.84	184	1426
0.34	206	3938	0.89	195	1425
0.35	163	3020	0.92	151	1072
0.35	163	3020	1.06	174	1064
0.38	152	2596	1.14	249	1490
0.41	195	3094	1.33	206	936
0.43	158	1966	1.5	206	893

The maximum and the minimum bend angle achievable bend angle were 1.5° and 0.1°, respectively. Due to low melting temperature of the material, it was not possible to use high power or low scan speed, as it deteriorated the surface. The bends were generated in the sheets in small increments at moderate value of power

and speed. Thus, more passes are required to achieve the target bend angle. Table 5.5 shows the combinations of process parameters used for various targeted bend angles.

Table 5.6 Pass schedule in multipass laser bending of small angles for Aluminum alloy (5052-H32) (assumed model error=±40% and desired accuracy=±0.1°)

Desired bend angle	Pass 1 bend angle		Pass 2 bend angle		Pass 3 bend angle		Pass 4 bend angle		Pass 5 bend angle		Pass 6 bend angle		Pass 7 bend angle		Final bend angle
	T.	A.	T.	A.	T.	A.	T.	A.	T.	A.	T.	A.	T.	A.	
0.5	0.43	0.31	0.19	0.21	-	-	-	-	-	-	-	-	-	-	0.52
0.5	0.43	0.27	0.23	0.18	-	-	-	-	-	-	-	-	-	-	0.45
0.5	0.43	0.36	0.17	0.22	-	-	-	-	-	-	-	-	-	-	0.58
1	0.79	0.57	0.38	0.51	-	-	-	-	-	-	-	-	-	-	1.08
1	0.79	0.61	0.35	0.47	-	-	-	-	-	-	-	-	-	-	1.08
1	0.79	0.65	0.32	0.41	-	-	-	-	-	-	-	-	-	-	1.06
1.5	1.14	0.97	0.45	0.31	0.23	0.16	-	-	-	-	-	-	-	-	1.44
1.5	1.14	1.02	0.41	0.27	0.22	0.19	-	-	-	-	-	-	-	-	1.48
1.5	1.14	1.13	0.34	0.41	-	-	-	-	-	-	-	-	-	-	1.54
2	1.5	1.31	0.56	0.38	0.29	0.37	-	-	-	-	-	-	-	-	2.06
2	1.5	1.39	0.51	0.33	0.27	0.35	-	-	-	-	-	-	-	-	2.07
2	1.5	1.27	0.59	0.41	0.3	0.37	-	-	-	-	-	-	-	-	2.05
5	1.5	1.29	1.5	1.33	1.5	1.53	0.68	0.79	-	-	-	-	-	-	4.94
5	1.5	1.37	1.5	1.32	1.5	1.57	0.6	0.67	-	-	-	-	-	-	4.93
5	1.5	1.24	1.5	1.39	1.5	1.51	0.69	0.77	-	-	-	-	-	-	4.91
8	1.5	1.25	1.5	1.27	1.5	1.41	1.5	1.37	1.5	1.31	1.06	1.23	0.19	0.11	7.95
8	1.5	1.32	1.5	1.36	1.5	1.59	1.5	1.39	1.5	1.27	0.84	0.93	0.17	0.22	8.08
8	1.5	1.34	1.5	1.37	1.5	1.44	1.5	1.38	1.5	1.33	0.89	1.02	0.15	0.2	8.08

T. =Target (Equation), A. =Actual (Experimental). All bend angles are in degree.

Further, the strategy was tested with ±20% model error and ±0.1% accuracy for small bend angles. The results are presented in Table 5.7. It is observed that the number of pass remains same even after reducing the model error from ±40% to ±20%. The results do not indicate any improvement in the production time. The range of the replicates for 1° desired bend angle was 0.17°. This may be attributed to the fact that the error between the target and actual bend angle exceeds ±20% in some passes. Thus, it is appropriate to use a model error of ±40% for Aluminium alloy (5052-H32) sheets.

Table 5.7 Pass schedule in multipass laser bending of small angles for Al 5052 alloy (assumed model error =±20% and desired accuracy=±0.1)

Desired bend angle	Pass 1 bend angle		Pass 2 bend angle		Pass 3 bend angle		Final bend angle
	T.	A.	T.	A.	T.	A.	
0.5	0.5	0.36	0.2	0.16	-	-	0.52
0.5	0.5	0.31	0.24	0.19	-	-	0.5
0.5	0.5	0.41	0.16	0.11	-	-	0.52
1	0.92	0.71	0.33	0.21	-	-	0.92
1	0.92	0.83	0.23	0.12	-	-	0.95
1	0.92	0.68	0.35	0.41	-	-	1.09
1.5	1.33	1.04	0.47	0.33	0.19	0.21	1.58
1.5	1.33	0.92	0.57	0.39	0.24	0.17	1.48
1.5	1.33	0.89	0.59	0.44	0.22	0.14	1.47

5.3.3 Stainless steel (SS304) sheet

Assuming ±40% model error, multipass experiments were carried out on stainless steel (SS304) sheets and bend angles of 2°, 5° and 8° were achieved with 0.1° accuracy following the strategy proposed in Section 5.3. The material properties of stainless steel (SS304) are as follows: $\alpha_{th}=1.73\times10^{-5}$ /°C, $\rho=7.88\times10^{3}$ kg/m^3, $c_p=4.9\times10^{2}$ J/kg.K (Deng and Murakawa, 2006). The results are presented in Table 5.9. The ranges of 3 replicates were 0.08°, 0.01° and 0.16° for the desired bend angles of 2°, 5° and 8°, respectively. Due to high melting temperature of stainless steel (SS304), it is possible to produce higher bend angle using high power and low scan speed. Thus, a bend angle of 2.73° can be targeted in a single pass to achieve bend angles of 5° and 8°. It was further verified experimentally that both low power/high speed and high power/low speed can be applied for achieving higher bend angles, depending on the production requirement. Table 5.8 shows the combinations of process parameters used for various targeted bend angles.

Table 5.8 Process parameters for various targeted bend angles for stainless steel (SS304)

Bend angle (Degree)	Laser power (W)	Scan speed (mm/min)	Bend angle (Degree)	Laser power (W)	Scan speed (mm/min)
0.17	350	5493	0.64	325	1355
0.19	400	5617	0.65	500	2052
0.21	300	3811	0.66	475	1920
0.22	300	4000	0.67	450	1792
0.23	400	4640	0.74	600	2163
0.25	300	3202	0.78	575	1967
0.26	425	4361	0.86	600	1861
0.32	550	4586	1.5	550	978
0.33	525	4245	1.75	600	915
0.36	400	2964	1.87	475	678
0.39	350	2394	1.91	525	733
0.43	375	2327	1.95	500	684
0.49	400	2178	2.24	475	566
0.51	425	2223	2.28	450	527
0.53	450	2265	2.29	425	495
0.59	350	1583	2.73	800	782
0.61	300	1312			

Table 5.9 Pass schedule in multipass laser bending for stainless steel (SS304) assumed model error=±40% and desired accuracy =±0.1°)

Desired bend angle	Pass 1 bend angle		Pass 2 bend angle		Pass 3 bend angle		Pass 4 bend angle		Pass 5 bend angle		Final bend angle
	T.	A.	T.	A.	T.	A.	T.	A.	T.	A.	
2	1.5	1.41	0.49	0.42	0.19	0.22	-	-	-	-	2.05
2	1.5	1.39	0.51	0.46	0.17	0.13	-	-	-	-	1.98
2	1.5	1.36	0.53	0.45	0.21	0.16	-	-	-	-	1.97
5	2.73	2.49	1.87	1.76	0.61	0.54	0.22	0.27	-	-	5.06
5	2.73	2.37	1.95	1.84	0.64	0.57	0.23	0.29	-	-	5.07
5	2.73	2.43	1.91	1.85	0.59	0.45	0.26	0.34	-	-	5.07
8	2.73	2.35	2.73	2.37	2.73	2.44	0.67	0.53	0.22	0.29	7.98
8	2.73	2.39	2.73	2.45	2.73	2.33	0.66	0.59	0.19	0.15	7.91
8	2.73	2.33	2.73	2.39	2.73	2.46	0.65	0.57	0.25	0.32	8.07

T. =Target (Equation), A. =Actual (Experimental). All bend angles are in degree.

Multipass experiments were also carried out to achieve bend angles of 2°, 5° and 8° assuming a model error of ±20%. The pass schedules are shown in Table 5.10. It is observed that the strategy provides an accuracy of ±0.1° could be achieved. The range of 3 replicates for the desired bend angle is 0.16°. In this case, the number of passes required to achieve the desired bend angle was reduced by one pass, which decreases the production time. The range of 3 replicates for the desired bend angle of 2° was 0.16°.

Table 5.10 Pass schedule in multipass laser bending for stainless steel (SS304) sheets (assumed model error =±20% and desired accuracy=±0.1°)

Desired bend angle	Pass 1 bend angle		Pass 2 bend angle		Pass 3 bend angle		Pass 4 bend angle		Final bend angle
	T.	A.	T.	A.	T.	A.	T.	A.	
2	1.75	1.63	0.39	0.29	-	-	-	-	1.92
2	1.75	1.59	0.43	0.34	-	-	-	-	1.93
2	1.75	1.67	0.36	0.41	-	-	-	-	2.08
5	2.73	2.35	2.29	2.37	0.32	0.26	-	-	4.98
5	2.73	2.37	2.28	2.34	0.33	0.25	-	-	4.96
5	2.73	2.41	2.24	2.31	0.32	0.23	-	-	4.95
8	2.73	2.33	2.73	2.45	2.73	2.39	0.78	0.86	8.03
8	2.73	2.29	2.73	2.36	2.73	2.42	0.86	0.98	8.05
8	2.73	2.37	2.73	2.49	2.73	2.35	0.74	0.82	8.03

T. =Target (Equation), A. =Actual (Experimental). All bend angles are in degree.

5.4 Improving the Strategy with Experiential Learning

It is likely that the experimental bend angle differ from that predicted (Eq. 5.2). The experimental bend angle α_a can be represented by Eq. 5.3

$$\alpha_a = k_p \frac{3\alpha_{\text{th}} P\eta}{\rho c_{\text{p}} v t^2}, \qquad 5.3$$

where k_p is the proportionality constant, which may vary from experiment to experiment. Considering the laser power and scan speed as the two process parameters, a neural network can be fitted for predicting the proportionality constant as a function of laser power and scan speed. The accuracy of prediction will depend on the number of training data to a large extent. In most of the neural network

predictions, the trained network predicts only the most likely estimate. However, neural networks can also be trained to predict lower, upper and most likely estimates of an output as discussed by Dixit and Chandra (2003), Kohli and Dixit (2004) and Sonar et al., (2006). In that case, the model prediction error can be defined as

$$\varepsilon_l = \frac{\text{most likely estimate} - \text{lower estimate}}{\text{most likely estimate}} \times 100, \quad \varepsilon_u = \frac{\text{upper estimate} - \text{most likely estimate}}{\text{most likely estimate}} \times 100 \tag{5.4}$$

where ε_l is the lower bound side error and ε_u is the upper bound side error. For simplicity, the error ε for both side of the most likely estimate can be taken as the maximum.

Suppose initial estimate of model error is ±40%. After sufficient number of practical data, a neural network gets trained to predict the proportionality constant k_p along with its upper and lower bound. Then the model error for each data can be obtained. It is to be noted that the model error may vary from data to data. The reliability of the model error for a particular set of input parameters will be more if there is some similar data in the training set. A measure of similarity is the Euclidian distance norm. It is hypothesized that the probability of the correct estimate will be exponentially decaying as the prediction data moves away from the training data. Following expression can be used for the probability of obtaining a prediction within the range of model error:

$$p = \exp\left(-\frac{5d}{d_{\max}}\right), \tag{5.5}$$

Where d is the distance between prediction data and the nearest training data, d_{max} is the distance between two farthest data points. For d=0, the probability will be 1 and for d= d_{max}, the probability will be 0.0067, a very small value. Once the probability of correct prediction has been estimated, the decision to modify the initial error estimate of ±40% can be taken based on the mathematical expectation of an optimization goal. For example, if the optimization goal is the minimization of the production time, the mathematical expectation, E can be calculated as

$$\begin{aligned} E_m = {} & p \times (\text{saving in production time by assuming reduced prediction error}) \\ & + (1-p) \times (\text{loss due to scrap as a result of wrong assumption}). \end{aligned} \tag{5.6}$$

If E_m is positive, the estimate of model error is modified, otherwise initial error estimate of 40% continues till the further data improves the confidence. With continuous learning, the uncertainty in prediction will keep on reducing.

5.5 Estimation of Coefficient of Proportionality (k_p)

The proportionality constant (k_p) may be defined as the ratio of experimental bend angle to the calculated bend angle. Here, the calculated bend angle is given by the Vollertsen's formula (Eq. 5.2). Its value varies from experiment to experiment. The different values of k_p are obtained for mild steel (AH36), aluminum alloy (5052-H32) alloy and Stainless steel (SS304). For example, to achieve a bend angle of 8°, the variation of k_p values with the number of passes in multipass experiments for all three materials are shown in Figure 5.3. The value of k_p did not deviate much in case of Stainless steel (SS304) with the number of passes. In case of mild steel (AH36), the deviation in the value of k_p was very small up to 3 passes and in the subsequent pass it fluctuates abruptly. In case of aluminum alloy (5052-H32), the value of k_p fluctuates randomly for all passes. Thus, the variation in the value of k_p does not follow a unique trend for all materials.

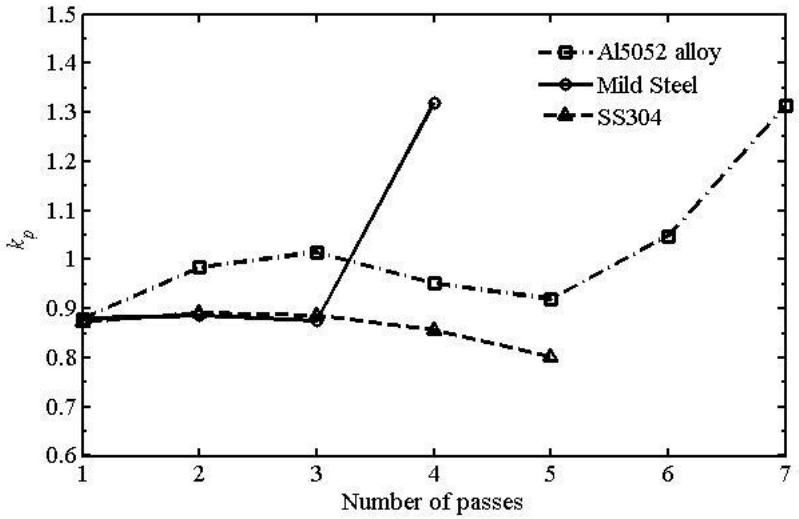

Figure 5.3 Variation of k_p with number of passes to achieve 8° bend angle in multipass laser bending of Aluminium alloy (5052-H32), mild steel (AH36) and Stainless steel (SS304) sheets

The variation in k_p values with number of passes to achieve a smaller bend angle of 2° is also shown in Figure 5.4 for aluminum alloy (5052-H32), mild steel (AH36) and Stainless steel (SS304) sheets. The deviations in the k_p values for various materials are small up to 2 passes. The deviations are high in the third pass. Thus, in case of smaller bend angle, the value of k_p fluctuates as the number of passes increase.

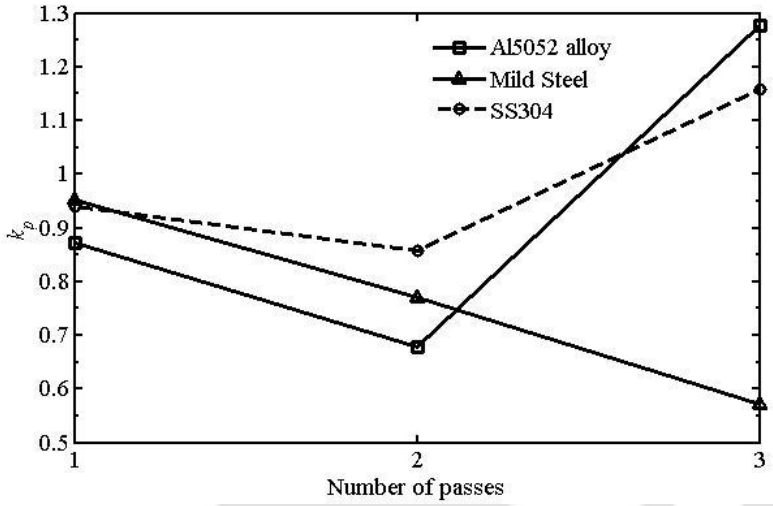

Figure 5.4 Variation of k_p with number of passes to achieve 2° bend angle in multipass laser bending of Aluminium alloy (5052-H32), mild steel (AH36) and Stainless steel (SS304) sheets

The variation in the k_p value from experiment to experiment for a particular material is affected by many parameters such as material property, input parameters, number of laser passes and higher or lower bend angles. Estimation of k_p is not governed by any mathematical relationship. It is a random function of number of passes and experimental conditions.

5.6 Conclusion

In this work, a heuristic strategy is proposed for obtaining the accurate bending in multipass laser line heating. The strategy is capable of producing a bend angle with ±0.1° accuracy which is better than the results reported in the literature. The strategy is simple and can be easily implemented on the shop floor. Here, it has been verified for mild steel (AH36), aluminum alloy and stainless steel. With appropriate

hardware and software, the process can be fully automated. By conducting shop floor experiments, it was verified that simple Vollertsen's formula can be used for achieving prescribed accuracy. First a fixed model prediction error of ±40% was assumed. Later on the model prediction error was taken as ±20% for assessing the reduction in the number of passes for a required bend angle. In fact it is proposed that the estimate of prediction error may be modified with the help of neural network. The more the experiential data for training the neural network, the greater will be the accuracy of estimates. Hence, the final decision to modify the estimate of model prediction error is taken with the help of probability theory. The proposed strategy can also be used for some other multipass manufacturing processes, such as multipass machining.

As a result of a number of experiments on 2 mm sheets of mild steel, aluminium alloy and stainless steel, the following useful observations were also obtained:

- The bend angle in one laser pass was between 2.5° and 3° for steels, but less than 1.6° for aluminium alloy due its high reflectivity and thermal conductivity.
- It was difficult to achieve a bend angle of less than 0.1° by laser bending
- A bend angle of 2° could be achieved in 2-3 passes for all the materials. For mild steel, a bend angle of 15° could be achieved in seven laser passes. For aluminium alloy, a bend angle of 8° required eight passes, whilst for stainless steel; a bend angle of 8° required four passes. Thus, the required number of laser passes depends on the type of material.
- For all the materials, good repeatability and accuracy in bend angle could be obtained. This indicates that by following the proposed strategy, precise bend angles can be produced by laser line heating.

Chapter 6

Laser Assisted Straightening by Permanent Magnet

6.1 Introduction

Laser bending is a non-contact manufacturing process, in which the thermal stresses cause plastic deformation. The process is influenced by a number of process parameters such as laser power, scan speed, laser beam spot diameter and number of scans. In comparison to laser forming, laser assisted forming can achieve larger deformation with less laser energy. It is due to the fact that laser is mainly use to soften the material and assisting force has been used to give the desired shape.

Compared to bending with the help of lasers, the reverse process, i.e., straightening, has been investigated very sparsely. From the limited literature, it is noted that straightening process is not as simple as it appears. Dearden et al. (2003) conducted experiments to straighten the distorted aluminum sheets and observed that some distortion always remained in the worksheet. Ueda et al. (2009) attempted to flatten the projections in the carbon steel and stainless steel sheets and developed irradiation strategies based on the numerical computations of plastic strain in the worksheet. Ueda et al. (2011) employed lasers for flattening the protrusions induced in a metallic worksheet mechanically. They observed that laser scanning on the convex surface of the protrusion is more efficient in reducing the height of protrusion as compared to laser scanning on the concave side. Thus, the convex surface should be exposed to higher temperature to induce larger tensile stresses for obtaining a flat surface. Chakraborty et al. (2015b) used temperature gradient mechanism (TGM) dominated laser bending to reduce the bend angle in mechanically bent stainless steel jobs. The change in bend angle was more when laser beam was irradiated on the convex side of the bent worksheet. Garg et al. (2016) suggested that the workpiece should be kept unclamped in an inverted V-

shape to ensure proper absorption of the laser irradiation during straightening. Nevertheless, a large number of scans were needed even for a slightly bent sheet.

This work introduces a new technique of laser-assisted straightening utilizing magnetic force along with laser irradiation. Magnetic force has the advantage that it can be applied to inaccessible regions and is also easily controllable. A parametric study was carried out to get an approximate estimate of optimum laser power, scan speed and number of laser pass. Further experiments were conducted on as-formed as well as heat treated (stress relieved and annealed) bent mild steel strips focused on magnetic-force-assisted laser straightening with continuous four passes of laser irradiation. Additionally, micro-hardness and microstructure were investigated after laser straightening to understand the detrimental effects of the process, if any.

6.2 Laser Assisted Straightening Setup

To perform laser straightening, the AH36 steel workpieces were bent mechanically at 15°. Then black color spray coating was applied along bend line to enhance the absorptivity during laser irradiation. The samples were kept for drying for one day. The laser straightening was performed by using a 2.5 kW continuous wave mode CO_2 laser machine (Make: LVD, Model: Orion 3015). One side of each specimen was fixed at a fixture in a cantilevered way. The free end of the sheet got attached with a magnet during laser irradiation as shown in Figure 6.1.

Initial study reveals that due to the presence of residual stresses perfect straightening was difficult to achieve in the as-formed specimens. Therefore, it was decided to perform stress relieving treatment before straightening operation. After mechanical bending, the strips were subjected to two kinds of treatment. One group of mechanically bent strips were kept in furnace for 1 hour at 500 °C and then allowed to cool in air (Krauss, 2015) for relieving residual stresses. While another group of 27 numbers of mechanically bent samples were kept in furnace at 700°C for 1 hour and then allowed to cool in furnace for 24 hours up to ambient temperature to facilitate subcritical annealing (Rajan et al., 2011). Finally, all heat treated samples were coated with special black paint spray applied along the bend line to enhance the absorptivity during laser irradiation. The specimens were kept

for drying for one day. The final results after straightening for stress-relieved specimens are depicted in Figure 6.8 and 6.9.

Before fixing the number of laser scans, preliminary experiments were carried out by using laser power of 1000 W, scan speed of 800 mm/min and beam diameter of 3.87 mm with Case 1 (four passes applied continuously). Table 6.1 shows straightening of a strip mechanically bent to an angle of 15^{o}. It was observed that four passes provided significant straightening without any visible defects (melting). In case of laser straightening, some experiments were carried out without magnetic force to straighten the bent sheets, but it required about 15 passes.

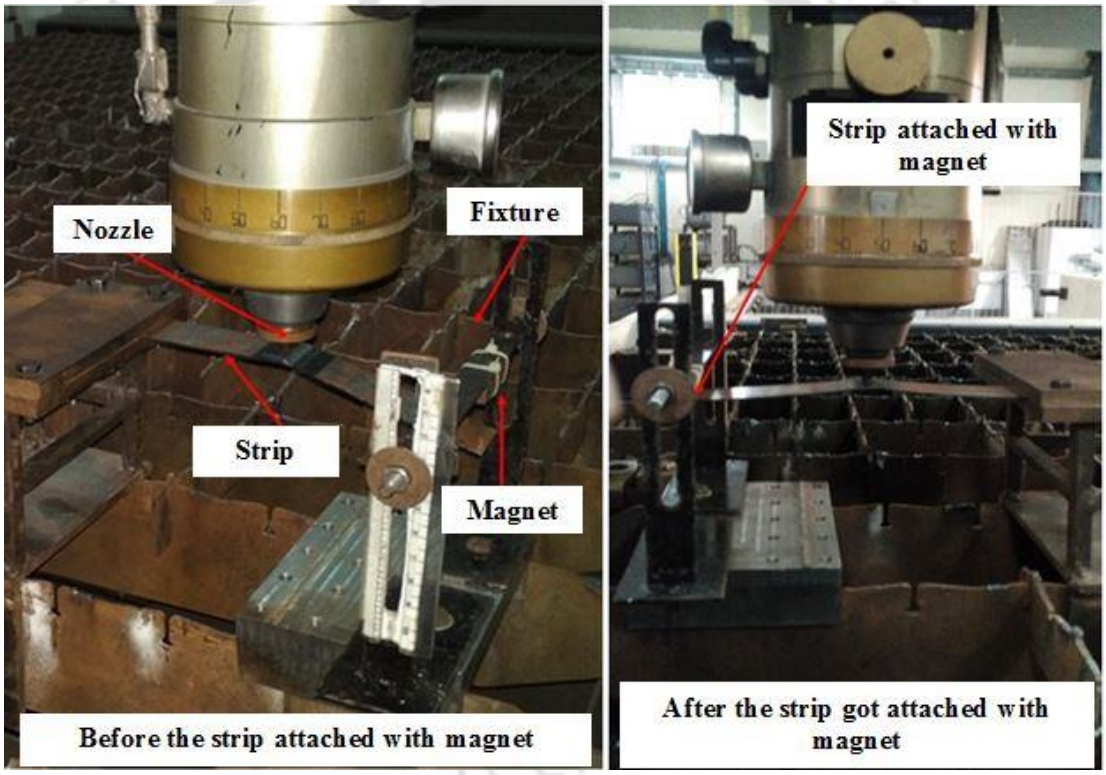

Figure 6.1 Photograph of the experimental setup before and after attaching the work-strip with magnet

Table 6.1 Selection of number of pass for laser assisted straightening by magnetic force

Laser power: 1 kW, Scan speed: 800 mm/min, Beam diameter: 3.87 mm Thickness: 1.5 mm				
Number of laser pass	**Reduction in bend angle**			
	Replicate 1	**Replicate 2**	**Replicate 3**	**Average**
1	4.32°	4.13°	3.96°	4.14°
2	6.41°	6.61°	6.21°	6.41°
3	8.16°	7.94°	7.86°	7.98°
4	9.42°	9.28°	8.47°	9.06°
5	10.22° (melted)	10.40° (melted)	10.12° (melted)	10.25°

To select the proper laser scan schemes, the full factorial experimentation (27) was chosen for as-formed, stress relieve and annealed sample as shown in Table 6.2. Laser scanning was carried out exactly along the bend line in width direction at a distance of 100 mm away from the free end of the strip. The magnet holder could be easily moved up and down through a slot for varying its vertical position as shown in Figure 6.2. In the figure, for each configuration, the original bent strip is shown in the solid line and its position when the laser beam heats it is shown by dotted lines. Before laser irradiation, the work plate was securely fixed with the magnet. The bend angle was reduced (for straightening) by following three laser scan schemes:

Scheme 1: As shown in Figure 6.2 (a), in this scheme the magnet was fixed in a location to make the strip horizontal. Without changing its location, four laser passes were applied continuously.

Scheme 2: As shown in Figure 6.2 (b), here the magnet was located midway to carry out half-straightening. At this position two laser passes were applied. After that the magnet was fixed at a location to make the strip horizontal and two laser passes were applied in this position.

Scheme 3: As shown in Figure 6.2 (c), in this scheme, the straightening was carried out incrementally in four steps. In each step, approximately one fourth of the total bend angle got reduced due to the application of one laser pass.

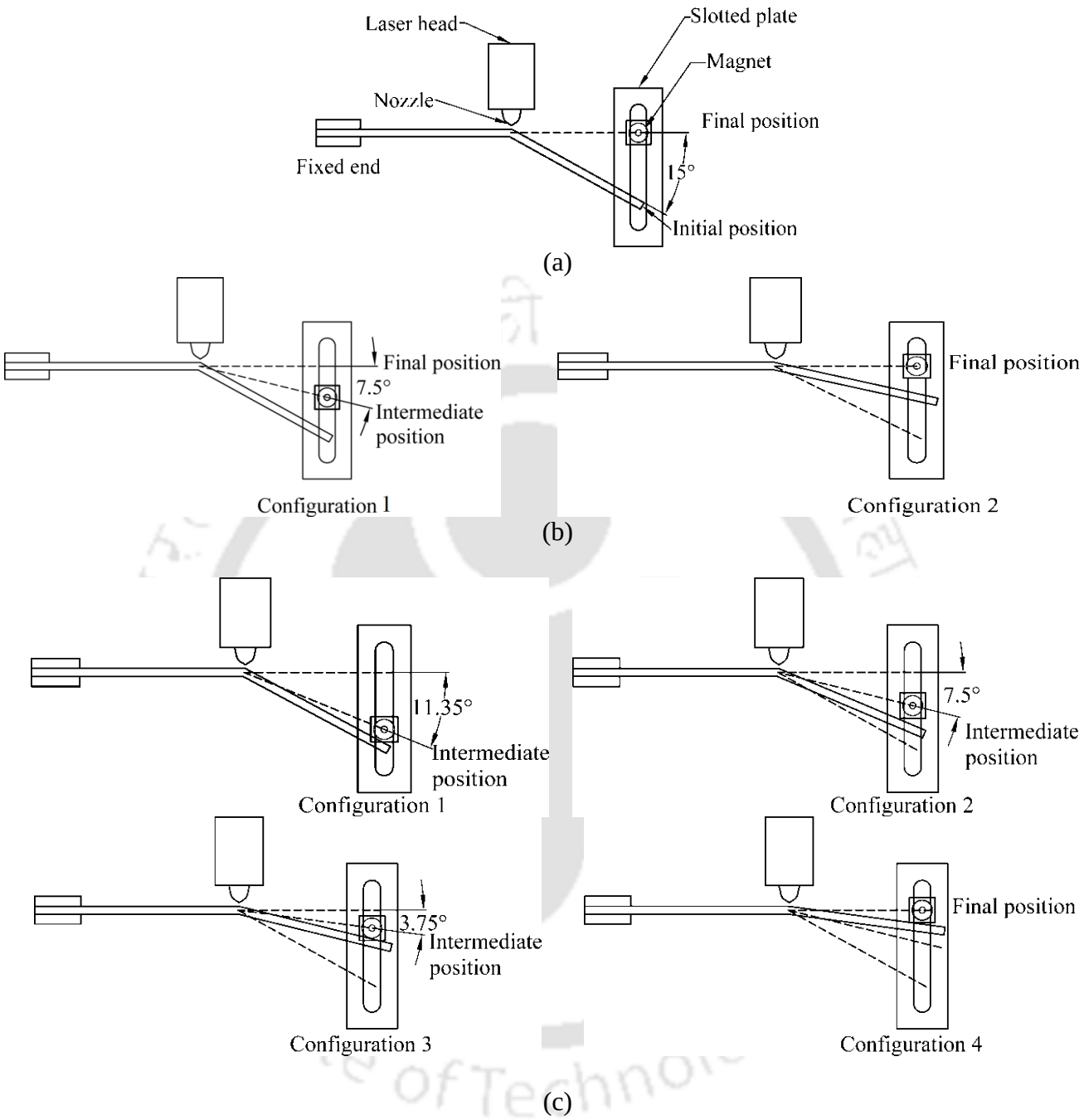

Figure 6.2 Different schemes of laser assisted straightening of strip: (a) Scheme 1 (single magnet-position), (b) Scheme 2 (two magnet-positions) and (c) Scheme 3 (four magnet-positions)

Table 6.2 Process parameters for laser assisted straightening (1000 W laser power, 800 mm/min scan speed and 3.87 mm laser beam diameter)

Test No.	Specimen type	Scheme used	Sheet thickness (mm)	Final bend angle (degree)
1	As-formed	Scheme 1	1	5.39
2	As-formed	Scheme 1	1.5	6.76
3	As-formed	Scheme 1	2	7.53
4	As-formed	Scheme 2	1	4.09
5	As-formed	Scheme 2	1.5	4.84
6	As-formed	Scheme 2	2	6.14
7	As-formed	Scheme 3	1	1.73
8	As-formed	Scheme 3	1.5	2.09
9	As-formed	Scheme 3	2	2.67
10	Stress-relieved	Scheme 1	1	3.56
11	Stress-relieved	Scheme 1	1.5	4.97
12	Stress-relieved	Scheme 1	2	5.43
13	Stress-relieved	Scheme 2	1	1.44
14	Stress-relieved	Scheme 2	1.5	2.16
15	Stress-relieved	Scheme 2	2	2.51
16	Stress-relieved	Scheme 3	1	1.39
17	Stress-relieved	Scheme 3	1.5	2.11
18	Stress-relieved	Scheme 3	2	2.24
19	Annealed	Scheme 1	1	1.19
20	Annealed	Scheme 1	1.5	1.81
21	Annealed	Scheme 1	2	2.31
22	Annealed	Scheme 2	1	1.24
23	Annealed	Scheme 2	1.5	1.76
24	Annealed	Scheme 2	2	2.29
25	Annealed	Scheme 3	1	1.27
26	Annealed	Scheme 3	1.5	1.69
27	Annealed	Scheme 3	2	2.41

6.3 Result and Discussion

The behavior of material components under laser assisted straightening by permanent magnetic force process is influenced by combinations of laser process parameters, thickness of workpiece, scan schemes and heat treatment of workpiece. In this work, the effect of laser process parameters on straightening, scan scheme on straightening, effect of heat treatment of specimen on straightening were studied.

Change in tensile and impact strength after straightening was also checked. Microhardness and microstructure evaluation were also performed.

6.3.1 Validation of FEM simulation

The detail of FEM simulation was discussed in Chapter 3. Few simulation has been performed for few selected cases (9 simulations) considering Scheme 1 (4 continuous laser pass) to compare the bend angle and profile of the workpiece with experimental result. Table 6.3 shows a good agreement between experiment and simulation. At a particular laser power of 900 W and scan speed of 800 mm/min, the maximum deviation was 11%. Figure 6.3 shows experimental and numerical shape of the work strip after straightening operation that depicts a convex profile in the locality of laser irradiation for both the conditions considering same laser process parameter.

Table 6.3 Experimental and numerical simulation results

Test number	Bend angle (degree)		Deviation
	Exp.	Sim.	(%)
1	5.39	5.93	10.02
4	6.76	7.42	9.76
7	7.53	8.14	8.11
10	1.19	1.30	9.24
13	1.81	1.94	7.18
16	2.31	2.56	10.82
18	3.56	3.87	8.71
22	4.97	5.49	10.46
25	5.43	5.90	8.65

Figure 6.3 Experimental and numerical deformed shape after straightening operation

The profile of the straightened (corrected) work plate was influenced by process parameters. Figure 6.4 depicts typical shapes generated during laser straightening. Type 1 means convex (viewed in direction of laser beam). Type 2

means incremental step type profile at the locality of straightening line. Type 3 is straight line surface generated during straightening. Type 3 is the most desirable profile during magnetic force assisted laser straightening. It was also observed that in most of cases in scheme 1, Type 1 shape developed. Similarly in most cases, Scheme 2 and Scheme 3 produce type 1 and Type 3 shapes respectively.

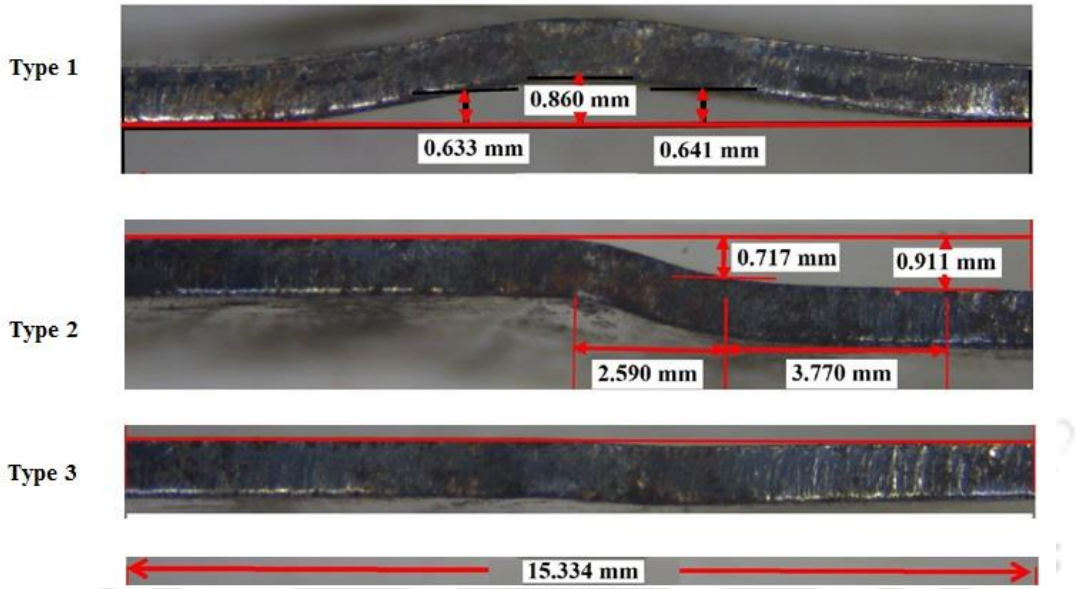

Figure 6.4 The profile of the laser straightened specimens at different scanning schemes

6.3.2 Selection of laser scan scheme

For the selection of proper scheme of straightening, 27 experiments were conducted as shown in Figure 6.5. The results show that for straightening of as-formed specimens, only Scheme 3 is suitable for getting sufficient reduction in the bend angle. Hence, for as-formed strips, Scheme 3 was selected. In case of stress-relieved specimens, Scheme 2 and Scheme 3 provided almost similar results. Considering the production time, Scheme 2 was selected. While in case of annealed specimens, Scheme 1 was selected considering its simplicity; other two schemes fared similarly. Initial experiments revealed that selection of proper scheme with proper parameters can straighten the strips.

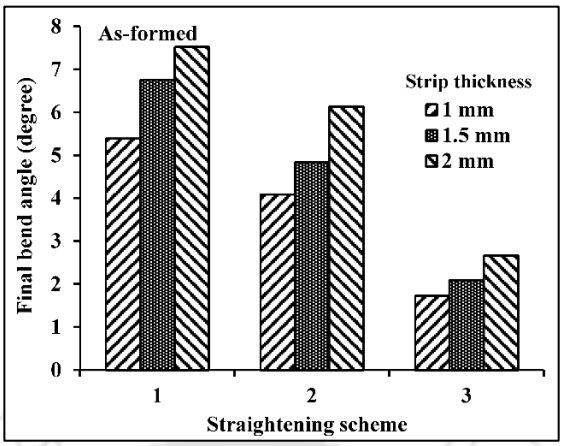

(a)

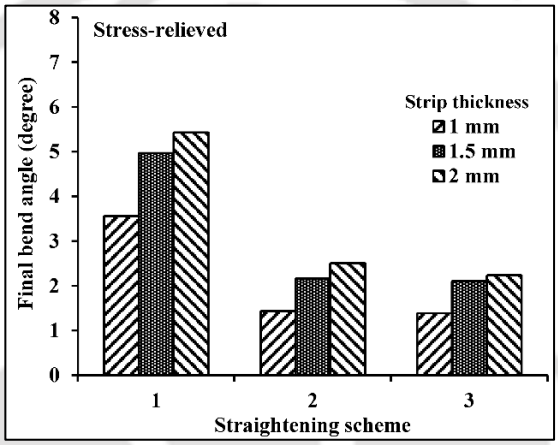

(b)

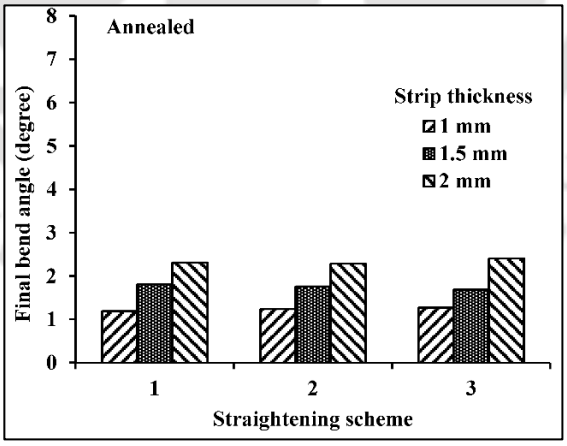

(c)

Figure 6.5 Final bend angle remained after straightening (at 1 kW laser power of and 0.8 m/min scan speed) by three schemes for strips of different thicknesses and types: (a) as-formed, (b) stress- relieved and (c) annealed

6.3.3 Angle reduction during annealing

An interesting phenomenon was observed during annealing of the samples. As shown in Table 6.4 after annealing, all samples showed a slight reduction in bend angle. This is due to the total release of residual stresses after annealing. The bend angle reduced in the range of 0.17°–0.61° in 1 mm thick strips, 0.31°–0.94° in 1.5 mm thick strips and 0.73°–1.32° in 2 mm thick strips, respectively. In the case of stress-relieved strips, no significant change in the bend angle was observed.

Table 6.4 Reduction in bend angle after annealing

Test Number	Strip thickness (mm)	Bend angle (°)		Reduction (°)
		Before annealing	After annealing	
1	1.0	15.79	15.32	0.47
2	1.5	15.52	15.01	0.51
3	2.0	14.85	14.12	0.73
4	1.0	15.47	15.12	0.35
5	1.5	15.66	15.09	0.57
6	2.0	14.95	14.19	0.76
7	1.0	14.95	14.45	0.5
8	1.5	16.03	15.09	0.94
9	2.0	15.40	14.13	1.27
10	1.0	14.62	14.37	0.25
11	1.5	14.42	14.11	0.31
12	2.0	16.25	14.98	1.27
13	1.0	15.27	15.04	0.23
14	1.5	14.92	14.34	0.58
15	2.0	16.89	15.57	1.32
16	1.0	14.56	14.39	0.17
17	1.5	14.44	14.02	0.42
18	2.0	16.39	15.14	1.25
19	1.0	14.35	14.13	0.22
20	1.5	14.67	14.24	0.43
21	2.0	16.29	15.33	0.96
22	1.0	14.84	14.23	0.61
23	1.5	14.81	14.33	0.48
24	2.0	16.29	15.11	1.18
25	1.0	14.57	14.12	0.45
26	1.5	14.57	14.09	0.48
27	2.0	16.23	15.19	1.04

A set of experiments was performed to determine the effects of laser power, scan speed and scan sequence. The full factorial experimentation was chosen to predict the effect of parameters on laser straightening. First, experiments were conducted for as-formed specimens. Scheme 3, *i.e.*, four passes in four positions, was selected for straightening the bent strips. The bend angle remaining after four laser passes is shown in Figure 6.6 for different cases. It is worth noting that at a laser power of 1000 W and scan speed of 800 mm/min, 1.5 mm thick strip could be fully straightened. For other cases also, the reduction in bend angle is significant. Following subsections discuss the effect of various parameters with the help of articulate figures.

6.3.4 Effect of laser power and scan speed for as-formed strips

As shown in Figure 6.6, for the same scan speed and number of scans, amount of straightening is dependent on the laser power, scan speed and strip thickness. For 1 mm strip thickness, the amount of straightening is the maximum at 900 W laser powers as depicted in Figure 6.6(a). At 1000 W power, some amount of melting is observed, which reduces the reverse bending. For strips of 1.5 mm and 2 mm thickness, the amount of straightening is the maximum at 1000 W laser power due to high thermal gradient. In all the cases, the straightening was the maximum at the lowest scan speed of 800 mm/min, which allowed the sufficient interaction time of the material with the laser beam. The final bend angle lies within the range of 1.07°–3.93° for 1 mm thickness strips (Figure 6.7a), 1.12°–2.77° for 1.5 mm thickness strips (Figure 6.7b) and 0.31°–0.73° for 2 mm thickness strips (Figure 6.7c), respectively. The best straightening with a 0.31° remained angle occurred with a laser power of 1000 W and scan speeds of 800 mm/min for 2 mm thick strip.

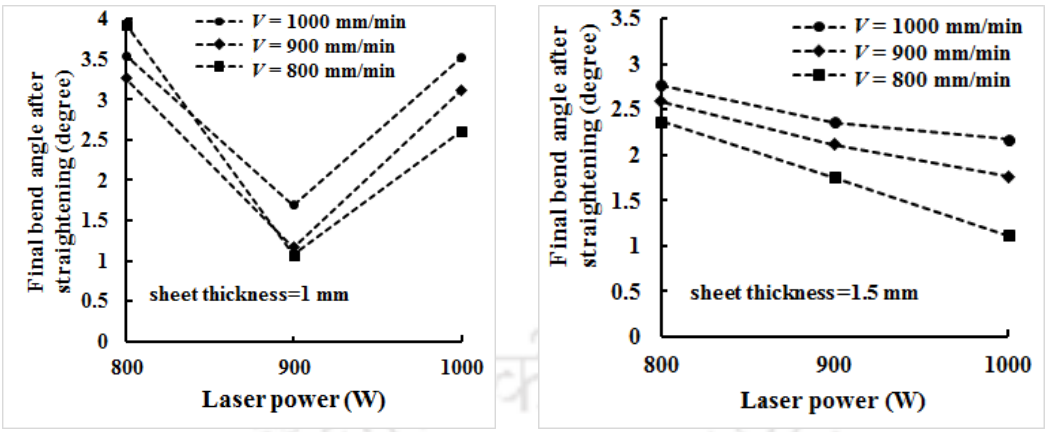

(a) (b)

(c)

Figure 6.6 Variation of degree of straightening with laser power for (a) 1mm, (b) 1.5 mm and (c) 2 mm sheet for as-formed strips

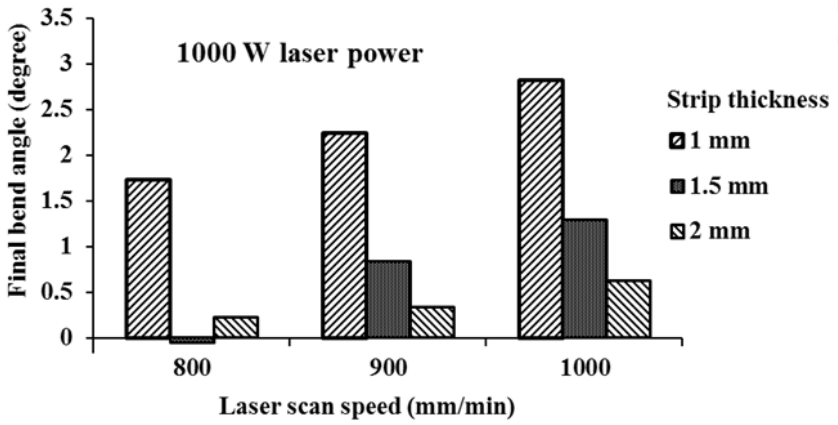

(a)

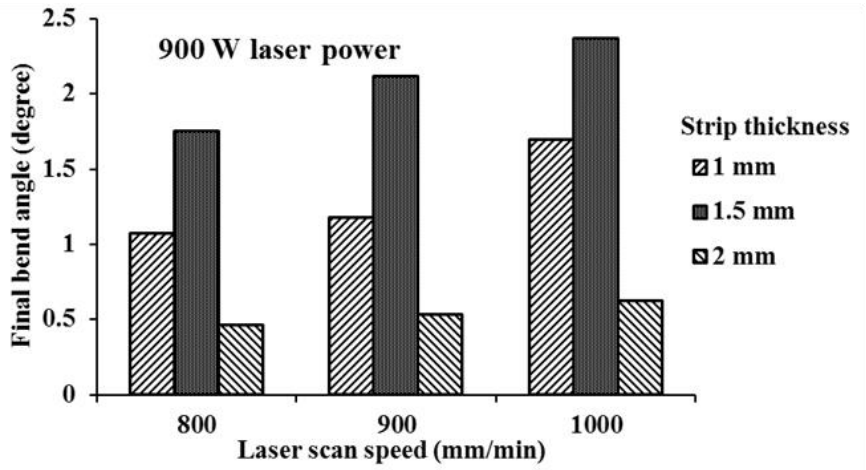

(b)

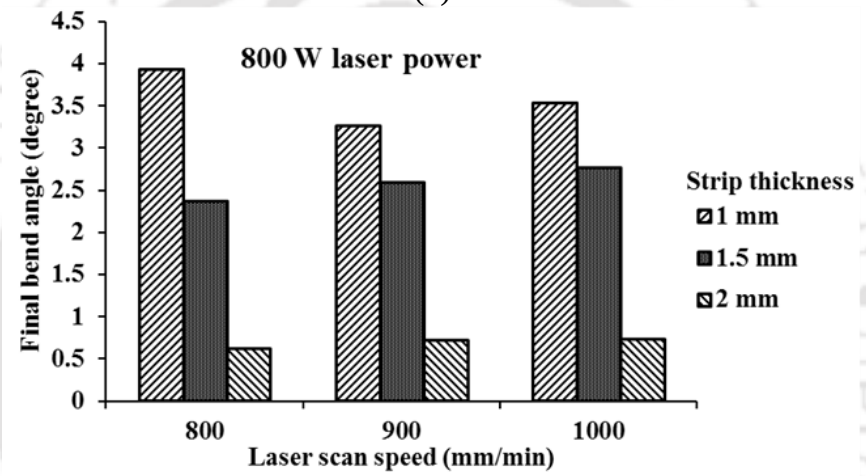

(c)

Figure 6.7 Final bend angle remained after straightening of as-formed strips at different scan speeds and laser power of (a) 1000 W, (b) 900 W and (c) 800 W.

Three replicates were performed for results having final angle value ≤ 0.5°. The final bend angle was within the range of 0.28°–0.43° for laser power of 1000 W and scan speed of 800 mm/min, 0.34°–0.59° for laser power of 1000 W and scan speed of 900 mm/min and 0.41°–0.59° for laser power of 900 W and scan speed of 800 mm/min for 2 mm thick strips. Thus, repeatability of the process is good.

6.3.5 Effect of laser power and scan speed for stress-relieved strips during Straightening

As shown in Figure 6.8, for the same scan speed and number of scans, the amount of straightening is the maximum at 900 W laser power for 1 mm thick strips.

For other types of strip, the straightening was the maximum at 1000 W laser power. The straightening was the maximum at a scan speed of 800 mm/min in all the cases. These trends are similar to those for as-formed strips; however here the amount of straightening is greater. The final bend angle was within the range of 0°–3.81° in 1 mm thick strips (Figure 6.9a). The final bend angle was within the range of 0°–1.89° for 1.5 mm thick strips (Figure 6.9b) and 0.22°–0.73° for 2 mm thick strips (Figure 6.9c), respectively. The perfect straightening, with no bend angle remained, occurred at laser power of 900 W and scan speed of 800 mm/min for 1 mm strips. For 1.5 mm strip, the perfect straightening occurred at a laser power of 1000 W and scan speed of 800 mm/min.

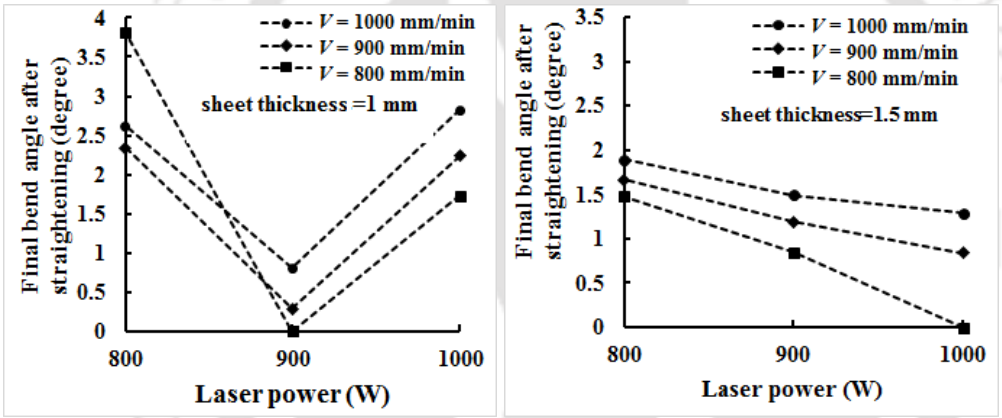

(a) (b)

(c)

Figure 6.8 Variation of degree of straightening with laser power for (a) 1mm, (b) 1.5 mm and (c) 2 mm sheet for stress-relieved strips

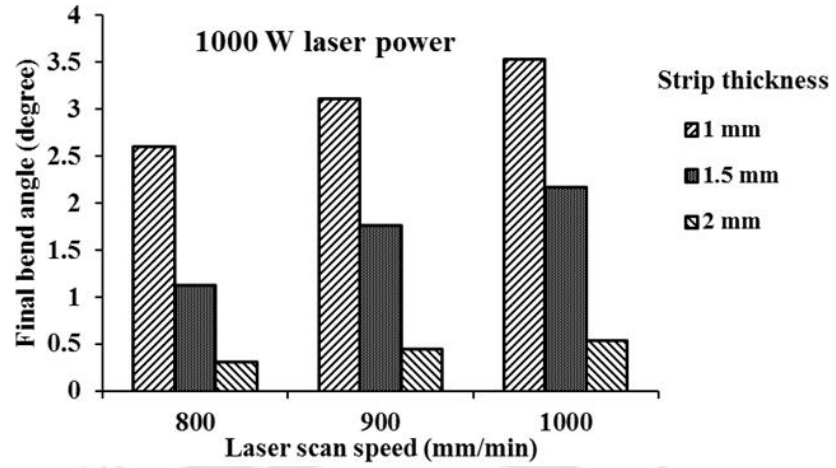

(a)

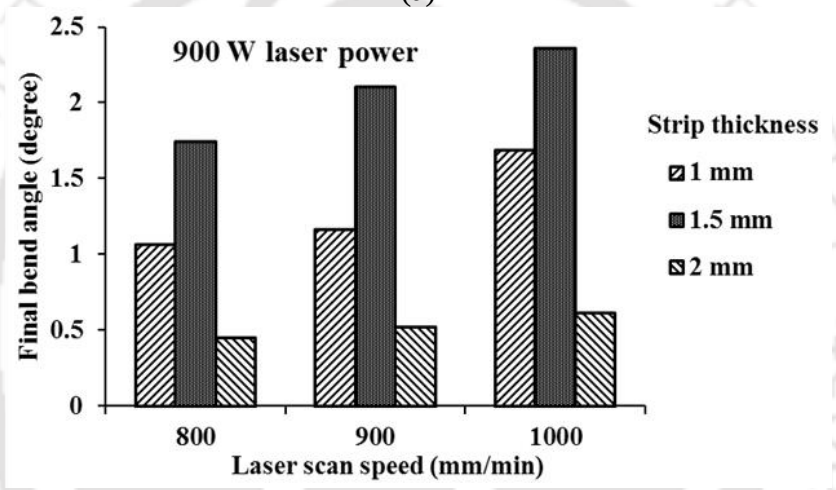

(b)

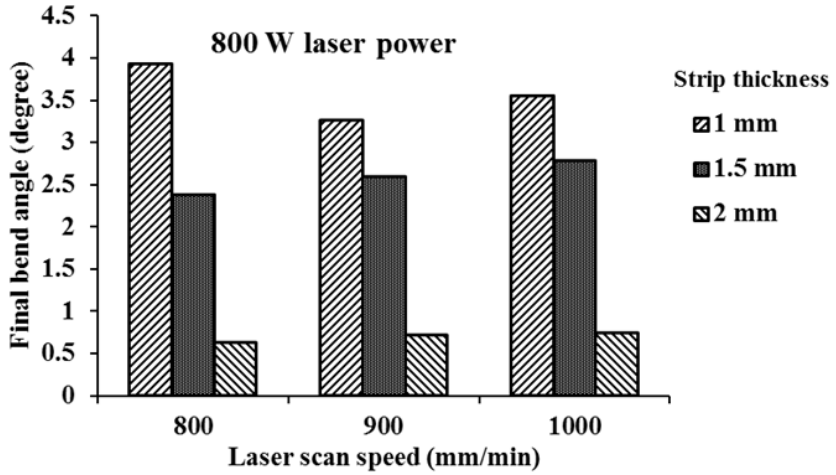

(c)

Figure 6.9 Final bend angle remained after straightening of stress-relieved strips at different scan speeds and laser power of (a) 1000 W, (b) 900 W and (c) 800 W.

Replicates were performed for results having final angle value ≤ 0.22°. The final bend angle was within the range of 0.0°–0.11° for laser power of 900 W and scan speed of 800 mm/min for 1 mm thick strip, 0.09°–0.18° for laser power of 1000 W and scan speed of 800 mm/min for 1.5 mm thick strip, and 0.19°–0.36° for laser power of 1000 W and scan speed of 800 mm/min for 2 mm thick strip. All cases showed good repeatability.

The stress-relieved specimens showed significant improvement over previous experiments on as-formed steel both in result and process. This was due to the release in lock-in stresses present in the specimen. However, stress-relieving by air cooling increase the hardness of the material which has been discussed later elaborately. At times, the increase in the hardness may be undesirable. Therefore, a study was conducted on the sub critically annealed samples subjected to laser straightening by Scheme 1. The final results after laser assisted straightening are presented in Figures 6.10 and 6.11.

6.3.6 Effect of laser power and scan speed for sub critically annealed specimen during straightening

As shown in Figure 6.10, for the same scan speed and number of scans, the amount of straightening is the maximum at 900 W laser power for 1 mm thick strips. For other types of strip, the straightening was the maximum at 1000 W laser power. The straightening was the maximum at a scan speed of 800 mm/min in all the cases. Although the trends are similar to the other types of strips, annealed strips could be straightened more properly than as-formed and stress relieved strips. The final bend angle was within the range of 0°–2.01° for 1 mm thick strip (Figure 6.11a), 0°–0.79° for 1.5 mm thick strip (Figure 6.11b) and 0.0°–0.53° for 2 mm thick strip (Figure 6.11c), respectively. The perfect straightening occurred at a laser power of 900 W and scan speed of 800 mm/min for 1 mm thick strip. For 1.5 mm thick strip, the perfect straightening occurred at a laser power of 1000 W and scan speed of 800 mm/min. Laser power of 1000 W and scan speed of 800 mm/min provided the perfect straightening for 2 mm thick strip.

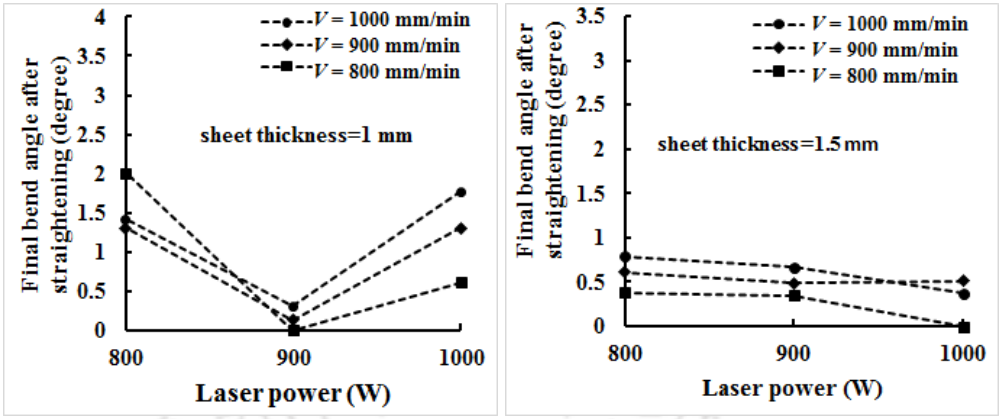

(a) (b)

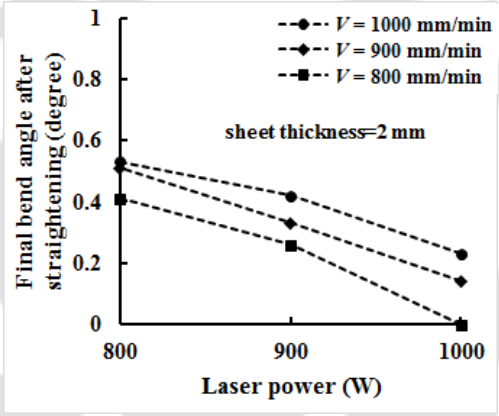

(c)

Figure 6.10 Variation of degree of straightening with laser power for (a) 1mm, (b) 1.5 mm and (c) 2 mm specimens for annealed strips

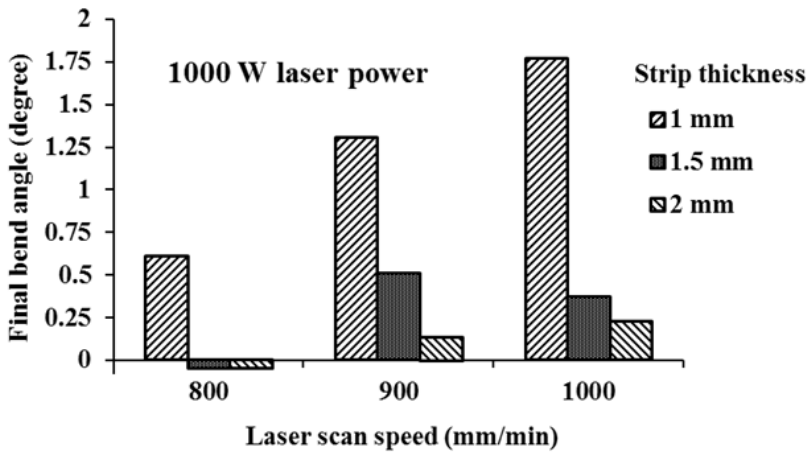

(a)

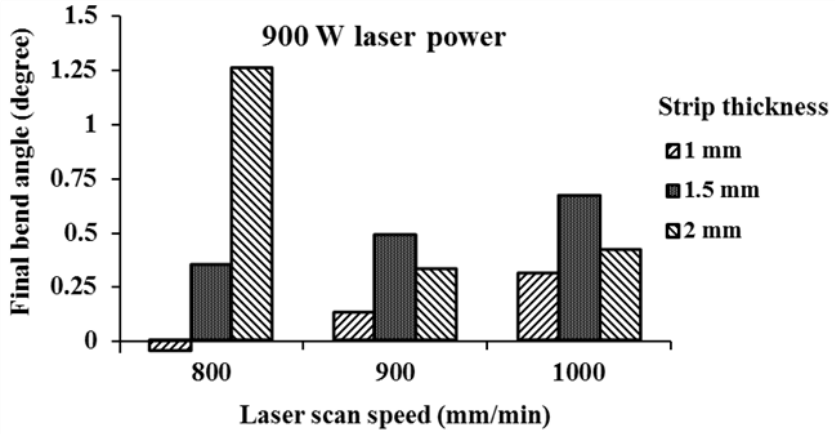

(b)

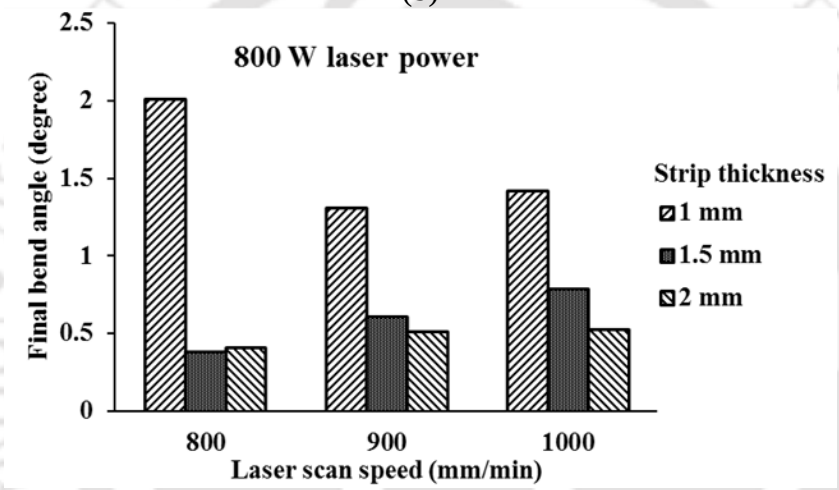

(c)

Figure 6.11 Final bend angle remained after straightening of annealed strips at different scan speeds and laser power of (a) 1000 W, (b) 900 W and (c) 800 W.

Replicates were performed for the perfect straightening cases. The final bend angle was within the range of 0°–0.13° at laser power of 900 W and scan speed of 800 mm/min for 1.0 mm thick strips, 0°–0.16° at laser power of 1000 W and scan speed of 800 mm/min for 1.5 mm thick strips and 0°–0.12° at laser power of 1000 W and scan speed of 800 mm/min for 2 mm thick strips. All cases showed good repeatability.

It was observed that annealing improved the process as well as the final results. Due to the implementation of Scheme 1, *i.e.*, fixing the magnet in the single horizontal position, caused significant decrease in processing time; thereby productivity increased. Also the maximum value of final bend angle was much less

than that for stress-relieved and as-formed steel. The reason behind this improvement was the annealing process that removed the residual stresses present in mechanically bent strip. This improvement was also observed in stress-relieved samples. However, due to air cooling sufficient time was not available to release the stresses to a significant level. Hence, annealing is the better option to increase the productivity and quality of product in laser assisted straightening. The final profile shape in case of stress relieved and annealed specimens were either straight or straight with very small incremental step (Type 3 and Type 2 in Figure 6.4).

6.3.7 Microhardness Tests

Figure 6.12 shows the variation of micro-hardness of as-formed straightened strips along perpendicular to laser scanning line for different laser powers and scan speeds. Three readings were taken along thickness direction from top (irradiated side) and average results were reported. For fixed laser power of 900 W, hardness decreases with increase in scan velocity from 800 mm/min to 1000 mm/min. Lower scan speed contributes to more heating of material and increases the hardness. For fixed laser scan speed value of 900 mm/min, hardness value increases with the increase in laser power from 800 W to 1000 W. Higher laser power contributes to higher heating of material and increases the hardness. The maximum hardness is 205 HV at laser irradiated region. The hardness decreases as the distance from the laser heating line increases and the minimum hardness is 130 HV at both the edges. The average hardness value of the base material was 130 HV. The maximum hardness of the mechanically bent specimen was 170 HV. Thus, there is the maximum 21% increase in the micro-hardness due to thermo-mechanical effect of laser straightening.

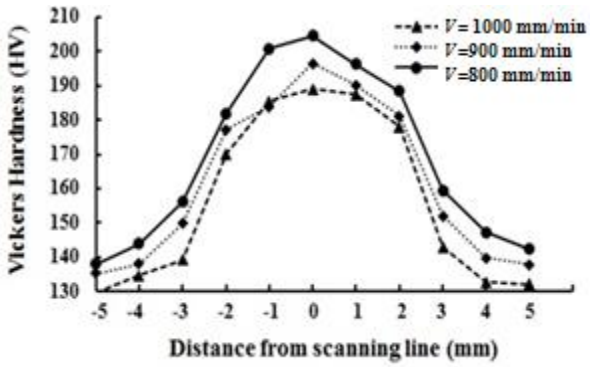

(a)

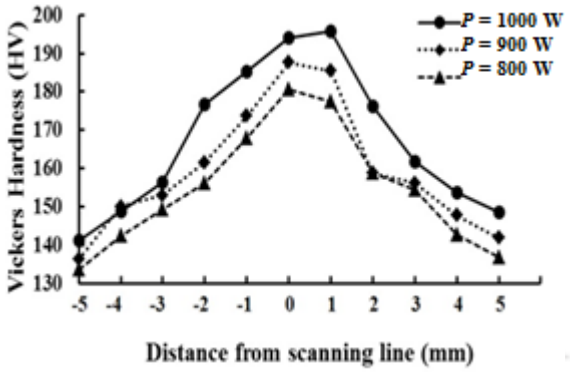

(b)

Figure 6.12 Micro-hardness profiles of the laser straightened strips at different (a) scan speeds and (b) laser powers for as-formed straightened strips

Figure 6.13 shows the variation of micro-hardness along perpendicular to laser scanning line of stress-relieved straightened strips. For fixed laser power of 900 W, hardness value decreases with increasing scan velocity from 800 mm/min to 1000 mm/min (Figure 13a). Again for fixed laser scan speed of 900 mm/min, hardness value increases with increase in laser power from 800 W to 1000 W (Figure 13b). Lower scan speed and higher laser power contributes to higher heating of material and increases the hardness. The maximum hardness value is 221 HV at laser irradiated region. The value decreases as the distance from the laser heating line increases and is the minimum at 151 HV at both the edges. Due to stress-relieving operation the hardness value increased compared to the as-formed steel.

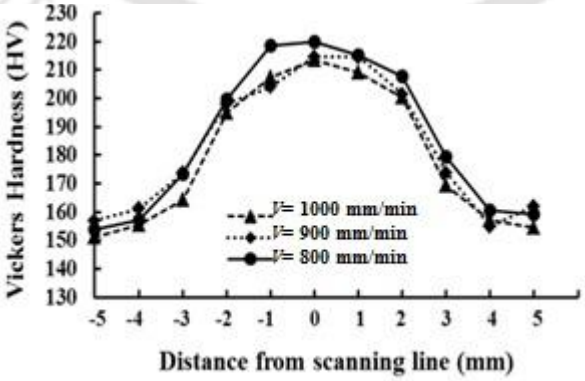

(a)

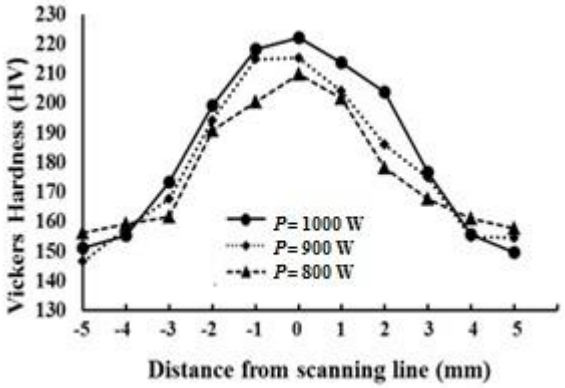

(b)

Figure 6.13 Micro-hardness profile of the laser straightening process at different (a) scan speeds and (b) laser powers for stress-relieved straightened strips

Figure 6.14 shows the variation of micro-hardness along perpendicular to laser scanning line of laser irradiated specimens with annealing. For fixed laser power value of 900 W, hardness value decreases with the increase in scan velocity from 800 mm/min to 1000 mm/min (Figure 6.14a). Again for fixed laser scan speed value of 900 mm/min, hardness increases with the increase in laser power from 800 W to 1000 W (Figure 6.14b). Lower scan speed or higher laser power contributes to higher heating of material and increases the hardness. The maximum hardness value is 178 HV at laser irradiated region. This is only 5% greater than the maximum hardness in the mechanical bent sheet. The value decreases as the distance from the laser heating line increases and reaches the minimum of 102 HV at both the edges. Due to annealing the hardness value decreases. Hence the process becomes convenient for achieving straightening.

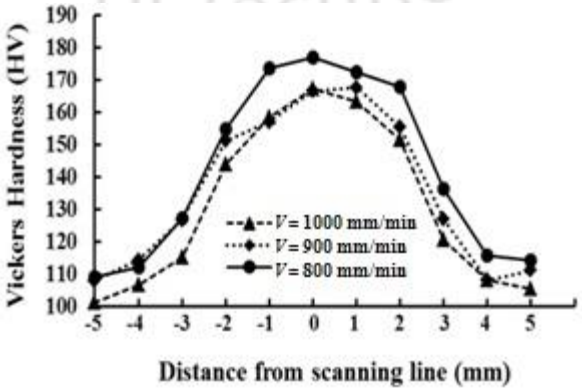

(a)

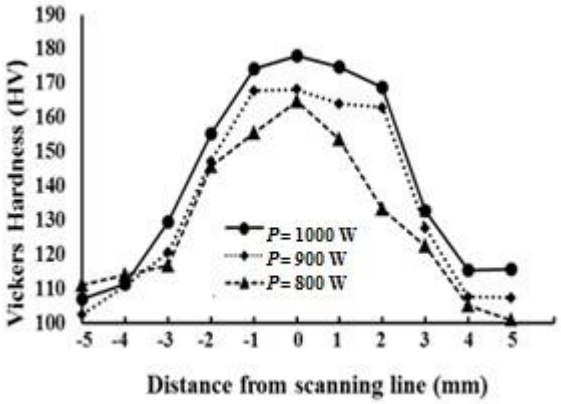

(b)

Figure 6.14 Micro-hardness profile of the laser straightening process at different (a) scan speed and (b) laser powers for annealed straightened strips

6.3.8 Microstructure evolution

Figure 6.15 (a–c) shows the optical microstructure of magnetic-force-assisted laser straightened as-formed strips along thickness direction with Scheme 3 at a laser power of 1000 W and scan speed of 800 mm/min. The study was confined to the laser irradiated zone and its vicinity only. The heat affected region showed a smaller average grain size of 14 µm (Figure 6.15b) as compared to the base material region with average grain size of 26 µm (Figure 6.15 a). The deformed and elongated grain was formed due to mechanical bending applied in the laser irradiated region as shown in Figure 6.15 (c). During laser straightening the heating time was not sufficient for reformation of the grain at that region. Figure 6.16 shows high resolution views for laser irradiated zones. At ×100 magnification, bigger grains were observed. Further small grains are seen in SEM image at ×5500 magnification (Figure 6.16 c) with very small average grain size of 1.25 µm.

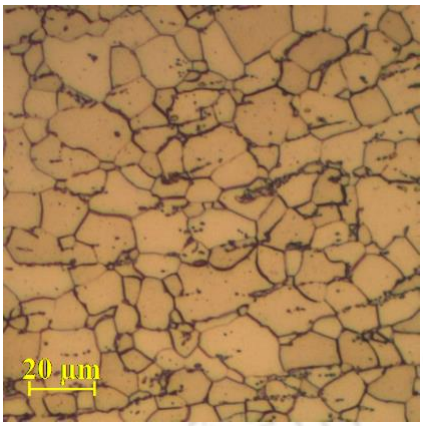

(a)

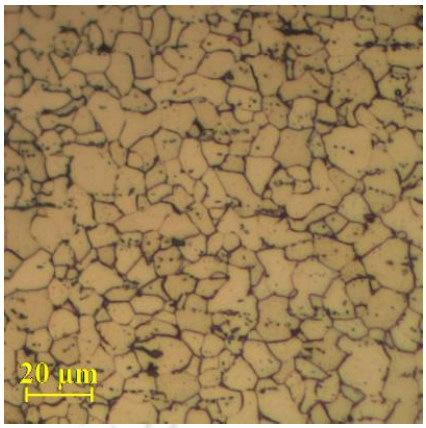

(b)

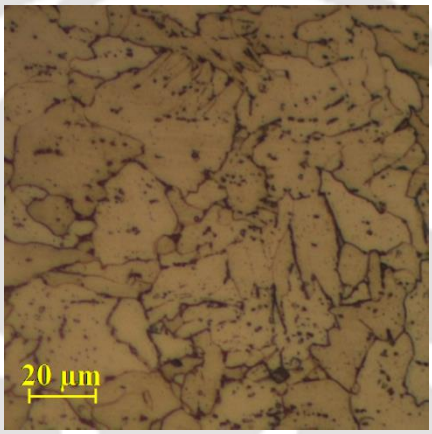

(c)

Figure 6.15 Optical microstructures (X50 magnification) along thickness for as-formed specimens: (a) base plate (un-deformed region) (b) heat affected region and (c) laser irradiated region

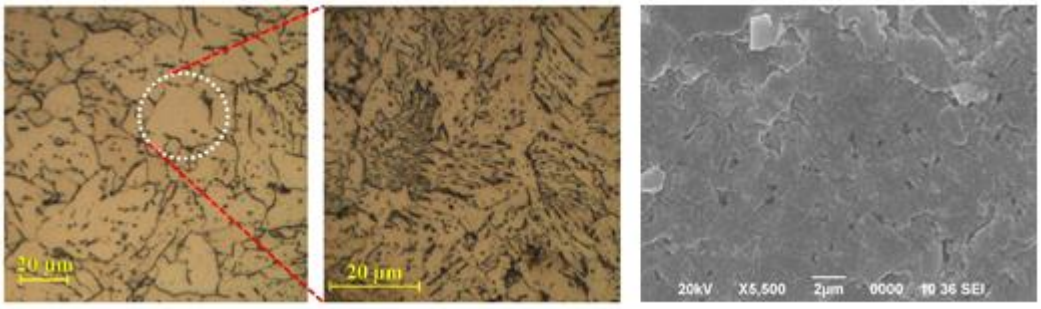

(a) (b) (c)

Figure 6.16 Microstructures at laser irradiated region for as-formed specimen: (a) ×50 magnification with optical microscope (b) ×100 magnification with optical microscope and (c) ×5500 magnification with SEM

Figure 6.17 **(**a–c) shows the optical microstructure of magnetic-force-assisted laser straightened stress-relieved strip along thickness direction at a laser power of 1000 W and a scan speed of 800 mm/min. The laser irradiated region showed fine grain size (Figure 6.17c) with average grain size of 16 µm compared with the base material region (Figure 6.17 a) having average grain size of 41 µm. The transition of base material to laser irradiated region with transition in grain size can be clearly seen in Figure 6.17 b. It can be observed that due to stress-relieving operation grain size is smaller in center but larger in the base material region. Also in stress-relieving operation, the grain size and grain boundary was not uniform as air-cooling provided insufficient time for grain reformation.

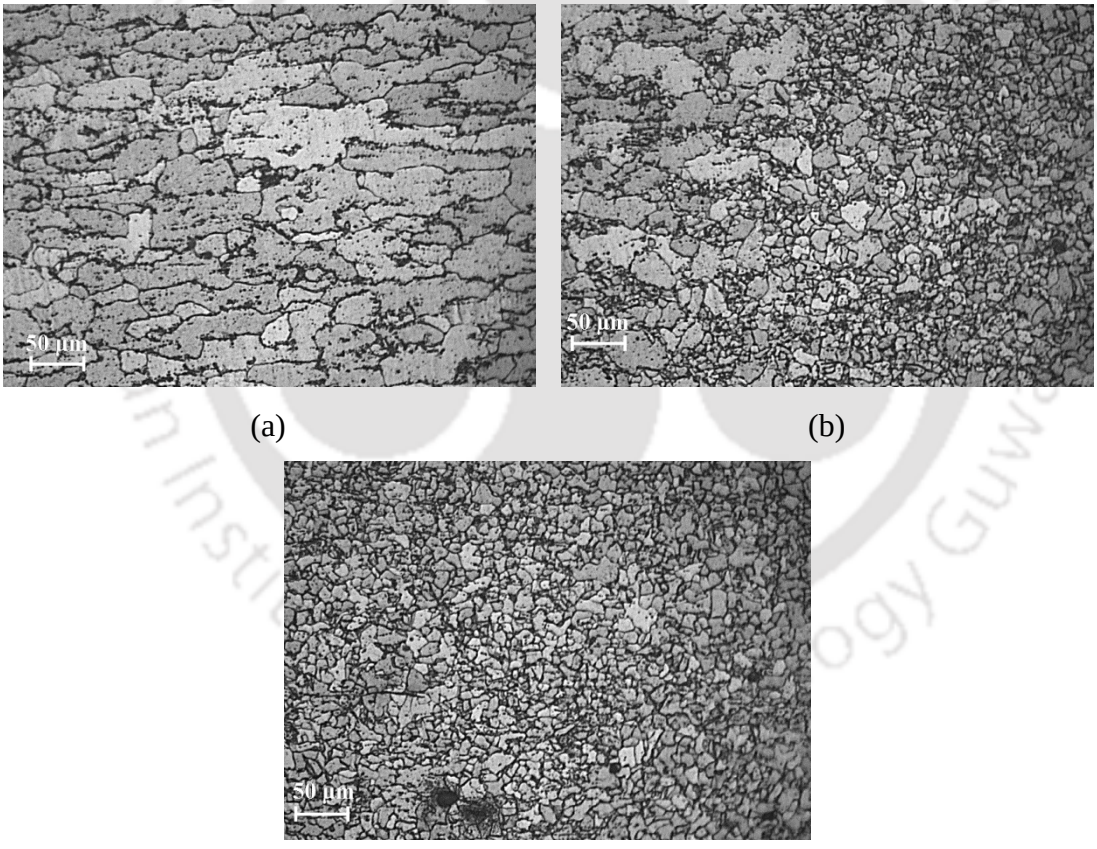

(a) (b)

(c)

Figure 6.17 Optical microstructures along thickness for stress-relieved specimens: (a) base plate (un-deformed region) (×50 magnification) (b) heat affected region (×50 magnification) and (c) laser irradiated region (×50 magnification)

Figure 6.18 (a–c) shows the optical microstructure of magnetic-force-assisted laser straightened subcritical-annealed strips along thickness direction at a laser power of 1000 W and scan speed of 800 mm/min for specimens with annealing. The heat affected region showed smaller grain size (Figure 6.18b) with average grain size of 36 µm compared with the base material region (Figure 6.18 a) having average grain size of 73 µm. The laser irradiated region (Figure 6.18 c) consisted of smaller grains compared to base material region with an average grain size of 27 µm. During annealing uniform and coarse grain reformation occurred throughout the specimen. However, after laser irradiation the grain size in the irradiated and heat affected regions became comparatively smaller.

(a) (b) (c)

Figure 6.18 Optical microstructures at the cross-section for specimens after annealing: (a) base plate (un-deformed region) (×50 magnification) (b) heat affected region (×50 magnification) and (c) laser irradiated region (×50 magnification)

In summary, during furnace cooling, grain reformed into uniform coarse grain with clear grain boundaries as evident from Figure 6.18. In case of stress-relieving by air-cooling, grain structure could not reform perfectly to coarse size as evident from Figure 6.17. However, average grain size of a stress relieved straightened strip was bigger than that of an as-formed straightened strip.

6.3.9 Tensile and Charpy impact tests

The tensile and Charpy impact tests were carried out on raw and straightened strips. In each scheme of straightening, the best straightened samples were chosen. The detail of Tensile and Charpy impact tests was given in Chapter 3. The results of

the ultimate tensile strength (UTS) and the maximum percentage elongation and Charpy impact values are reported in Table 6.5. It is observed that UTS of the annealed and straightened strip is almost the same as that of the raw (before bending) strip. Therefore stress-relieve and annealing treatment did not change the ductility of the material significantly. After straightening as-formed and stress-relieved strips, 15-16% reduction in UTS was observed due to thermo-mechanical processing that generates internal stresses. However, the maximum elongation is about 25% in all the cases. This indicates that although there is some enhancement in hardness during the process, the ductility is unaffected.

Table 6.5 Ultimate tensile strength, the maximum percentage elongation and Charpy impact value of various strips

Strip / Property	Raw (Base material)	As-formed straightened	Stress-relieved straightened	Annealed straightened
UTS (MPa)	352	300	297	355
Maximum elongation (%)	25.1	25.1	24.8	25.2
Impact value (J)	166	148	143	162

The Charpy impact value of raw strip was 166 J. The impact value reduced to 148 J and 143 J for as-formed and stress-relieved straightened strip, respectively. However, when the straightening was carried out after annealing, the impact value came out to be 162 J, which is only about 2% less compared to impact value of raw strip. Annealing relieves the residual stresses and increases the toughness. Without annealing, the residual stresses are not relaxed. Tensile residual stresses enhance the chances of fracture, thus reducing the toughness. Overall, it is ascertained that there is no significant deterioration of mechanical properties during the straightening of the annealed strips.

6.3 Conclusion

The magnet-assisted-laser straightening process is an effective and efficient process. It can contribute to higher production with better efficiency. Use of proper heat treatment also enhances the process and material properties significantly. Study

of microstructure and mechanically showed that there was no serious adverse effect of magnetic-force-assisted laser straightening upon material properties. In some cases, the hardness increased without reduction in the ductility. The following are the specific conclusions:

1. Magnetic-force-assisted laser straightening was much more efficient than conventional laser straightening due to decrease in the number of laser passes than conventional straightening. A bend angle of 15° could be straightened with 4 passes only compared to conventional one which took 10–15 passes for the same set of process parameters.
2. It is possible to achieve desired straightness with proper selection of process parameters and heat treatment process. The best straightening was obtained when the bent strips were annealed. For 1 mm thick strip, the best performance was obtained at 900 W laser power and 800 mm/min scan speed. On the other hand, for 1.5 mm and 2 mm thick strips, the best parameters were 1000 W laser power and 800 mm/min scan speed. Hence, it is important to select proper process parameters for each job.
3. Micro-hardness value increased in the case of straightened as-formed and stress-relieved strips, while it increased only marginally in the case of straightened annealed strips. Micro-hardness value was the highest in the vicinity of the laser scan line and kept on reducing while moving away from the scan line.
4. The microstructure showed smaller grains in the heat affected zone and coarse grain size in the base material region in all three types of samples. In the laser irradiated region, grains were elongated and deformed with small grain size for straightened as-formed strips. The grains were fine in case of stress-relieved and annealed straightened strips in laser irradiated region. However, grain size of stress-relieved specimen was smaller than annealed specimen.
5. Although annealed strips provided the overall best performance in straightening, the annealing process takes more time and may not be feasible in some cases. Stress relieving can be a better option in those cases.

Prima facie the proposed magnetic-force-assisted laser straightening appears to be a potential industrial-scale process. It is specifically suitable for straightening of micro components, even in the assembled form. For bigger jobs, instead of permanent magnet, an electro-magnet can be employed. As the laser heating reduces the flow stress of the material drastically, the power of the electromagnet need not be very high. Use of electromagnet assisted bending and straitening is discussed in Chapter 7.

Chapter 7

Laser Assisted Bending and Straightening by Electromagnetic Force

7.1 Introduction

Use of laser for bending different metallic and non-metallic components is an emerging and important subject of several researchers since last three decades. In ship building industries, laser based bending can replace flame or roll bending processes in the fabrication of hull, enhancing the accuracy and productivity. In automotive industries, it can be used for forming as well as distortion correction of car body panels and doors. Automotive industries have started using magnesium alloys due to their high specific strength. However, magnesium alloys possess poor formability during mechanical bending, thus making a strong case in favor of laser based bending. In aerospace industries, laser based forming can be used to fabricate structures made of aluminum and titanium. It can also be used in forming compressor blades. Although there is no comprehensive report in open literature on the existing share of laser forming in manufacturing sector, information staggered in various research papers and a number of funded projects indicate its growing importance. Different process parameters such as laser power, scan speed, laser beam spot diameter and number of scans greatly influence the process. The main challenge is to make the process accurate and efficient. Hennige et al. (1997) proposed a methodology to enhance accuracy of bend angle. The process efficiency may be improved in different ways. Enhancing the absorptivity by different coatings is one of the ways Gautam et al. (2015). Another way is to implement laser assisted bending where assisting load is used to support the deformation process.

This study is inspired from the work carried out by Fetene et al. (2017).They used permanent magnets to enhance efficiency of laser bending; however, process produces a permanent attraction between magnet and workpiece. It creates problem while fixing and removing the workpiece. Moreover, due to the action of magnetic force the final bend may vary during unloading, which may affect the accuracy of the process. In this work, an electromagnetic force has been used to assist the laser bending and straightening process. Controlled magnetic force was applied along with laser heating that does not require physical contact and can reach to inaccessible areas. Possibility for simulation of a newly proposed methodology is also an important aspect. There are a number of attempts to simulate laser bending (Vivek et al. 2011 and Eideh et al. 2015). In this work, along with the experimental work, it was demonstrated that the process could be simulated with a fair degree of confidence.

Objective of this work is to achieve desirable bending and straightening by suitable laser assisted bending process. An electromagnet was developed to provide controlled assisting force. The force measurement was performed and force equation was also developed. Thereafter experimental analysis on laser assisted bending and straightening with simulation was performed. Then effect of parameter and study on edge effect was performed. Later microhardness testing was also performed.

7.2 Magnetic Force Measurement Based on Current and Air Gap

Magnet pulling force strength is affected by material properties, air gap (distance between magnet and work plate), thickness and electric current. Magnetic saturation in the plate limits the effective attractive force between the workpiece and electromagnet. This section elaborates about development of electromagnet and the setup for electromagnetic force measuring.

7.2.1 Development of the electromagnet

For this work an electromagnet was developed as shown in Figure 7.1. Depending on the requirement, electromagnet may have different shapes and sizes. For the present work, an electromagnet has been designed with specific dimensions suitable for the job. As shown in Figure 7.1, the electromagnet had two main

components— the core and the coil. A number of very thin sheets called laminations are fixed together to form this core. The material of the core is similar to the non-grain oriented electrical steel used in electrical machines. The reason the for use of sheets is to minimize the eddy current loss. Due to the excessive eddy current loss, high heating and other problems may appear during application, which may lead to deterioration of the winding. The coil is composed of laminated copper wire of 22 gauge dia wrapped with 900 turns around the core. The operating condition for the electromagnet is 12 V direct current (DC) and range of current is 1−7 A.

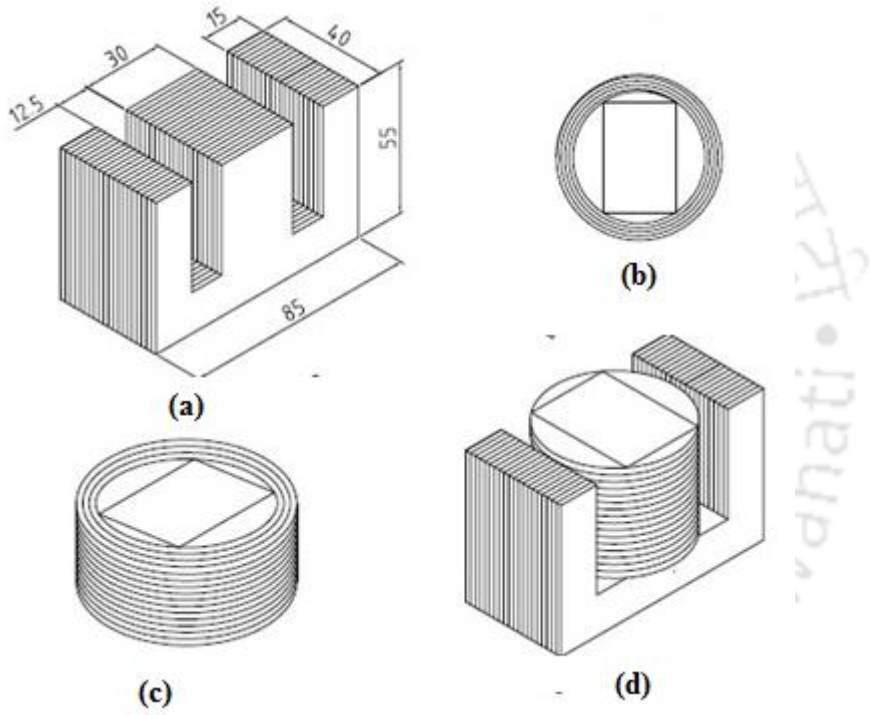

Figure 7.1 Electromagnet (a) core composed of laminations (b) coil wrapped in core (top view) (c) coil wrapped in core (isometric view) and (d) the complete assembly. All dimensions are in mm.

7.2.2 Electromagnetic force measuring setup

Magnetic force of attraction is affected by air gap (distance between the magnet and work plate) and workpiece thickness as reported by Fetene et al. (2017). Magnetic flux saturation in the plate limits the effective attractive force between the work plate and magnet. Figure 7.2 shows a setup for measuring the magnetic force. The setup was developed for the measurement of magnetic force. As shown in

Figure 7.2, it consists of a metal strip free at one end and other end fixed by a hinge. The electromagnet was kept below the work strip. The gap between the magnet and strip can be changed according to the requirement. The free end is connected to a weighing scale while the other end of scale was fixed to the arm of the stand as shown. Due to electromagnetic force the free end was attracted and the force displayed in the digital scale was recorded. The net magnetic force was measured at the following gaps between the bottom surface of the workpiece and the top surface of the magnet: 5, 10, 15, 20, 25 and 30 mm. Details of electromagnetic force measurement are discussed in Section 7.4.1

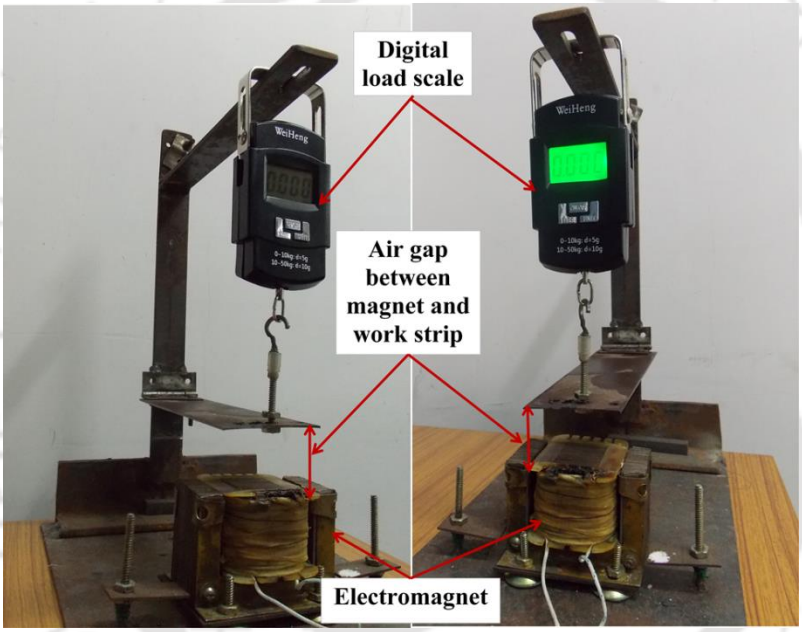

Figure 7.2 Experimental setup to measure the magnetic force on work plate with variable applied current

7.3 Experimental Plan

For electromagnetic force assisted bending by laser, the strip was properly clamped on one side. The magnet holder was at the top side of the workpiece as shown in Figure 7.3. The magnet holder could easily be moved up and down though a slot for varying the distance between magnets and workpiece. During laser irradiation, the electromagnet was activated by using a switch. A 12 V DC source, connecting wire, a rheostat and an ammeter was also used to get a controlled current for generating required electromagnetic force. The gap between the top surface of

the workpiece and magnets was initially 20 mm. The experiments were performed on a 2.5 kW continuous wave mode CO_2 laser machine (Make: LVD, Model: Orion 3015). The laser beam was irradiated at a distance of 100 mm away from free end (Middle of the strip). After the laser beam irradiation, the heated specimens were allowed to cool naturally. For straightening of bent strip, one side of each specimen was fixed at a fixture in a cantilevered way. The free end of the strip was kept below the electromagnet. For all the experiments AH36 steel strips were used.

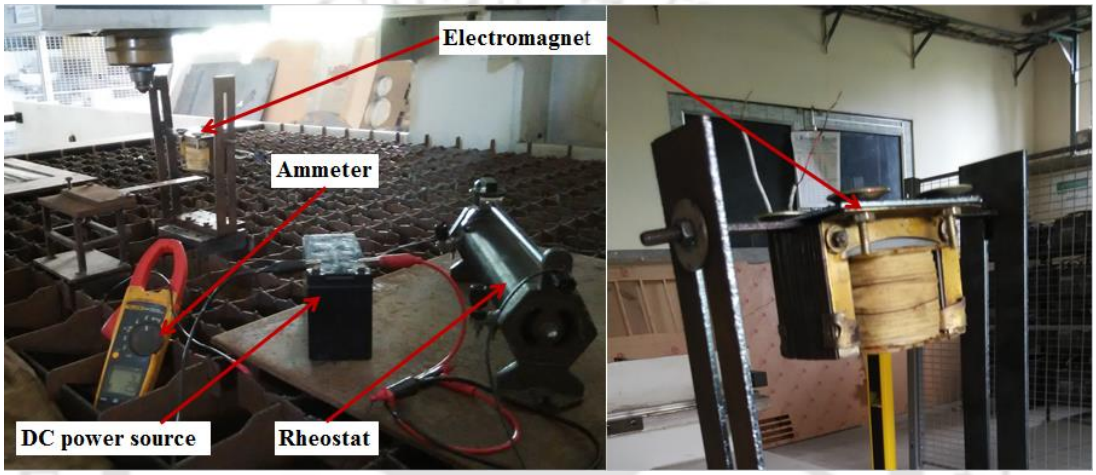

Figure 7.3 Experimental setup with electromagnet

The CO_2 laser has been utilized at different laser parameters. The experiments were carried out at different process parameters as listed in Table 7.1. The process parameters are as follows: laser power (*P*), laser beam diameter (*D*), scan speed (*v*), applied current (*I*) and air gap (*G*).

Table 7.1 Experimental and simulation process parameters

Parameters	Symbol	Unit	Values
Laser power	*P*	W	500–1000
Laser beam diameter	*D*	mm	3.87 (fixed)
Scan speed	*v*	mm/min	500–1000
Current	*I*	A	3, 4, 5, 6 and 7
Air gap	*G*	mm	5, 10, 15, 20, 25 and 30

7.4 Results and Discussion

In this section experimental as well as simulation results are discussed. A comparison between two results is made. The simulation procedure is already discussed in Chapter 3. The result clearly demonstrates effectiveness of the proposed process.

7.4.1 Magnetic force result based on current and air gap

The magnetic force of attraction has been measured using the setup as explained in Figure 7.2. For different air gap, i.e. 5 mm, 10 mm, 15 mm, 20 mm, 25 mm and 30 mm, the force of attraction and its variation with applied current were measured. The variation in current was taken in the increments of 0.5 A for each gap as shown in Figure 7.4. As shown in the figure, for a fixed distance magnetic force of attraction increases with increase in applied current.

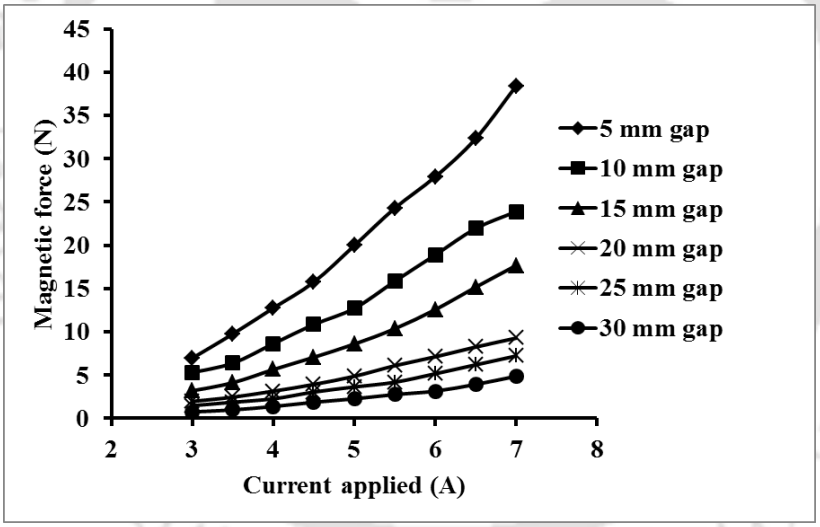

Figure 7.4 Change in magnetic force with applied current for different air gaps

It was observed that electromagnetic force of attraction is a function of applied current and air gap between magnet and workpiece. Considering force as a function of current and distance, an equation was fitted as

$$F = 0.00186 I^{1.98} G^{-1.19}, \quad 7.1$$

where F is electromagnetic force of attraction, I is the applied current and G is the air gap between workpiece and magnet. However, while comparing with experimental results, this equation provides up to 25% variation. Also the curve fitting was done with R^2 value of 0.95. Therefore, considering individual gap,

individual equations were fitted as shown in Table 7.2. Such approach provides very less error with high R^2.

Table 7.2 The equation for each gap considering force as function of current (I)

Gap (mm)	Equation	R^2
5	$F = 0.799I^{1.99}$	0.9991
10	$F = 0.0.654I^{1.863}$	0.9963
15	$F = 0.334I^{2.03}$	0.9987
20	$F = 0.232I^{1.899}$	0.9974
25	$F = 0.174I^{1.892}$	0.9949
30	$F = 0.682I^{2.171}$	0.9966

7.4.2 Validation FEM results with experimental results

Effect of parameters on variation of final bend angle has been evaluated both experimentally and numerically. Figure 7.5 shows a comparison between the simulation and experimental results of the final deformed shapes of the strip. The experiment has been carried out at a laser power of 750 W, scan speed of 600 mm/min, current of 4.5 A and an air gap of 20 mm. The same parameters have been considered for the numerical simulation by taking an absorptivity of 0.67. Both the simulated and experimental profiles looked identical. In fact, superimposition of simulated image on experimental image makes them indistinguishable. Experimental bend angle was measured as 10.03° against the simulated bend angle of 9.56°. Thus, the deviation between the experimental and numerical bend angles was 4.7%.

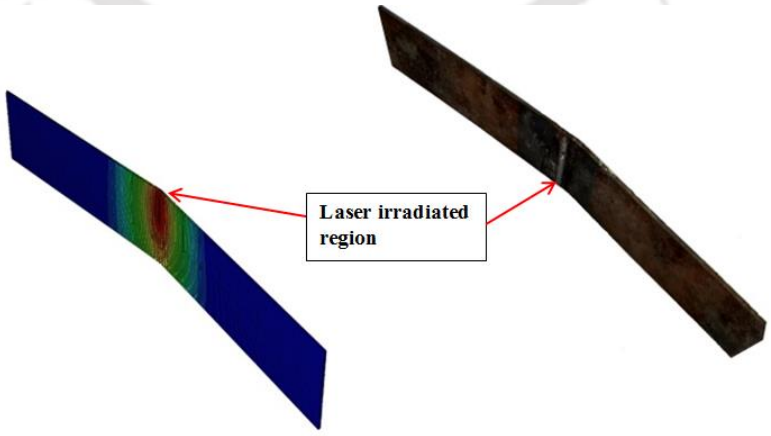

Figure 7.5 Comparison for deformed shape of work strip after bending for both simulation and experimental results with isometric view

Figure 7.6 a−c show the experimental and simulation result of bend angle for 1 mm, 1.5 mm and 2 mm thick strip at different laser power. It is observed that the bend angle increases with the increase in laser power. The maximum bend angle is obtained in case of 1 mm thick strip. Bend angle remained almost constant after a laser power of 800 W. Similar trend was observed in the case of 1.5 and 2 mm strips also at different laser powers. The maximum bend angles were obtained at the maximum laser power of 1100 W— 10.97°, 8.03° and 5.2° for 1, 1.5 and 2 mm thick strips, respectively. Here some melting was observed. However, in all the three cases, the maximum bend angles without any melting were obtained at considerably low power level. For 1 mm thick strip at 650 W laser power maximum bend angle of 8.8° was achieved. Similarly for 1.5 and 2 mm strip maximum value of bend angle

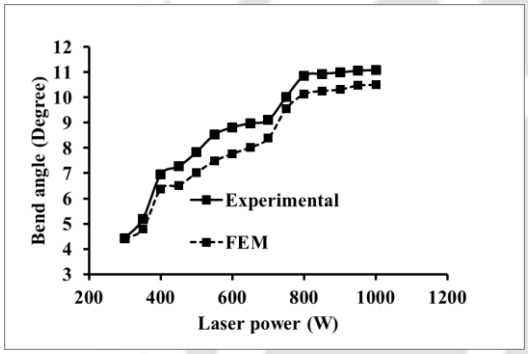

(a)

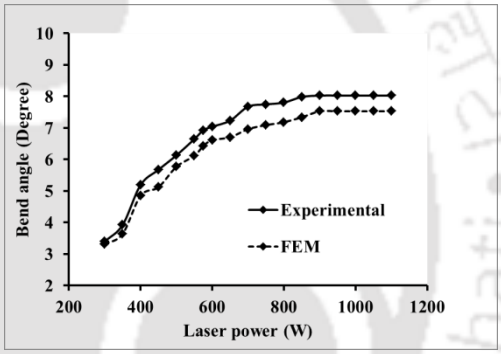

(b)

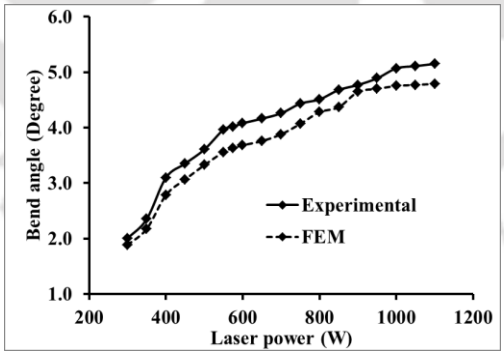

(c)

Figure 7.6 Comparisons of experimental and simulation results for bend angle with change in laser power at 600 mm/min scan speed and 4.5 A applied current for (a) 1 mm (b) 1.5 mm and (c) 2.0 mm strip thickness. In all the cases, air gap between strip and magnet was 20 mm.

without any melting were 7.70° and 4.8° were obtained at 750 W and 900 W respectively. In all types of strips, after a specific value of laser power, the strip got attached to the magnet. It resulted almost uniform bend angle after that laser power.

Laser scan speed has significant effect on bend angle when laser power and applied current are kept fixed. In the case of 1 mm thick strip for the scan speed range of 500–800 mm/min, laser irradiated strip attached with magnet due to magnetic force and the softening of the material at the scanning line. Similar trends were observed in case of 1.5 mm and 2 mm strip with scan speed range of 500–700 mm/min for both. However, above this scan speed range, the work pieces did not attach with magnet. Figure 7.7 shows that the bend angle increased with decreasing scan speed for all strips. Good agreement between simulations with experimental

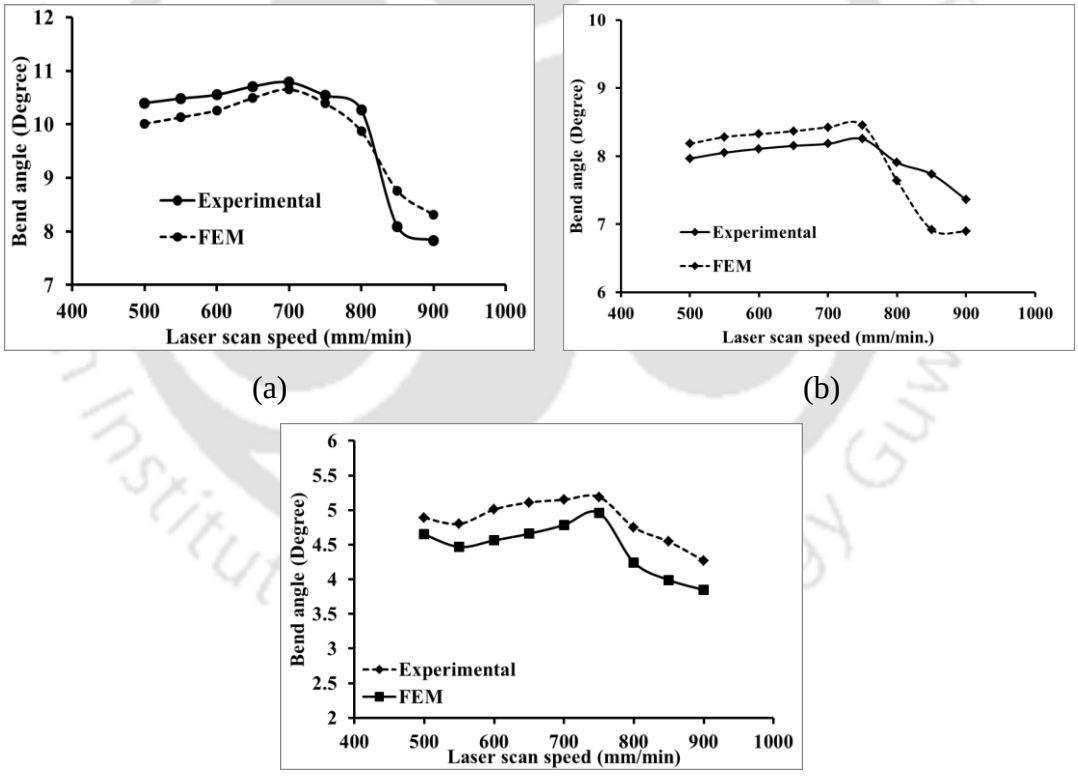

Figure 7.7 Comparisons of experimental and simulation results for bend angle with change in scan speed for fixed power of 900 W and 4.5 A applied current for (a) 1 mm (b) 1.5 mm and (c) 2.0 mm strip thickness. In all the cases, air gap between strip and magnet was 20 mm

result was obtained. For a specific range of scan speed the bend angle was almost uniform. The reason was that in all such cases the strip got attached to the magnet.

The gap between workpiece with magnet also affects the bend angle. Figure 7.8 shows change in bend angle with change in air gap for fixed parameters— 800 mm/min scan speed, 900 W power and 4.5 A applied current. For 1 mm and 1.5 mm strip the maximum bend occurred in the range of 20−25 mm air gap. For 2 mm the maximum bend occurred in 15 mm air gap. The gap should be judiciously selected considering the current and strip thickness.

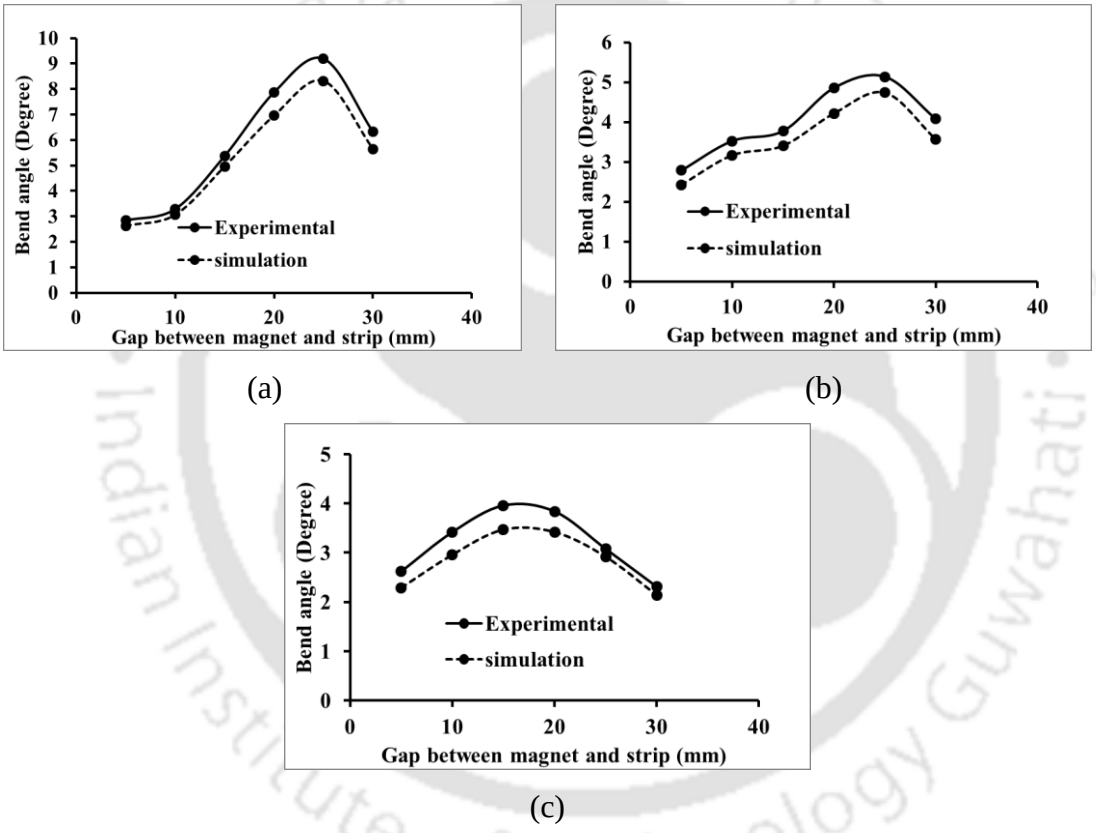

Figure 7.8 Comparisons of experimental and simulation results for bend angle with change in gap at 800 mm/min scan speed, 900W power and 4.5 A current for (a) 1 mm (b) 1.5 mm and (c) 2.0 mm sheet thickness.

Figure 7.9 shows influence of applied current on bend angle for different thickness of strip thickness. Applied current has significant effect on bend angle. Three cases were considered with three different levels of powers and scan speeds— (1) high power of 1000 W and low speed of 500 mm/min, (2) moderate power of 750 W and moderate speed of 750 mm/min and (3) low power of 500 W and high

speed of 1000 mm/min. In case 1, higher bend angle was achieved, even at low current. In case 2, required current also has to be medium range for higher bend angle. In case 3, due to low power and high scan speed, required current was very high for achieving higher bend angle. It can be observed that strip with higher thickness (2 mm) did not bend sufficiently even at higher current of 7 A.

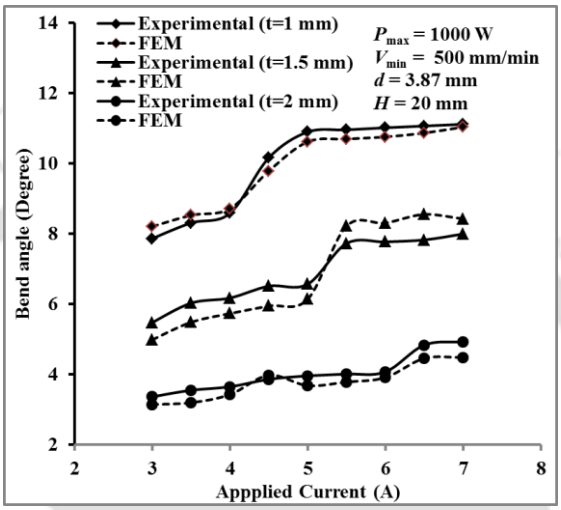

(a)

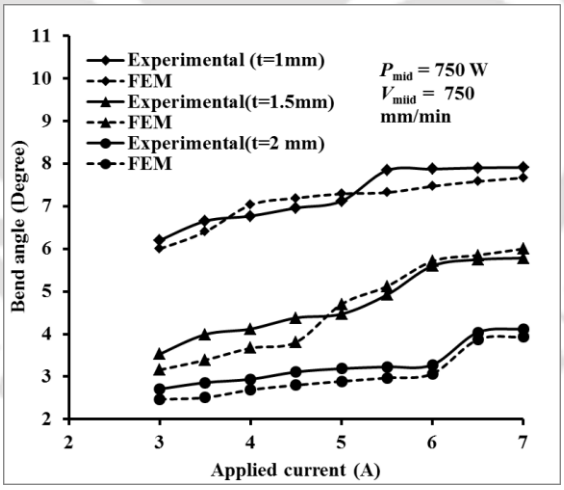

(b)

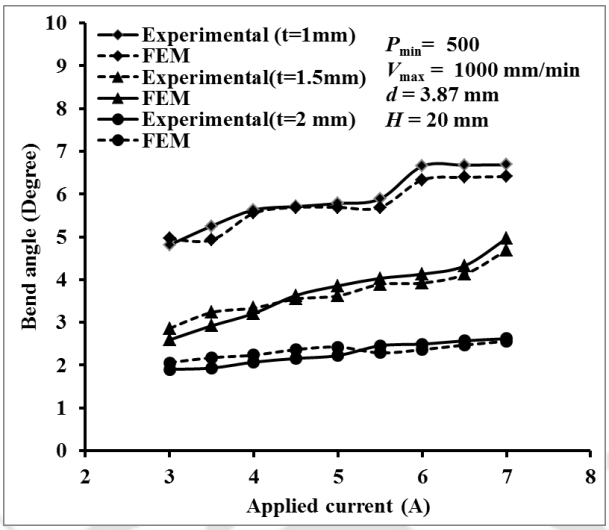

(c)

Figure 7.9 Bend angle versus applied current for (a) case1 (b) case 2 and (c) case 3

7.4.3 Edge effect

The variation of the bend angle along the laser scan direction (width direction) is called edge effect. It should be minimized for better quality of the product. Figure 7.10 shows the simulated and experiment bend angles along the laser scan directions. A good agreement is observed between them. It was observed that laser power, scan speed and applied current of magnet significantly affect the edge effect. The edge effect is lesser in case of high applied current, higher laser power and lower scan speed. In all three cases, the strip got stuck with the magnet and was not allowed to move freely. In a way, magnets acted as a fixture that restrained the movement of strip. Thus, uniform bend angle was obtained along the width direction.

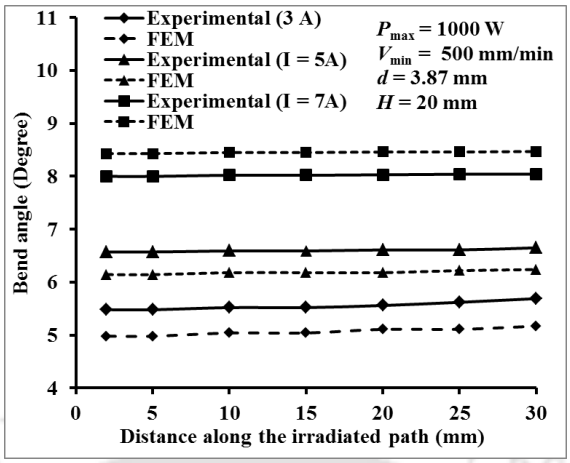

(a)

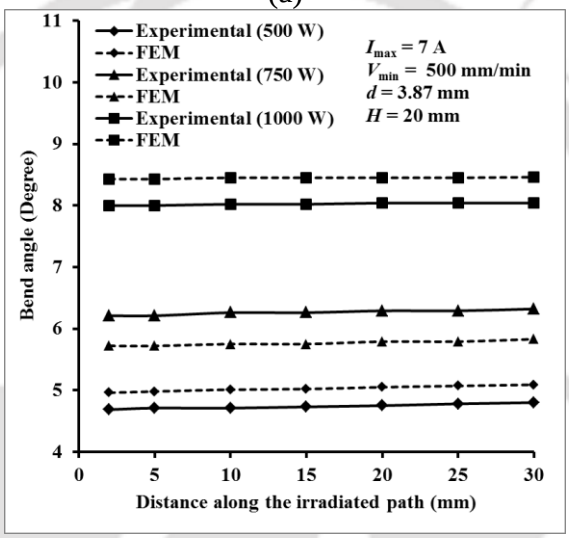

(b)

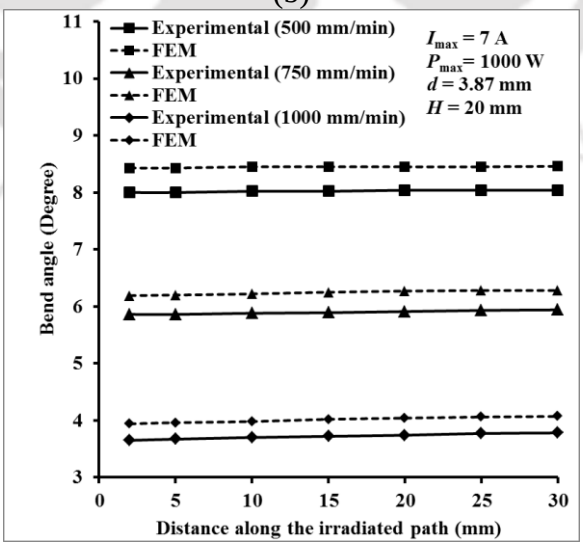

(c)

Figure 7.10 Variation of bend angle along the scan direction with (a) variation of current (b) variation of laser power and (c) variation of scan speed

7.4.4 Microhardness evaluation

Figure 7.11 shows the variation of micro-hardness of AH36 steel strips along perpendicular to laser scanning line for different applied currents, scan speeds and laser powers. Three readings were taken along thickness direction and average results are reported. For fixed laser power value of 900 W, hardness value decreases with increase in scan velocity from 800 mm/min to 1000 mm/min. Lower scan speed contributes to higher heating of material and increases the hardness. For fixed laser scan speed value of 900 mm/min, hardness value increases with increases in laser power from 800−1000 W. Higher laser power contributes to higher heating of material and increases the hardness. The maximum hardness value is 195 VHN at laser irradiated region. Micro-hardness also increases with increase in applied current with fixed value of laser power and scan speed. This occurs due to higher force of attraction due to increase in applied current which may lead to small plastic deformation along scanning line. In all cases, the hardness value decreases as the distance from the laser heating line increases and the minimum hardness value was about 130 VHN at both the edges.

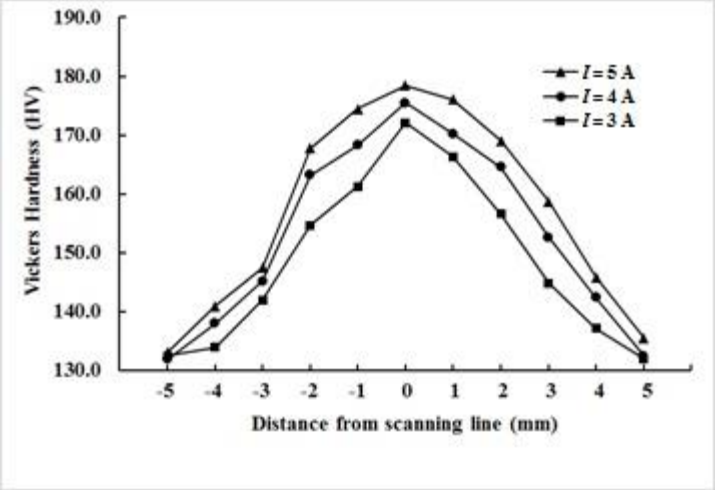

(a)

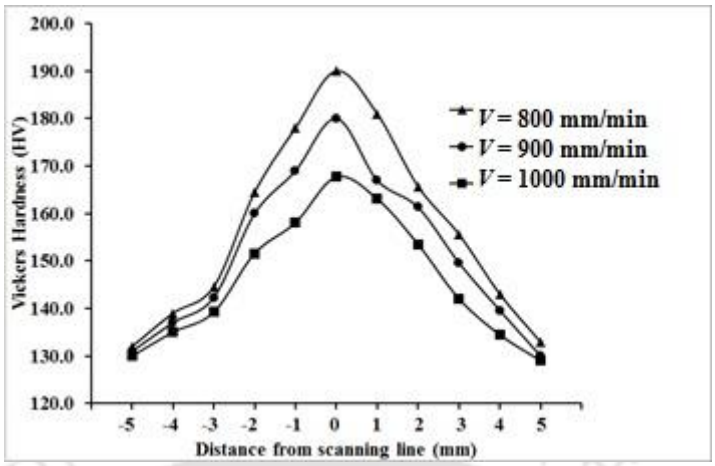

(b)

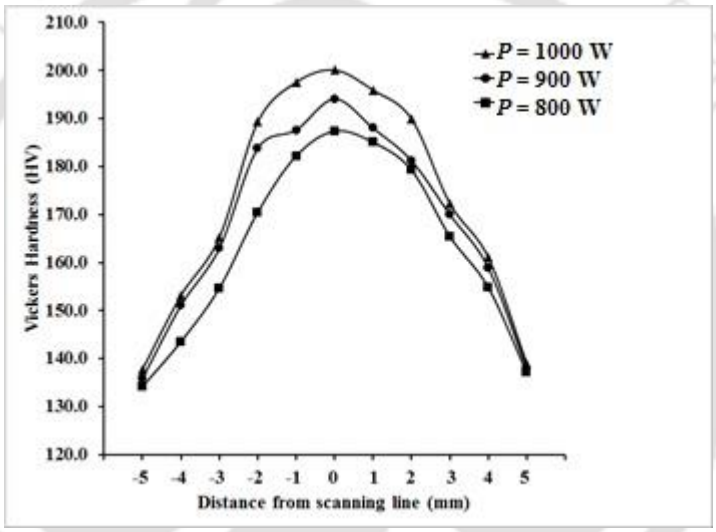

(c)

Figure 7.11 Change in micro-hardness with change of (a) applied current (b) scan speed and (c) laser power

7.4.5 Result of laser assisted straightening

Initial experiments with laser power of 1000 W, scan speed of 800 mm/min and laser beam diameter of 3.87 showed that only 3 passes were sufficient to attain considerable straightening. It was observed that three passes can be applied continuously to get sufficient straightening without any visible defects. As shown in Figures 7.12 and 7.13, in case of 1.5 mm thick strip for laser power of 1000 W, the amount of straightening is the maximum at 6 A applied current for scan speeds of 800 mm/min and 900 mm/min. The amount of straightening decreased with decrease in applied current. Similarly, for 2 mm thick strip, for laser power of 1000 W, the

amount of straightening was the maximum at 6 A applied current for scan speed 800 mm/min. Overall, perfect straightening was obtained in 2 cases and 1 case of 1.5 mm and 2 mm strip, respectively. The final bend angle was within the range of 0°–1.66° in 1.5 mm thick strips and within the range of 0.24°–2.31° in 2 mm strip. The perfect straightening, with no retained bend angle, occurred at a laser power of 1000 W and applied current of 6 A for scan speed of 800 mm/min and 900 mm/min in 1.5 mm thick strips. For 2 mm thick strip, the perfect straightening occurred at a laser. The small negative value in Figure 7.12 and 7.13 represent 0° straightening value. It is shown in this manner to provide clarity.

Table 7.3 Variation of bend angle after straightening with laser power, scan speed and applied current for an initial bend angle of (15°±1°)

Test No.	Laser Power (W)	Scan speed (mm/min)	Applied current (A)	Final bend angle(°)	
				1.5 mm	2 mm
1	1000	1000	4.0	1.57	2.07
2	1000	1000	5.0	0.91	1.25
3	1000	1000	6.0	0.16	0.33
4	1000	900	4.0	1.31	1.83
5	1000	900	5.0	0.78	1.07
6	1000	900	6.0	0	0.24
7	1000	800	4.0	1.12	1.51
8	1000	800	5.0	0.51	0.67
9	1000	800	6.0	0	0.17
10	900	1000	4.0	1.02	1.37
11	900	1000	5.0	0.74	1.02
12	900	1000	6.0	0.11	0.39
13	900	900	4.0	0.89	1.23
14	900	900	5.0	0.47	0.67
15	900	900	6.0	0.13	0.31
16	900	800	4.0	0.74	1.03
17	900	800	5.0	0.46	0.65
18	900	800	6.0	0	0.27
19	800	1000	4.0	1.52	2.07
20	800	1000	5.0	1.19	1.63
21	800	1000	6.0	0.21	0.43
22	800	900	4.0	1.38	1.91
23	800	900	5.0	1.11	1.53
24	800	900	6.0	0.21	0.41
25	800	800	4.0	1.66	2.31
26	800	800	5.0	1.03	1.42
27	800	800	6.0	0.12	0.33

power of 1000 W and scan speed of 800 mm/min only. Variation of bend angle with laser power, scan speed and applied current for 1.5 mm and 2 mm thick strip is shown in Table 7.3.

Replicates were performed for results having perfect straightening (final angle value almost 0°). The final bend angle was within the range of 0.0°–0.12° for laser power of 1000 W and scans speed of 900 mm/min for 1.5 mm thick strip and 0.0°–0.10° for laser power of 1000 W and scan speed of 800 mm/min for 1.5 mm thick strip. The final bend angle was within the range of 0.0°–0.17° for laser power of 1000 W and scan speed of 800 mm/min for 2 mm thick strip. All cases showed good repeatability.

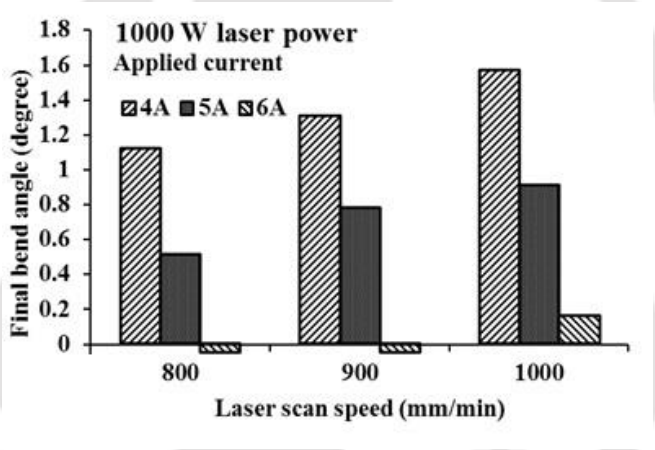

(a)

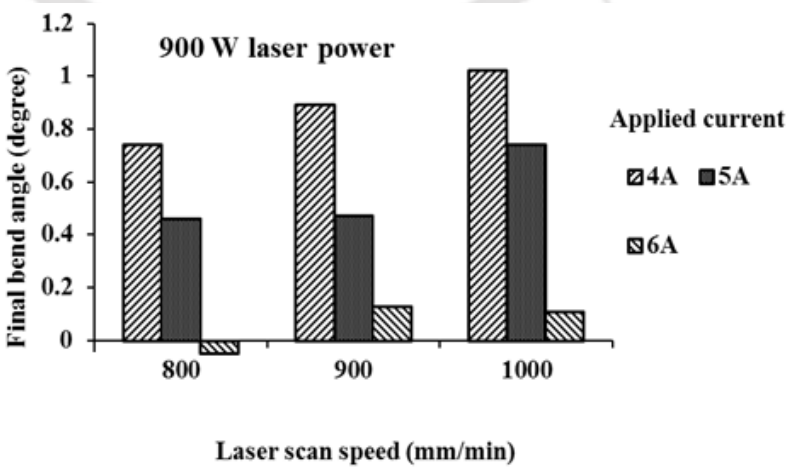

(b)

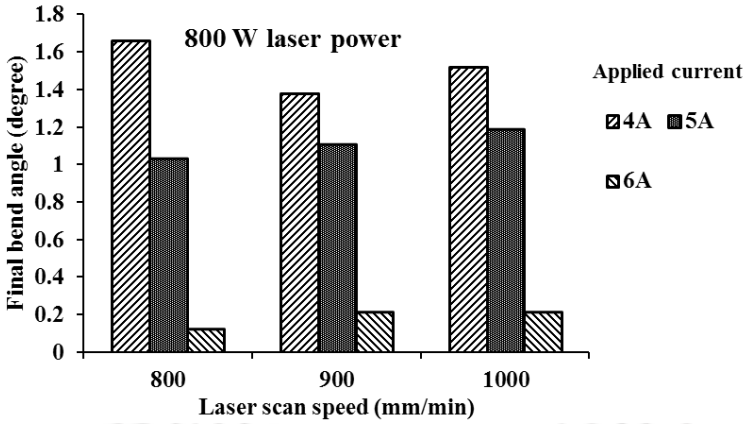

(c)

Figure 7.12 Variation of final bend angle with scan speed for three different schemes at applied current of 4 A, 5 A and 6 A for (a) 1000 W, (b) 900 W and (c) 800 W laser powers. (Thickness =1.5 mm)

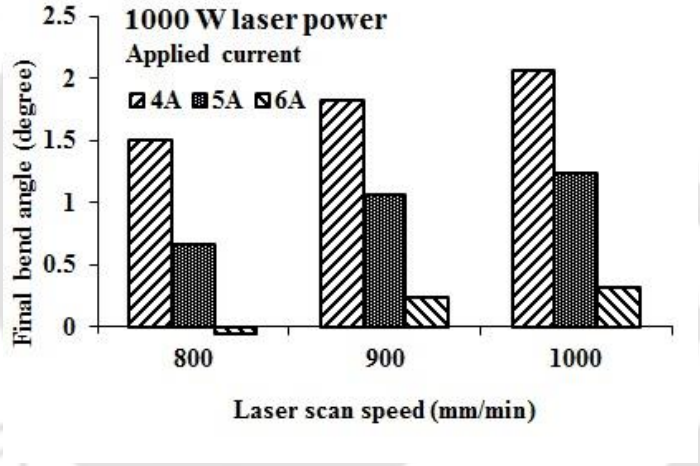

(a)

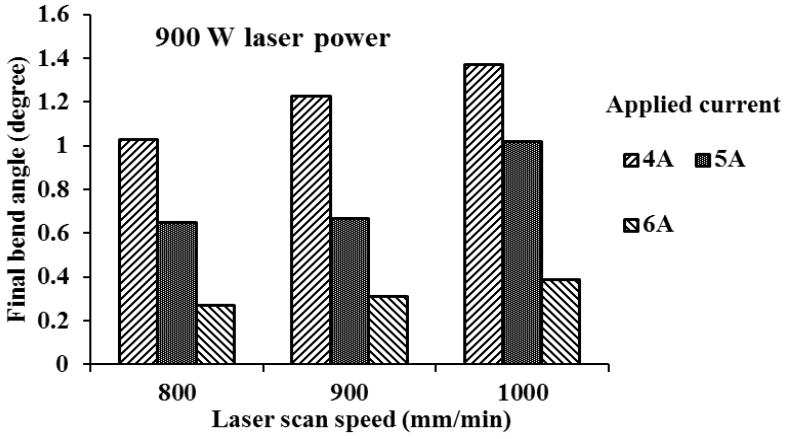

(b)

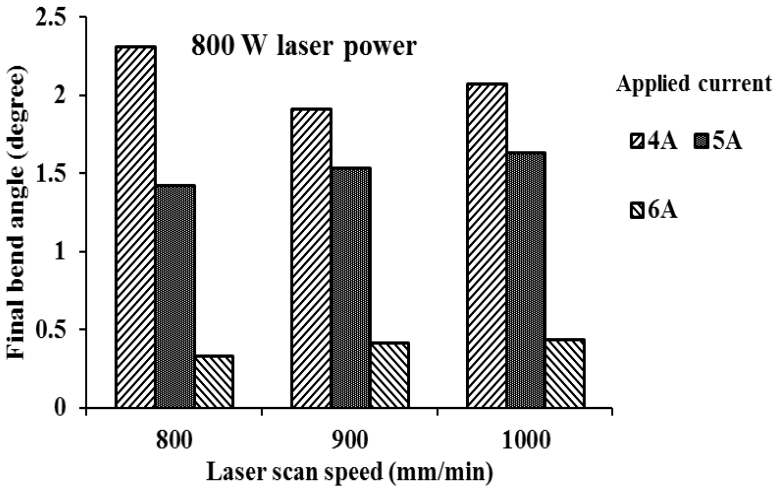

(c)

Figure 7.13 Variation of final bend angle with scan speed for three different schemes at applied current of 4 A, 5 A and 6 A for (a) 1000W, (b) 900 W and (c) 800 W laser powers. (Thickness = 2 mm)

7.5 Conclusion

In this work, a forming process is proposed to obtain large bend angles by laser irradiation with controlled electromagnetic force. The process was also used for straightening of the bent sheets. The following are the salient findings from this work:

- Application of electromagnetic force could result in significant increase in the bend angle. Bend angle increases with increase in laser power and decreases with increase in scan speed for a particular applied current.
- Applied current plays an important role in bend angle. For a specific gap, bend angle increased with applied current up to a certain value. Then it got saturated due to mechanical restriction of movement. Increasing the gap further increased the bend angle.
- The bend angle was the highest at the end of the scan path. At high power, low scan speed and higher magnetic force, the bend angle reached saturation as the plate got stuck with the magnets. This also reduced the edge effect. Thus, the edge effect is very less in electromagnetically assisted laser bending.
- Spring-back effect was less at low scan speed, high laser power and high applied current. In all the cases the strip attached to the magnet during

irradiation. All three parameters contribute to higher bending with less spring back due to the attachment of strip to magnet.

- Micro-hardness increased with an increase in laser power and decreased with increased laser scan speed; in both the cases, generation of higher temperature is responsible for heat treatment. It also shows a moderate increase with applied current as increase in current leads to high force of attraction which may create certain mechanical forming.
- Electromagnetic-force-assisted laser straightening was much more efficient than conventional laser straightening due to decrease in number of laser passes. A bend angle of 15° could be straightened with 3 passes only, conventional unassisted laser straightening took 10–15 passes for the same set of process parameters. It is possible to achieve desired straightness with proper selection of process parameters. In a few cases the best straightening with 0° bend was obtained.

The main advantage of electromagnetic force over other kind of assisting force described in literature is that it can be controlled properly according to process requirement. It can be exactly engaged and disengaged during starting and completion of laser irradiation leading to convenience and accuracy. Other encouraging observation about the proposed electromagnetic force assisted laser bending is that it could be simulated with reasonable accuracy. This is good for the acceptability of the process for industrial implementation. Moreover, a single laser source can be used for cutting, welding, heat treatment and forming, thus increasing the overall production efficiency.

Chapter 8

Epilogue

8.1 Introduction

Laser based bending and straightening are important manufacturing processes in industrial sectors including, automobile, railway, shipbuilding and aerospace industries. Different studies of laser bending and a few on straightening are available in literature. Nevertheless, development of proper multipass bending strategy and verification for accuracy in laser bending, laser assisted straightening of bend strip by permanent magnet and laser assisted bending and straightening by electromagnet was not explored methodically. To understand the process and based on the research gap recognized in the literature, present work was carried out. In this thesis, experimental study and numerical simulations were carried out on the laser bending as well as laser assisted bending and straightening processes. The result of laser bending or straightening is dependent on process parameters and workpiece geometry. Therefore systematic approach was used for enhancement of performance in accuracy and efficiency of the process.

8.2 Overall Conclusion

Initially enhancement in bend angle produced in multi pass laser bending was done by using black spray paint. This process was modelled numerically and results were compared with which shows the process to be promising. In next work a strategy has been developed and verified in shop floor with three different materials. The strategy for increased accuracy of bend angle produced was innovative and effective with promising features for industrial work. Results of laser assisted straightening process showed that it was possible to generate perfect straightness for deformed sheet. The simulation results are also promising. Microhardness and microstructure study with tensile and impact test result confirmed that there was no serious change or deterioration after straightening. The

process further enhanced with controlled electromagnet for both laser bending and straightening which seemed to be potential field of research both in term of accuracy and efficiency of result. The different technical findings and overall conclusions are as follows:

1. Use of black enamel spray paint with proper coating scheme enhances the bending significantly.
2. The bend angle in one laser pass was between 2.5° and 3° for steels, but less than 1.6° for aluminium alloy due its high reflectivity and thermal conductivity.
3. It was difficult to achieve a bend angle of less than 0.1° by laser bending in steel.
4. The required number of laser passes depends on the type of material. For mild steel, a bend angle of 15° could be achieved in seven laser passes. For aluminium alloy, a bend angle of 8° required eight passes, whilst for stainless steel, a bend angle of 8° required four passes.
5. For all the materials, good repeatability and accuracy in bend angle could be obtained. This indicates that by following the proposed strategy, precise bend angles can be produced by laser line heating.
6. Magnetic-force-assisted laser straightening was much more efficient than conventional laser straightening due to decrease in number of laser passes than conventional straightening. A bend angle of 15° could be straightened with 4 passes only compared to conventional one which took 10–15 passes for the same set of process parameters.
7. It is possible to achieve desired straightness with proper selection of process parameters and heat treatment process. The best straightening was obtained when the bent strips were annealed. For 1 mm thick strip, the best performance was obtained at 900 W laser power and 800 mm/min scan speed. On the other hand, for 1.5 mm and 2 mm thick strips, the best parameters were 1000 W laser power and 800 mm/min scan speed. Hence, it is important to select proper process parameters for each job.

8. Micro-hardness value increased in the case of straightened as-formed and stress-relieved strips, while it increased only marginally in the case of straightened annealed strips. Micro-hardness value was the highest in the vicinity of the laser scan line and kept on reducing while moving away from the scan line.
9. The microstructure showed smaller grains in the heat affected zone and coarse grain size in the base material region in all three types of samples. In the laser irradiated region, grains were elongated and deformed with small grain size for straightened as-formed strips.
10. Application of magnetic force could result in significant increase in the bend angle. Bend angle increases with increase in laser power and decreases with increase in scan speed for a particular applied current.
11. Applied current plays an important role in bend angle. For a specific gap, bend angle got increased with applied current up to a certain value. Then it got saturated due to mechanical restriction of movement. Increasing the gap further increased the bend angle.
12. The bend angle was the highest at the end of the scan path. At high power, low scan speed and higher magnetic force, the bend angle reached saturation as the plate got stuck with the magnets. This also reduced the edge effect. Thus, the edge effect is very less in electromagnetically assisted laser bending.
13. Spring-back effect was less at low scan speed, high laser power and high applied current. In all the cases the strip attached to the magnet during irradiation. All three parameters contribute to higher bending with less spring back due to the attachment of strip to magnet.
14. Micro-hardness increased with increase in laser power and decreased with increased laser scan speed; in both the cases, generation of higher temperature is responsible for heat treatment. It also shows a moderate increase with applied current as increase in current leads to high force of attraction which may create certain mechanical forming.

15. Electromagnetic-force-assisted laser straightening was much more efficient than conventional laser straightening due to decrease in number of laser passes.

8.3 Scope for Future Work

Although a lot of research findings are available on laser based bending in the literature, there are several issues that need further investigations. Some of these are as follows:

1. There are some publications in the literature on use of different coating in laser bending process. However this aspect may further investigated to enhance the process.
2. The strategy proposed for improving accuracy of bend angle may further extend to different types of material at different condition. The strategy may be further improved by experiential learning in the shop floor. Based on the strategy a complete close looped expert system can be developed to make the process fully automated.
3. There is a need to carry out more experimental investigation on the metallurgical and mechanical properties of specimen after laser assisted bending and straightening by electromagnet.
4. The FEM model for laser assisted bending and straightening by using permanent magnet and electromagnet, needs modification over the current work.
5. Optimization of the laser based bending and straightening process considering all operating process parameters is an important research area.

References

- Akinlabi, S.A., Pietra, F. and Akinlabi, E.T., 2015. Experimental and numerical investigation on laser beam forming of steel sheets. Proceedings of the Institution of Mechanical Engineers, Part L: Journal of Materials: Design and Applications, Vol. 229, No. 6, pp.455–471.
- Arısoy, Y.M., Criales, L.E., Özel, T., Lane, B., Moylan, S. and Donmez, A., 2017. Influence of scan strategy and process parameters on microstructure and its optimization in additively manufactured nickel alloy 625 via laser powder bed fusion. The International Journal of Advanced Manufacturing Technology, Vol. 90, No. 5-8, pp.1393–1417.
- Bammer, F., Schuöcker, D., Schumi, T., Holzinger, B. and Humenberger, G., 2011. A diode-laser-system for laser-assisted bending of brittle materials. Advances in Optical Technologies, 2011, pp.1–4.
- Barletta, M., Casamichele, L. and Tagliaferri, V., 2006. Line bending of Al_2O_3 coated and uncoated aluminium thin sheets. Surface and Coatings Technology, Vol. 201, Nos. 3–4, pp.660–673.
- Barletta, M., Gisario, A. and Guarino, S., 2009. Hybrid forming process of AA 6108 T4 thin sheets: modelling by neural network solutions. Proceedings of the Institution of Mechanical Engineers, Part B: Journal of Engineering Manufacture, Vol. 223, No. 5, pp.535–545.
- Bartkowiak, K., Dearden, G. and Watkins, K.G., 2004. 2-D Laser forming comparative study on Nd:Yag of titanium alloy Ti-6Al-4V. 23rd International Congress on Applications of Lasers and Electro-optics (ICALEO 2004), San Francisco, Vol. 97, pp.528.
- Behnagh, R.A., Besharati Givi, M.K. and Akbari, M., 2012. Mechanical properties, corrosion resistance, and microstructural changes during friction stir processing of 5083 aluminum rolled plates. Materials and Manufacturing processes, Vol. 27, No. 6, pp.636–640.
- Bejan, A. and Kraus, A.D. (Eds.), 2003. Heat Transfer Handbook, Vol. 1, John Wiley and Sons, Hoboken, New Jersey, USA.

- Belghazi, H., El Ganaoui, M. and Labbe, J.C., 2010. Analytical solution of unsteady heat conduction in a two-layered material in imperfect contact subjected to a moving heat source. International Journal of Thermal Sciences, Vol. 49, No. 2, pp.311–318.
- Birnbaum, A.J., Cheng, P. and Yao, Y.L., 2007. Effects of clamping on the laser forming process, Journal of Manufacturing Science and Engineering, Vol. 129, No. 6, pp.1035–1044.
- Carey, C., Cantwell, W.J., Dearden, G., Edwards, K.R., Edwardson, S.P., Mullett, J.D., Williams, C.J. and Watkins, K.G., 2007. Effects of laser interaction with graphite coatings. Proceedings of the Laser Assisted Net Shape Engineering, Vol. 5, pp.673–686.
- Casalino, G. and Ludovico, A.D., 2002. Parameter selection by an artificial neural network for a laser bending process. Proceedings of the Institution of Mechanical Engineers, Part B: Journal of Engineering Manufacture, Vol. 216, No. 11, pp.1517–1520.
- Casamichele, L., Quadrini, F. and Tagliaferri, V., 2007. Process-efficiency prediction in high power diode laser forming. Journal of Manufacturing Science and Engineering, Vol. 129, No. 5, pp.868–873.
- Cavaliere, P. and De Marco, P.P., 2007. Friction stir processing of AM60B magnesium alloy sheets. Materials Science and Engineering: A, Vol. 462, No. 1, pp.393–397.
- Chakraborty, S.S., Maji, K., Racherla, V. and Nath, A.K., 2015a. Investigation on laser forming of stainless steel sheets under coupling mechanism. Optics and Laser Technology, Vol. 71, pp.29–44.
- Chakraborty, S.S., More, H., Racherla, V. and Nath, A.K., 2015b. Modification of bent angle of mechanically formed stainless steel sheets by laser forming. Journal of Materials Processing Technology, Vol. 222, pp.128–141.
- Chakraborty, S.S., More, H. and Nath, A.K., 2016. Laser forming of a bowl shaped surface with a stationary laser beam. Optics and Lasers in Engineering, Vol. 77, pp.126–136.

- Chan, K.C. and Liang, J., 2000a. Effect of microstructures on deformation behaviour of aluminium matrix composites in laser bending. Texture, stress and Microstructure, Vol. 34, No. 1, pp.43–54.
- Chan, K.C. and Liang, J., 2000b. Laser bending of an Al6013/SiC_p aluminium matrix composite sheet. Journal of Materials Processing Technology, Vol. 100, No. 1, pp.214–218.
- Chandrasekaran, M., Muralidhar, M., Krishna, C.M. and Dixit, U.S., 2012. Online machining optimization with continuous learning. In Computational Methods for Optimizing Manufacturing Technology: Models and Techniques (pp. 85–110). IGI Global.
- Chang, C.I., Du, X.H. and Huang, J.C., 2007. Achieving ultrafine grain size in Mg-Al-Zn alloy by friction stir processing. Scripta Materialia, Vol. 57, No. 3, pp.209–212.
- Chehrghani, A., Torkamany, M.J., Hamedi, M.J. and Sabbaghzadeh, J., 2012. Numerical modeling and experimental investigation of TiC formation on titanium surface pre-coated by graphite under pulsed laser irradiation. Applied Surface Science, Vol. 258, No. 6, pp.2068–2076.
- Chen, G., Xu, X., Poon, C.C. and Tam, A.C., 1998. Laser-assisted microscale deformation of stainless steels and ceramics. Optical Engineering, Vol. 37, No. 10, pp.2837–2843.
- Chen, G., Xu, X., Poon, C.C. and Tam, A.C., 1999. Experimental and numerical studies on microscale bending of stainless steel with pulsed laser. Journal of Applied Mechanics, Vol. 66, No. 3, pp.772–779.
- Chen, G. and Xu, X., 2001. Experimental and 3D finite element studies of CW laser forming of thin stainless steel sheets. Journal of Manufacturing Science and Engineering, Vol. 123, No. 1, pp.66–73.
- Chen, D.J., Xiang, Y.B., Wu, S.C. and Li, M.Q., 2002. Simulation and experiment of curve irradiated laser bending process of titanium alloy sheet. Materials Science and Technology, Vol. 18, No. 6, pp.673–676.

- Chen, D.J., Wu, S.C. and Li, M.Q., 2004a. Studies on laser forming of Ti-6Al-4V alloy sheet. Journal of Materials Processing Technology, Vol. 152, No. 1, pp.62–65.
- Chen, D., Wu, S. and Li, M., 2004b. Deformation behaviours of laser curve bending of sheet metals. Journal of Materials Processing Technology, Vol. 148, No. 1, pp.30–34.
- Chen, M.L., Jeswiet, J., Bates, P.J. and Zak, G., 2008. Experimental study on sheet metal bending with medium–power diode laser. Proceedings of the Institution of Mechanical Engineers, Part B: Journal of Engineering Manufacture, Vol. 222, No. 3, pp.381–389.
- Chen, J., Qi, Y., Shi, Y. and Bi, Z., 2010. An analytical model to predict bending angles in high-frequency induction heat forming. Proceedings of the Institution of Mechanical Engineers, Part C: Journal of Mechanical Engineering Science, Vol. 224, No. 3, pp.655–660.
- Cheng, P.J. and Lin, S.C., 2000a. An analytical model for the temperature field in the laser forming of sheet metal. Journal of Materials Processing Technology, Vol. 101, No. 1, pp.260–267.
- Cheng, P.J. and Lin, S.C., 2000b. Using neural networks to predict bending angle of sheet metal formed by laser. International Journal of Machine Tools and Manufacture, Vol. 40, No. 8, pp.1185–1197.
- Cheng, J. and Yao, Y.L., 2001. Cooling effects in multiscan laser forming. Journal of Manufacturing Processes, Vol. 3, No. 1, pp.60–72.
- Cheng, J. and Yao, Y.L., 2002. Microstructure integrated modeling of multiscan laser forming. Journal of Manufacturing Science and Engineering, Vol. 124, No. 2, pp.379–388.
- Cheng, J.G. and Yao, Y.L., 2004. Process synthesis of laser forming by genetic algorithm. International Journal of Machine Tools and Manufacture, Vol. 44, No. 15, pp.1619–1628.
- Cheng, P., Mika, D., Graham, M., Yao, Y.L. and Jones, M., 2005a. Laser forming of complex structures. The 1st International Workshop on Thermal Forming (IWOTF'05).

- Cheng, P., Yao, Y.L., Liu, C., Pratt, D. and Fan, Y., 2005b. Analysis and prediction of size effect on laser forming of sheet metal. Journal of Manufacturing Processes, Vol. 7, No. 1, pp.28–41.
- Cheng, P., Fan, Y., Zhang, J., Yao, Y.L., Mika, D.P., Zhang, W., Graham, M., Marte, J. and Jones, M., 2006. Laser forming of varying thickness plate—Part I: Process analysis. Journal of manufacturing science and engineering, Vol. 128, No. 3, pp.634–641.
- Cheng, G.J., Pirzada, D. and Ming, Z., 2007. Microstructure and mechanical property characterizations of metal foil after microscale laser dynamic forming. Journal of applied physics, Vol. 101, No. 6, pp.063108.
- Ciurana, J., Arias, G. and Ozel, T., 2009. Neural network modeling and particle swarm optimization (PSO) of process parameters in pulsed laser micromachining of hardened AISI H13 steel. Materials and Manufacturing Processes, Vol. 24, No.3, pp.358–368.
- Criales, L.E., Arısoy, Y.M., Lane, B., Moylan, S., Donmez, A. and Özel, T., 2017. Predictive modeling and optimization of multi-track processing for laser powder bed fusion of nickel alloy 625. Additive Manufacturing, Vol. 13, pp.14–36.
- Cui, G.R., Ma, Z.Y. and Li, S.X., 2009. The origin of non-uniform microstructure and its effects on the mechanical properties of a friction stir processed Al-Mg alloy. Acta Materialia, Vol. 57, No. 19, pp.5718–5729.
- Das, B. and Biswas, P., 2017. Effect of operating parameters on plate bending by laser line heating. Proceedings of the Institution of Mechanical Engineers, Part B: Journal of Engineering Manufacture, Vol. 231, No. 10, pp.1812-1819.
- Davim, J.P., Oliveira, C., Barricas, N. and Conceição, M., 2008a. Evaluation of cutting quality of PMMA using CO_2 lasers. The International Journal of Advanced Manufacturing Technology, Vol. 35, No.9–10, pp.875–879.
- Davim, J.P., Barricas, N., Conceicao, M. and Oliveira, C., 2008. Some experimental studies on CO2 laser cutting quality of polymeric materials. Journal of materials processing technology, Vol. 198, No. 1–3, pp.99–104.

- Dearden, G. and Edwardson, S.P., 2003. Some recent developments in two-and three-dimensional laser forming for ‘macro’ and ‘micro’ applications. Journal of Optics A: Pure and Applied Optics, Vol. 5, No. 4, p.S8.
- Dehghani, K. and Mazinani, M., 2011. Forming nanocrystalline surface layers in copper using friction stir processing. Materials and Manufacturing Processes, Vol. 26, No. 7, pp.922–925.
- Deng, D. and Murakawa, H., 2006. Numerical simulation of temperature field and residual stress in multi-pass welds in stainless steel pipe and comparison with experimental measurements. Computational materials science, Vol. 37, No. 3, pp.269–277.
- Dieter GE., 1991. Engineering design: a Materialistic and Processing Approach, 2nd edn. McGraw-Hill, New York.
- Dixit, U.S., Joshi, S.N. and Kumar, V.H., 2012. Microbending with laser. Micromanufacturing processes. CRC Press, Boca Raton, pp.283–303.
- Dixit, U.S., Joshi, S.N. and Kant, R., 2015. Laser forming systems: a review. International Journal of Mechatronics and Manufacturing Systems, Vol. 8, No. 3–4, pp.160–205.
- Dixit, U.S. and Fetene, B.N., 2016. A finite element modelling of laser bending of friction stir welded aluminium 5052-H32 sheets. International Journal of Mechatronics and Manufacturing Systems, Vol. 9, No. 3, pp.215-236.
- Dragos, V., Dan, V. and Kovacevic, R., 2000. Prediction of the laser sheet bending using neural network. In Circuits and Systems, 2000. Proceedings. ISCAS 2000 Geneva. The 2000 IEEE International Symposium on, Vol. 3, pp. 686–689, IEEE.
- Du, Y., Wang, X. and Silvanus, J., 2010. Improved BP network to predict bending angle in the laser bending process for sheet metal. Intelligent System Design and Engineering Application (ISDEA), 2010 International Conference on, Vol. 1, pp.839–843, IEEE.
- Dutta Majumdar, J. and Manna, I., 2011. Laser material processing. International materials reviews, Vol. 56, Nos. 5–6, pp.341–388.

- Edwardson, S.P., Watkins, K.G., Dearden, G. and Magee, J., 2001. 3D laser forming of saddle shapes. Proceedings of Laser Assisted Net Shaping, pp.559–568.
- Edwardson, S.P., Abed, E., Bartkowiak, K., Dearden, G. and Watkins, K.G., 2006. Geometrical influences on multi-pass laser forming. Journal of Physics D: Applied Physics, Vol. 39, No. 2, p.382.
- Edwardson, S.P., Abed, E., Carey, C., Edwards, K.R., Dearden, G. and Watkins, K.G., 2007. Factors influencing the bend per pass in multi-pass laser forming. Proceedings of the 5th LANE, 1, pp.557–568.
- Edwardson, S.P., Griffiths, J., Dearden, G. and Watkins, K.G., 2010a. Temperature gradient mechanism: overview of the multiple pass controlling factors, Physics Procedia, Vol. 5, Part A, pp.53–63.
- Edwardson, S.P., Griffiths, J., Edwards, K.R., Dearden, G. and Watkins, K.G., 2010b. Laser forming: overview of the controlling factors in the temperature gradient mechanism. Proceedings of the Institution of Mechanical Engineers, Part C: Journal of Mechanical Engineering Science, Vol. 224, No. 5, pp.1031–1040.
- Eideh, A. and Dixit, U.S., 2013. A robust and efficient inverse method for determining the thermal parameters during laser forming. In Proceedings of National Conference of Recent Advancements in Mechanical Engineering. NERIST, Nirjuli, India (pp. 38–43).
- Eideh A., 2014. Determination of Parameters During Laser Bending by Inverse Analysis, M. Tech. Thesis, Department of Mechanical Engineering, IIT Guwahati, India.
- Eideh, A., Dixit, U.S. and Echempati, R., 2015. A simple analytical model of laser bending process, laser based manufacturing, in Joshi, S.N. and Dixit, U.S. (Eds.): 5th International and 26th National All India Manufacturing Technology, Design and Research AIMTDR 2014, Chapter 1, pp.1–15.
- Fan, Y., Cheng, P., Yao, Y.L., Yang, Z. and Egland, K., 2005. Effect of phase transformations on laser forming of Ti-6Al-4V alloy. Journal of Applied Physics, Vol. 98, No. 1, p.013518-10.

- Fan, Y., Yang, Z., Cheng, P., Egland, K. and Yao, L., 2007. Investigation of effect of phase transformations on mechanical behavior of AISI 1010 steel in laser forming. Journal of Manufacturing Science and Engineering, Vol. 129, No. 1, pp.110–116.
- Feng, A.H. and Ma, Z.Y., 2007. Enhanced mechanical properties of Mg–Al–Zn cast alloy via friction stir processing. Scripta materialia, Vol. 56, No. 5, pp.397–400.
- Fetene, B.N., 2018. A Study on the Performance of Laser Based Bending, Ph.D. Thesis, Indian Institute of Technology Guwahati.
- Fetene, B.N., Shufen, R. and Dixit, U.S., 2018. FEM-based neural network modeling of laser-assisted bending. Neural Computing and Applications. Vol. 29, No. 6, pp.69-82.
- Fetene, B.N., Dixit, U.S. and Liao, H., 2017. Laser bending of friction stir processed and cement-coated sheets. Materials and Manufacturing Processes, Vol. 32, No. 14, pp.1628–1634.
- Fetene, B.N., Dixit, U.S. and Davim, J.P., 2017. Laser-assisted bending by magnetic force. The Journal of Engineering. Vol. 2017, No. 7, pp.343–353.
- Fetene, B.N., Kumar, V., Dixit, U.S. and Echempati, R., 2018. Numerical and experimental study on multi-pass laser bending of AH36 steel strips. Optics and Laser Technology, 99, pp.291–300.
- Folkersma, G., Brouwer, D. and Römer, G., 2016, Microtube laser forming for precision component alignment, ASME Journal of Manufacturing Science and Engineering, Vol. 138, No. 8, pp. 0810121–6.
- Garg, A., Sastry, P.S., Pandey, M., Dixit, U.S. and Gupta, S.K., 2007. Numerical simulation and artificial neural network modeling of natural circulation boiling water reactor. Nuclear engineering and design, Vol. 237, No. 3, pp.230–239.
- Gautam, S.S., Singh, S.K. and Dixit, U.S., 2015. Laser forming of mild steel sheets using different surface coatings. In Lasers based manufacturing (pp.17-39). Springer, New Delhi.
- Geiger, M., Vollertsen, F. and Deinzer, G., 1993. Flexible Straightening of Car Body Shells by Laser Forming. No. 930279, SAE Technical paper.

- Geiger, M. and Vollertsen, F., 1993. The mechanisms of laser forming. CIRP Annals-Manufacturing Technology, Vol. 42, No. 1, pp.301–304.
- Geiger, M., 1994. Synergy of laser material processing and metal forming. CIRP Annals-Manufacturing Technology, Vol. 43, No. 2, pp.563–570.
- Gisario, A., Barletta, M., Conti, C. and Guarino, S., 2011. Springback control in sheet metal bending by laser-assisted bending: Experimental analysis, empirical and neural network modelling. Optics and Lasers in Engineering, Vol. 49, No. 12, pp.1372–1383.
- Gisario, A., Barletta, M. and Venettacci, S., 2016. Improvements in springback control by external force laser-assisted sheet bending of titanium and aluminum alloys. Optics and Laser Technology, Vol. 86, pp.46–53.
- Gisario, A., Mehrpouya, M., Venettacci, S. and Barletta, M., 2017. Laser-assisted bending of Titanium Grade-2 sheets: Experimental analysis and numerical simulation. Optics and Lasers in Engineering, Vol. 92, pp.110–119.
- Gollo, M.H., Mahdavian, S.M. and Naeini, H.M., 2011. Statistical analysis of parameter effects on bending angle in laser forming process by pulsed Nd: YAG laser. Optics and Laser Technology, Vol. 43, No. 3, pp.475–482.
- Gould, R.G., 1959. The LASER, light amplification by stimulated emission of radiation. The Ann Arbor conference on Optical Pumping, the University of Michigan, Vol. 15, pp. 128.
- Griffiths, J., Edwardson, S.P., Dearden, G. and Watkins, K.G., 2010. Finite element modelling of laser forming at macro and micro scales. Physics Procedia, Vol. 5, Part B, pp.371–380.
- Guan, Y., Sun, S., Zhao, G. and Luan, Y., 2005. Influence of material properties on the laser-forming process of sheet metals. Journal of Materials Processing Technology, Vol. 167, No. 1, pp.124–131.
- Guglielmotti, A., Quadrini, F., Squeo, E.A. and Tagliaferri, V., 2009. Laser bending of aluminum foam sandwich panels. Advanced engineering materials, Vol. 11, No.11, pp.902–906.
- Hao, N. and Li, L., 2003a. Finite element analysis of laser tube bending process, Applied Surface Science, Vol. 208, pp.437–441.

- Hao, N. and Li, L., 2003b. An analytical model for laser tube bending, Applied Surface Science, Vols. 208, pp.432–436.
- Hassan, K.A., Prangnell, P.B., Norman, A.F., Price, D.A. and Williams, S.W., 2003. Effect of welding parameters on nugget zone microstructure and properties in high strength aluminium alloy friction stir welds. Science and Technology of Welding and joining, Vol. 8, No. 4, pp.257–268.
- Hennige, T., Holzer, S., Vollertsen, F. and Geiger, M., 1997. On the working accuracy of laser bending, Journal of Materials Processing Technology, Vol. 71, No. 3, pp.422–432.
- Holzer, S., Arnet, H. and Geiger, M., 1994. Physical and numerical modelling of the buckling mechanism. In Laser assisted net shape engineering, Proceedings of the LANE, Vol. 1, pp.379–386.
- Hsieh, H.S. and Lin, J., 2004a. Laser-induced vibration during pulsed laser forming. Optics and Laser Technology, Vol. 36, No. 6, pp.431–439.
- Hsieh, H.S. and Lin, J., 2004b. Thermal-mechanical analysis on the transient deformation during pulsed laser forming. International Journal of Machine Tools and Manufacture, Vol. 44, No. 2, pp.191–199.
- Hu, Z., Labudovic, M., Wang, H. and Kovacevic, R., 2001. Computer simulation and experimental investigation of sheet metal bending using laser beam scanning. International Journal of Machine Tools and Manufacture, Vol. 41, No. 4, pp.589–607.
- Hu, Z., Kovacevic, R. and Labudovic, M., 2002. Experimental and numerical modeling of buckling instability of laser sheet forming. International Journal of Machine Tools and Manufacture, Vol. 42, No. 13, pp.1427–1439.
- Hu, J., Dang, D., Shen, H. and Zhang, Z., 2012. A finite element model using multi-layered shell element in laser forming. Optics and Laser Technology, Vol. 44, No. 4, pp.1148–1155.
- Hu, J., Xu, H. and Dang, D., 2013. Modeling and reducing edge effects in laser bending. Journal of Materials Processing Technology, Vol. 213, No. 11, pp.1989–1996.

- Jamil, M.C., Sheikh, M.A. and Li, L., 2011a. A study of the effect of laser beam geometries on laser bending of sheet metal by buckling mechanism. Optics and Laser Technology, Vol. 43, No. 1, pp.183–193.
- Jamil, M.S.C., Sheikh, M.A. and Li, L., 2011b. A numerical study of the temperature gradient mechanism in laser forming using different laser beam geometries. Lasers in Engineering, Vol. 22, Nos. 5–6, pp.413–428.
- Jamil, M.C., Fauzi, E.I., Juinn, C.S. and Sheikh, M.A., 2015. Laser bending of pre-stressed thin-walled nickel micro-tubes. Optics and Laser Technology, Vol. 73, pp.105–117.
- Ji, Z. and Wu, S., 1998. FEM simulation of the temperature field during the laser forming of sheet metal. Journal of Materials Processing Technology, Vol. 74, No. 1, pp.89–95.
- Jovic, S., Makragic, S. and Jovanovic, M., 2017. Parameters influence of laser forming on shaped surface by soft computing technique. Optik-International Journal for Light and Electron Optics, Vol. 142, pp.451–454.
- Kannatey-Asibu Jr, E., 2009. Principles of Laser Materials Processing (Vol. 4). John Wiley and Sons.
- Kant, R. and Joshi, S. N., 2012a. Numerical simulation of laser bending of magnesium alloy AZ31B using FEM. Proc. of the International Conference IDDRG 2012, Vol. 2, pp.736–741.
- Kant, R. and Joshi, S. N., 2012b. Analysis of sheet-holding methods in laser bending process using FEM. Proc. of the 3rd Asian Symposium on Materials and Processing, ASMP - 2012, MCMTP6.
- Kant, R. and Joshi, S.N., 2013a. Numerical simulation of multi-pass laser bending processes using finite element method. In Proceedings of the 2nd international conference IRAM 2013, pp. 16–18.
- Kant, R. and Joshi, S.N., 2013b. Finite element simulation of laser assisted bending with moving mechanical load. International Journal of Mechatronics and Manufacturing Systems, Vol. 6, No. 4, pp.351–366.
- Kant, R. and Joshi, S.N., 2014. Numerical modeling and experimental validation of curvilinear laser bending of magnesium alloy sheets. Proceedings of the

Institute of Mechanical Engineering Part B: Journal of Engineering Manufacture, Vol. 228, pp.1036–1047.

- Kant, R., Joshi, S.N. and Dixit, U.S., 2015a. An integrated FEM-ANN model for laser bending process with inverse estimation of absorptivity. Mechanics of Advanced Materials and Modern Processes, Vol. 1, No. 1, pp. 6.
- Kant, R., Joshi, S.N. and Dixit, U.S., 2015b, Research Issues in the Laser Sheet Bending Process, Chapter 4 in Materials Forming and Machining: Research and Development, edited by J. Paulo Davim, Woodhead Publishing, Cambridge, pp. 73–95.
- Kant, R. and Joshi, S.N., 2016. Thermo-mechanical studies on bending mechanism, bend angle and edge effect during multi-scan laser bending of magnesium M1A alloy sheets. Journal of Manufacturing Processes, Vol. 23, pp.135–148.
- Karthikeyan, L., Senthil Kumar, V.S. and Padmanabhan, K.A., 2013. Investigations on superplastic forming of friction stir-processed AA6063-T6 aluminum alloy. Materials and Manufacturing processes, Vol. 28, No. 3, pp.294–298.
- Kennedy, E., Byrne, G. and Collins, D.N., 2004. A review of the use of high power diode lasers in surface hardening. Journal of Materials Processing Technology, Vol. 155, pp.1855–1860.
- Kim, H.K. and Oh, S.I., 2001. Evaluation of heat transfer coefficient during heat treatment by inverse analysis, Journal of Materials Processing Technology, Vol. 112, pp. 157–165.
- Kohli, A. and Dixit, U.S., 2005. A neural-network-based methodology for the prediction of surface roughness in a turning process. The International Journal of Advanced Manufacturing Technology, Vol. 25, No. 1, pp.118–129.
- Kratky, A., 2007. Laser assisted forming techniques. In XVI International Symposium on Gas Flow, Chemical Lasers, and High-Power Lasers (Vol. 6346, p. 634615). International Society for Optics and Photonics.
- Kraus, J., 1997. Basic process in laser bending of extrusion using the upsetting mechanism. Laser Assisted Net Shape Engineering 2, Proceedings of the

LANE, Vol. 97, pp.431–438.

- Kumar, V. and Dixit, U.S., 2018a. Selection of process parameters in a single-pass laser bending process. Engineering Optimization, Vol. 50, No. 9, pp.1609–1624.
- Kumar, V. and Dixit, U.S., 2018b. A model for the estimation of hardness of laser bent strips. Optics & Laser Technology, Vol. 107, pp.491–499.
- Kumar, V., Dixit, U.S. and Zhang, J., 2019. Determination of thermal conductivity, absorptivity and heat transfer coefficient during laser-based manufacturing. Measurement, Vol. 131, pp.319–328.
- Kyrsanidi, A.K., Kermanidis, T.B. and Pantelakis, S.G., 1999. Numerical and experimental investigation of the laser forming process, Journal of Materials Processing Technology, Vol. 87, No. 1, pp.281–290.
- Kyrsanidi, A.K., Kermanidis, T.B. and Pantelakis, S.G., 2000. An analytical model for the prediction of distortions caused by the laser forming process. Journal of Materials Processing Technology, Vol. 104, No. 1, pp.94–102.
- Labeas, G.N., 2008. Development of a local three-dimensional numerical simulation model for the laser forming process of aluminium components. Journal of materials processing technology, Vol. 207, No. 1, pp.248–257.
- Lambiase, F., 2012. An analytical model for evaluation of bending angle in laser forming of metal sheets. Journal of materials engineering and performance, Vol. 21, No. 10, pp.2044–2052.
- Lambiase, F. and Di Ilio, A., 2013. A closed-form solution for thermal and deformation fields in laser bending process of different materials. The International Journal of Advanced Manufacturing Technology, Vol. 69, No. 1–4, pp.849–861.
- Lambiase, F., Di Ilio, A. and Paoletti, A., 2013. An experimental investigation on passive water cooling in laser forming process, The International Journal of Advanced Manufacturing Technology, Vol. 64, No. 5–8, pp.829–840.

- Lambiase, F., Di Ilio, A. and Paoletti, A., 2015. Optimization of multi–pass laser bending by means of soft computing techniques. Procedia CIRP, Vol. 33, pp.502–507.
- Langlade, C., Roman, A., Schlegel, D., Gete, E. and Folea, M., 2016. Formation of a Tribologically Transformed Surface (TTS) on AISI 1045 steel by friction stir processing. Materials and Manufacturing Processes, Vol. 31, No. 12, pp.1565–1572.
- Lawrence, J., Schmidt, M.J. and Li, L., 2001. The forming of mild steel plates with a 2.5 kW high power diode laser. International Journal of Machine Tools and Manufacture, Vol. 41, No. 7, pp.967–977.
- Lawrence M. and Petterson A., 2002. Brain maker user's manual, 7th edn. California Scientific Software, Nevada City.
- Lee, K.C. and Lin, J., 2002. Transient deformation of thin metal sheets during pulsed laser forming. Optics and Laser Technology, Vol. 34, No. 8, pp.639–648.
- Li, W. and Yao, Y.L., 2000. Numerical and experimental study of strain rate effects in laser forming. Journal of Manufacturing Science and Engineering, Vol. 122, No. 3, pp.445–451.
- Li, W. and Yao, Y. L., 2001a. Numerical and experimental investigation of convex laser forming process. Journal of Manufacturing Processes, Vol. 3, No. 2, pp.73–81.
- Li, W. and Yao, Y. L., 2001b. Laser bending of tubes: mechanism, analysis and prediction. Journal of Manufacturing Science and Engineering, Vol. 123, No. 4, pp.674–681.
- Liechty, B.C. and Webb, B.W., 2008. Modeling the frictional boundary condition in friction stir welding. International Journal of Machine Tools and Manufacture, Vol. 48, No. 12, pp.1474–1485.
- Liu, C. and Yao, Y. L., 2002. Optimal and robust design of the laser forming process. Journal of Manufacturing Processes, Vol. 4, No. 1, pp.52–66.
- Liu, J., Sun, S. and Guan, Y., 2009. Numerical investigation on the laser bending of stainless steel foil with pre-stresses. Journal of materials processing technology, Vol. 209, No. 3, pp.1580–1587.

- Liu, F., Lin, X., Huang, C., Song, M., Yang, G., Chen, J. and Huang, W., 2011. The effect of laser scanning path on microstructures and mechanical properties of laser solid formed nickel-base superalloy Inconel 718. Journal of Alloys and Compounds, Vol. 509, No. 13, pp.4505–4509.
- Logothetis, N., 1992. Managing for Total Quality: from Deming to Taguchi and SPC. Prentice-Hall of India.
- Ma, Z.Y., 2008. Friction stir processing technology: a review. Metallurgical and materials Transactions A, Vol. 39, No. 3, pp.642–658.
- Ma, Z.Y., Mishra, R.S. and Liu, F.C., 2009. Superplastic behavior of micro-regions in two-pass friction stir processed 7075Al alloy. Materials Science and Engineering: A, Vol. 505, No. 1, pp.70–78.
- Magee, J. and De Vin, L.J., 2002. Process planning for laser-assisted forming. Journal of Materials Processing Technology, Vol. 120, No. 1, pp.322–326.
- Maji, K., Pratihar, D.K. and Nath, A.K., 2013. Analysis and synthesis of laser forming process using neural networks and neuro-fuzzy inference system. Soft Computing, Vol. 17, No. 5, pp.849–865.
- Maji, K., Pratihar, D.K. and Nath, A.K., 2014a. Laser forming of a dome shaped surface: Experimental investigations, statistical analysis and neural network modeling. Optics and Lasers in Engineering, Vol. 53, pp.31–42.
- Maji, K., Pratihar, D.K. and Nath, A.K., 2014b. Analysis of pulsed laser bending of sheet metal using neural networks and neuro-fuzzy system. Proceedings of the Institution of Mechanical Engineers, Part B: Journal of Engineering Manufacture, Vol. 228, No. 9, pp.1015–1026.
- Majumdar, J.D., Nath, A.K. and Manna, I., 2004. Studies on laser bending of stainless steel. Materials Science and Engineering: A, Vol. 385, No. 1, pp.113–122.
- Martin, R., 1979. Automated adjusting in precision engineering (German patent: Automatisiertesjustieren in der feinwerktechnik). Deutsches Patentamt, Offenlegungsschrift, Vol. 29, No. 18, pp.100.
- Mazhukin, V.I., Lobok, M.G. and Smurov, I., 2007. Transient effects in pulsed

laser irradiation. Applied Surface Science, Vol. 253, No. 19, pp.7744–7748.

- McGrath, P.J. and Hughes, C.J., 2007. Experimental fatigue performance of laser-formed components. Optics and lasers in engineering, Vol. 45, No. 3, pp.423–430.
- Merklein, M., Hennige, T. and Geiger, M., 2001. Laser forming of aluminium and aluminium alloys—microstructural investigation. Journal of Materials Processing Technology, Vol. 115, No. 1, pp.159–165.
- Mishra, R.S., Mahoney, M.W., McFadden, S.X., Mara, N.A. and Mukherjee, A.K., 1999. High strain rate superplasticity in a friction stir processed 7075 Al alloy. Scripta Materialia, Vol. 42, No. 2, pp.163–168.
- Mishra, R.S. and Ma, Z.Y., 2005. Friction stir welding and processing. Materials Science and Engineering: R: Reports, Vol. 50, Nos. 1–2, pp.1–78.
- Mishra, A. and Dixit, U.S., 2013. Determination of thermal diffusivity of the material, absorptivity of the material and laser beam radius during laser forming by inverse heat transfer. Journal of Machining and Forming Technology, Vol. 5, Nos. 3–4 pp.208–226.
- Morisada, Y., Fujii, H., Nagaoka, T., Nogi, K. and Fukusumi, M., 2007. Fullerene/A5083 composites fabricated by material flow during friction stir processing. Composites Part A: Applied Science and Manufacturing, Vol. 38, No. 10, pp.2097–2101.
- Mueller, S., Kruck, B. and Baudisch, P., 2013, April. LaserOrigami: laser-cutting 3D objects. In Proceedings of the SIGCHI Conference on Human Factors in Computing Systems (pp. 2585–2592). ACM.
- Nascimento, F., Santos, T., Vilaça, P., Miranda, R.M. and Quintino, L., 2009. Microstructural modification and ductility enhancement of surfaces modified by FSP in aluminium alloys. Materials Science and Engineering: A, Vol. 506, No. 1, pp.16–22.
- Ocana, J.L., Morales, M., Molpeceres, C., Garcia, O., Porro, J.A. and Garcia-Ballesteros, J.J., 2007. Short pulse laser microforming of thin metal sheets for MEMS manufacturing. Applied Surface Science, Vol. 254, No. 4, pp.997–1001.

- Okamoto, Y., Uno, Y., Ohta, K.I., Shibata, T., Kubota, S.I. and Namba, Y., 2000. Study on precision laser forming of plastic with YAG laser. Journal of the Japan Society for Precision Engineering, Vol. 66, No. 6, pp.891–895.
- Okamoto, Y., Miyamoto, I., Uno, Y. and Takenaka, T., 2004. Deformation characteristics of plastics in YAG laser forming, Fifth International Symposium on Laser Precision Microfabrication, Vol. 5662, pp. 576-582, International Society for Optics and Photonics.
- Palani, I.A., Naikwad, S., Padmanabhan, R., Shanmugam, S. and Natu, H., 2015. Parametric Investigation in Laser Forming of 8 mm FE-410 Plate Using High Power CO_2 Laser and Its Bend Angle Prediction. Materials Today: Proceedings, Vol. 2, Nos.4–5, pp.2013–2021.
- Park, S., Lee, C.G., Han, H.N., Ma, N. and Chung, K., 2008. Surface friction stir method to improve formability and spring-back of AA5052-H32 sheets. International Journal of Material Forming, Vol. 1, No. 1, pp.261–264.
- Paunoiu, V., Squeo, E.A., Quadrini, F., Gheorghies, C. and Nicoara, D., 2008. Laser bending of stainless steel sheet metals. International Journal of Material Forming, Vol. 1, No. 1, pp.1371–1374.
- Pérez, J.A., González, M. and Dopico, D., 2010. Adaptive neurofuzzy ANFIS modeling of laser surface treatments. Neural Computing and Applications, Vol. 19, No. 1, pp.85–90.
- Pitz, I., Otto, A. and Schmidt, M., 2010. Simulation of the laser beam forming process with moving meshes for large aluminium plates. Physics Procedia, Vol. 5, Part B, pp.363–369.
- Pretorius, T., 2009. Laser Forming, The Theory of Laser Materials Processing, edited by Dowden, J., Vol. 119, pp. 281–314, Springer, UK.
- Qi, L. and Namba, Y., 2011. Precision laser adjustment using CW diode laser, Precision Engineering, Vol. 35, No. 1, pp.126–132.
- Quadrini, F., Guglielmotti, A., Squeo, E.A. and Tagliaferri, V., 2010. Laser forming of open-cell aluminium foams. Journal of Materials Processing Technology, Vol. 210, No. 11, pp.1517–1522.

- Ramulu, P.J., Narayanan, R.G. and Kailas, S.V., 2013. Forming limit investigation of friction stir welded sheets: influence of shoulder diameter and plunge depth. International Journal of Advanced Manufacturing Technology, Vol. 69, Nos. 9–12, pp. 2757–2772.
- Risbood, K.A., Dixit, U.S. and Sahasrabudhe, A.D., 2003. Prediction of surface roughness and dimensional deviation by measuring cutting forces and vibrations in turning process. Journal of Materials Processing Technology, Vol. 132, No. 1, pp.203–214.
- Romer, G.R.B.E. and Meijer, J., 2000. Inverse calculation of power density for laser surface treatment. Annals of the CIRP, Vol. 49, pp. 135–138.
- Roohi, A.H., Gollo, M.H. and Naeini, H.M., 2012. External force-assisted laser forming process for gaining high bending angles. Journal of Manufacturing Processes, Vol. 14, No. 3, pp.269–276.
- Roohi, A.H., Naeini, H.M., Gollo, M.H., Soltanpour, M. and Abbaszadeh, M., 2015. On the random-based closed-cell metal foam modeling and its behavior in laser forming process. Optics and Laser Technology, Vol. 72, pp.53–64.
- Rouquette, S., Guo, J. and Le Masson, P., 2007. Estimation of the parameters of a Gaussian heat source by the Levenberg-Marquardt method: Application of the electron beam welding. International Journal of Thermal Sciences, Vol. 46, pp.128–138.
- Safdar, S., Li, L., Sheikh, M.A. and Liu, Z., 2007a. Finite element simulation of laser tube bending: Effect of scanning schemes on bending angle, distortions and stress distribution. Optics and Laser Technology, Vol. 39, No. 6, pp.1101–1110.
- Safdar, S., Li, L., Sheikh, M.A. and Liu, Z., 2007b. The effect of nonconventional laser beam geometries on stress distribution and distortions in laser bending of tubes. Journal of manufacturing science and engineering, Vol. 129, No. 3, pp.592–600.
- Safari, M. and Farzin, M., 2013. Experimental and numerical investigation of laser bending of tailor machined blanks. Optics and Laser Technology, Vol. 48, pp.513–522.

- Safari, M. and Farzin, M., 2014. A study on laser bending of tailor machined blanks with various irradiating schemes. Journal of Materials Processing Technology, Vol. 214, No. 1, pp.112–122.
- Safari, M. and Farzin, M., 2015. Experimental investigation of laser forming of a saddle shape with spiral irradiating scheme. Optics and Laser Technology, Vol. 66, pp.146–150.
- Samm, K., Terzi, M., Ostendorf, A. and Wulfsberg, J., 2009, Laser-assisted micro-forming process with miniaturised structures in sapphire dies, Applied Surface Science, Vol. 255, No. 24, pp.9830–9834.
- Sato, Y.S., Nelson, T.W., Sterling, C.J., Steel, R.J. and Pettersson, C.O., 2005. Microstructure and mechanical properties of friction stir welded SAF 2507 super duplex stainless steel. Materials Science and Engineering: A, Vol. 397, No. 1, pp.376–384.
- Scialpi, A., De Filippis, L.A.C., Cuomo, P. and Di Summa, P., 2008. Micro friction stir welding of 2024–6082 aluminum alloys. Welding International, Vol. 22, No. 1, pp.16–22.
- Sekban, D.M., Saray, O., Aktarer, S.M., Purcek, G. and Ma, Z.Y., 2015. Microstructure, mechanical properties and formability of friction stir processed interstitial-free steel. Materials Science and Engineering: A, Vol. 642, pp.57–64.
- Sharma, V., Gupta, Y., Kumar, B.M. and Prakash, U., 2016. Friction stir processing strategies for uniform distribution of reinforcement in a surface composite. Materials and Manufacturing Processes, Vol. 31, No. 10, pp.1384–1392.
- Sheikh, M.A. and Li, L., 2010. Understanding the effect of non-conventional laser beam geometry on material processing by finite-element modelling. Proceedings of the Institution of Mechanical Engineers, Part C: Journal of Mechanical Engineering Science, Vol. 224, No. 5, pp.1061–1072.
- Shen, Z.H., Zhang, S.Y., Lu, J. and Ni, X.W., 2001. Mathematical modeling of laser induced heating and melting in solids. Optics and laser technology, Vol. 33, No. 8, pp.533–537.

- Shen, H., Shi, Y., Yao, Z. and Hu, J., 2006. An analytical model for estimating deformation in laser forming. Computational Materials Science, Vol. 37, No. 4, pp.593–598.
- Shen, H., 2008. Mechanism of laser micro-adjustment. Journal of Physics D: Applied Physics, Vol. 41, No. 24, p.245106.
- Shen, H. and Yao, Z., 2009. Study on mechanical properties after laser forming. Optics and Lasers in Engineering, Vol. 47, No. 1, pp.111–117.
- Shen, H. and Vollertsen, F., 2009. Modelling of laser forming–An review. Computational Materials Science, Vol. 46, No. 4, pp.834–840.
- Shen, H., Ran, M., Hu, J. and Yao, Z., 2014. An experimental investigation of underwater pulsed laser forming. Optics and Lasers in Engineering, Vol. 62, pp.1–8.
- Shi, Y., Shen, H., Yao, Z., Hu, J. and Xia, L., 2006a. Application of similarity theory in the laser forming process. Computational Materials Science, Vol. 37, No. 3, pp.323–327.
- Shi, Y., Yao, Z., Shen, H. and Hu, J., 2006b. Research on the mechanisms of laser forming for the metal plate. International Journal of Machine Tools and Manufacture, Vol. 46, No. 12, pp.1689–1697.
- Shi, Y., Shen, H., Yao, Z. and Hu, J., 2007a. An analytical model based on the similarity in temperature distributions in laser forming. Optics and lasers in engineering, Vol. 45, No. 1, pp.83–87.
- Shi, Y., Shen, H., Yao, Z. and Hu, J., 2007b. Temperature gradient mechanism in laser forming of thin plates. Optics and Laser Technology, Vol. 39, No. 4, pp.858–863.
- Shi, Y., Hu, J. and Dong, C., 2011. Analysis of the geometric effect on the forming accuracy in laser forming. Proceedings of the Institution of Mechanical Engineers, Part B: Journal of Engineering Manufacture, Vol. 225, No. 10, pp.1792–1800.
- Shi, Y., Liu, Y., Yi, P. and Hu, J., 2012. Effect of different heating methods on deformation of metal plate under upsetting mechanism in laser forming. Optics and Laser Technology, Vol. 44, No. 2, pp.486–491.

- Shi, Y., Lu, X., Liu, Y. and Yi, P., 2013. Forming accuracy analysis of plate in multi-scanning laser bending process. Proceedings of the Institution of Mechanical Engineers, Part E: Journal of Process Mechanical Engineering, Vol. 227, No. 3, pp.225–228.
- Shi, Y., Zhang, C., Sun, G. and Li, C., 2016. Study on reducing edge effects by using assistant force in laser forming. Journal of Materials Processing Technology, Vol. 227, pp.169–177.
- Shichun, W. and Jinsong, Z., 2001. An experimental study of laser bending for sheet metals. Journal of Materials Processing Technology, Vol. 110, No. 2, pp.160–163.
- Shidid, D.P., Gollo, M.H., Brandt, M. and Mahdavian, M., 2013. Study of effect of process parameters on titanium sheet metal bending using Nd: YAG laser. Optics and Laser Technology, Vol. 47, pp.242–247.
- Shidfar, A., Jazbi, B. and Alinejadmofrad, M., 2012. Inverse estimation of pulse parameters of a time-varying laser pulse to obtain desired temperature at the material surface. Optics and Laser Technology, Vol. 44, pp.1675–1680.
- Singh, K., Joshi, S.N., Ray, A.K. and Dixit, U.S., 2013a, August. A comparison of bend quality of mechanical and laser bending of mild steel. In Proceedings of National Symposium on Miniature Manufacturing in 21st Century (NSMMIC–2013), IIT (BHU), Varanasi, India.
- Singh, K., Ray, A.K., Joshi, S.N. and Dixit, U.S., 2013b, November. Effect of lime and graphite grease coatings on the absorptivity of mild steel sheet in line heating by CO_2 laser. In Proceedings of national conference on recent advancements in mechanical engineering (pp. 8–9).
- Sonar, D.K., Dixit, U.S. and Ojha, D.K., 2006. The application of a radial basis function neural network for predicting the surface roughness in a turning process. The International Journal of Advanced Manufacturing Technology, Vol. 27, No. 7, pp.661–666.
- Sun, H., 1998. Thin lens equation for a real laser beam with weak lens aperture truncation. Optical Engineering, Vol. 37, No. 11, pp.2906–2914.

- Surekha, K., Murty, B.S. and Rao, K.P., 2009. Effect of processing parameters on the corrosion behaviour of friction stir processed AA 2219 aluminum alloy. Solid state sciences, Vol. 11, No. 4, pp.907–917.
- Tam, A.C., Poon, C.C. and Crawforth, L., 2001. Laser bending of ceramics and application to manufacture magnetic head sliders in disk drives, Analytical Sciences/Supplements, Vol. 17, pp.s419–s421.
- Teixidor, D., Ferrer, I., Ciurana, J. and Özel, T., 2013. Optimization of process parameters for pulsed laser milling of micro-channels on AISI H13 tool steel. Robotics and Computer-Integrated Manufacturing, Vol.29, No.1, pp.209–218.
- Tewari, A., Spowart, J.E., Gokhale, A.M., Mishra, R.S. and Miracle, D.B., 2006. Characterization of the effects of friction stir processing on microstructural changes in DRA composites. Materials Science and Engineering: A, Vol. 428, No. 1, pp.80–90.
- Thomson, G. and Pridham, M., 2001. Material property changes associated with laser forming of mild steel components. Journal of Materials Processing Technology, Vol. 118, No. 1, pp.40–44.
- Toros, S., Ozturk, F. and Kacar, I., 2008. Review of warm forming of aluminium–magnesium alloys. Journal of materials processing technology, Vol. 207, No. 1, pp.1–12.
- Ueda, T., Sentoku, E., Yamada, K. and Hosokawa, A., 2005. Temperature measurement in laser forming of sheet metal. CIRP Annals-Manufacturing Technology, Vol. 54, No. 1, pp.179–182.
- Ueda, T., Sentoku, E., Wakimura, Y. and Hosokawa, A., 2009. Flattening of sheet metal by laser forming. Optics and Lasers in Engineering, Vol. 47, No. 11, pp.1097–1102.
- Ueda, T., Wakimura, Y., Furumoto, T., Hosokawa, A. and Tanaka, R., 2011. Experimental investigation on laser flattening of sheet metal. Optics and Lasers in Engineering, Vol. 49, No. 1, pp.137–144.
- Valvi, S.R., Krishnan, A., Das, S. and Naryanan, G.R., 2015. Prediction of microstructural features and forming of friction stir welded sheets using cellular

automata finite element (CAFE) approach. International Journal of Materials Forming, DOI 10.1007/s12289-015-1216-0.

- Van Elsen, M., Baelmans, M., Mercelis, P. and Kruth, J.P., 2007. Solutions for modelling moving heat sources in a semi-infinite medium and applications to laser material processing. International Journal of heat and mass transfer, Vol. 50, No. 23, pp.4872–4882.
- Vásquez-Ojeda, C. and Ramos-Grez, J., 2009. Bending of stainless steel thin sheets by a raster scanned low power CO_2 laser. Journal of Materials Processing Technology, Vol. 209, No. 5, pp.2641–2647.
- Venkadeshwaran, K., Das, S. and Misra, D., 2012. Bend angle prediction and parameter optimisation for laser bending of stainless steel using FEM and RSM. International Journal of Mechatronics and Manufacturing Systems, Vol. 5, Nos. 3–4, pp.308–321.
- Venkateswarlu, G., Davidson, M.J. and Tagore, G.R.N., 2012. Modelling studies of sheet metal formability of friction stir processed Mg AZ31B alloy under stretch forming. Materials and Design, Vol. 40, pp.1–6.
- Vivek, A., Kim, K.H. and Daehn, G.S., 2011, Simulation and instrumentation of electromagnetic compression of steel tubes, Journal of Materials Processing Technology, Vol. 211, No. 5, pp. 840–850.
- Vollertsen, F., Geiger, M. and Li, W.M., 1993. FDM and FEM simulation of laser forming: a comparative study. In Advanced technology of plasticity, Proceedings of the fourth international conference on technology of plasticity (pp. 1793–1798), Beijing, 19–24 September.
- Vollertsen, F. and Rodle, M., 1994. Model for the temperature gradient mechanism of laser bending. Proc. of the LANE'94, pp.371–378.
- Vollertsen, F., Komel, I. and Kals, R., 1995. The laser bending of steel foils for microparts by the buckling mechanism-a model. Modelling and Simulation in Materials Science and Engineering, Vol. 3, No. 1, pp.107–119.
- Vollertsen, F. and Sakkiettibutra, J., 2010. Different types to use laser as a forming tool. Physics Procedia, Vol. 5, pp.193–203.
- Walczyk, D.F. and Vittal, S., 2000. Bending of titanium sheet using laser

forming. Journal of Manufacturing Processes, Vol. 2, No. 4, pp.258–269.

- Wang, Y. and Mishra, R.S., 2007. Finite element simulation of selective superplastic forming of friction stir processed 7075 Al alloy. Materials Science and Engineering: A, Vol. 463, No. 1, pp.245–248.
- Wang, X.Y., Xu, W.X., Xu, W.J., Hu, Y.F., Liang, Y.D. and Wang, L.J., 2011. Simulation and prediction in laser bending of silicon sheet. Transactions of Nonferrous Metals Society of China, Vol. 21, pp.s188–s193.
- Wang, X., Ma, X., Li, Z. and Wang, R., 2016. A study of thickening phenomenon in laser bending zone of a metal laminated plate. Procedia CIRP, Vol. 42, pp.454–459.
- Watkins, K.G., Edwardson, S.P., Magee, J., Dearden, G., French, P., Cooke, R.L., Sidhu, J. and Calder, N.J., 2001. Laser forming of aerospace alloys (No. 2001–01–2610). SAE Technical Paper.
- Woo, H.G. and Cho, H.S., 1999. Three-dimensional temperature distribution in laser surface hardening processes. Proceedings of the Institution of Mechanical Engineers, Part B: Journal of Engineering Manufacture, Vol. 213, No. 7, pp.695–712.
- Woodfield, P. L., Monde, M. and Mitsutake, Y., 2007. On estimating thermal diffusivity using analytical inverse solution for unsteady one-dimensional heat conduction, International Journal in Heat and Mass transfer, Vol. 50, pp.1202–1205.
- Wu, D.J., Ma, G.Y., Liu, S., Wang, X.Y. and Guo, D.M., 2010a. Experiments and simulation on laser bending of silicon sheet with different thicknesses, Applied Physics A, Vol. 101, No. 3, pp.517–521.
- Wu, D., Zhang, Q., Ma, G., Guo, Y. and Guo, D., 2010b. Laser bending of brittle materials. Optics and Lasers in Engineering, Vol. 48, No. 4, pp.405–410.
- Xu W., Zhang L.C. and Wang X., 2013, Laser bending of silicon sheet: absorption factor and mechanisms, ASME Journal of Manufacturing Science and Engineering, Vol. 135, No. 6, pp.061005–7.
- Yang,Y.C., Wu, T.S. and Wei, E.J., 2007. Modelling of simultaneous estimating the laser heat flux and melted depth during laser processing by inverse

methodology. International Communication in Heat and Mass transfer, Vol. 34, pp.440–447.

- Yang, L.J., Tang, J., Wang, M.L., Wang, Y. and Chen, Y.B., 2010. Surface characteristic of stainless steel sheet after pulsed laser forming. Applied Surface Science, Vol. 256, No. 23, pp.7018–7026.
- Yanjin, G., Sheng, S., Guoqun, Z. and Yiguo, L., 2003. Finite element modeling of laser bending of pre-loaded sheet metals. Journal of Materials Processing Technology, Vol. 142, No. 2, pp.400–407.
- Yau, C.L., Chan, K.C. and Lee, W.B., 1998. Laser bending of lead frame materials. Journal of Materials Processing Technology, Vol. 82, No. 1, pp.117–121.
- Yilbas, B.S. and Akhtar, S.S., 2014. Laser bending of metal sheet and thermal stress analysis. Optics and Laser Technology, Vol. 61, pp.34–44.
- Yu, G., Masubuchi, K., Maekawa, T. and Patrikalakis, N.M., 2001. FEM Simulation of laser forming of metal plates. Journal of Manufacturing Science and Engineering, Vol. 123, No. 3, pp.405–410.
- Zahrani, E.G. and Marasi, A., 2013a. Modeling and optimization of laser bending parameters via response surface methodology. Proceedings of the Institution of Mechanical Engineers, Part C: Journal of Mechanical Engineering Science, Vol. 227, No. 7, pp.1577–1584.
- Zahrani, E.G. and Marasi, A., 2013b. Experimental investigation of edge effect and longitudinal distortion in laser bending process. Optics and Laser Technology, Vol. 45, pp.301–307.
- Zhang, X.R., Chen, G. and Xu, X., 2002. Numerical simulation of pulsed laser bending. Transactions-American Society of Mechanical Engineers Journal of Applied Mechanics, Vol. 69, No. 3, pp.254–260.
- Zhang, L., Reutzel, E.W. and Michaleris, P., 2004. Finite element modeling discretization requirements for the laser forming process. International Journal of Mechanical Sciences, Vol. 46, No. 4, pp.623–637.
- Zhang, X.R. and Xu, X., 2005a. Laser bending for adjusting curvatures of hard disk suspensions. Microsystem Technologies, Vol. 11, No. 11, pp.1197–1203.

- Zhang, X.R. and Xu, X., 2005b. Laser bending for high-precision curvature adjustment of microcantilevers, Applied Physics Letters, Vol. 86, No. 2, p.021114.
- Zhang, P., Yu, J. and Zheng, X., 2009. Deformation behaviors of laser forming of ring sheet metals. Tsinghua Science and Technology, Vol. 14, Supplement 1, pp.132–136.
- Zhou, J., Shen, H., Yu, X., Hu, J. and Yao, Z., 2013. On the competition between in-plane and out-of-plane deformations in laser thermal adjustment. Optics and Laser Technology, Vol. 45, pp.689–696.

Appendix

Appendix A

Important specification of CO_2 laser machine

Make and Model	: Orion 3015 from LVD
Type	: GE FANUC HF excited CO_2 laser
Maximum power	: 2.5 kW
Wave length	: 10.6 µm
Sheet size	: 3000 mm × 1500 mm
Maximum sheet weight	: 570 kg
X-axis travel	: 3080 mm
Y-axis travel	: 1555 mm
Z-axis travel	: 290 mm
Machine dimension	: 7975 mm × 2825 mm × 2200 mm
Total weight installation	: 11500 kg
Maximum position speed	
X-Y axis	: 100 m/min
Z-axis	: 15 m/min
Repetitive accuracy	: ± 0.02 mm
Position accuracy	: ± 0.05 mm/m
Controlling parameters	
CNC control	: GE FANUC 16 iLB with Pentium processor
Software	: CADMAN-L3D
Laser power	: 50–2500W
Output stability	: ±1% – ±2%
focal lens	: 5 to 7.5 inches focal length
Duty cycle	: 5 to 100%
Frequency	: Continuous wave, pulsed 1 to 2000 Hz
Laser gas composition	: He (60%), N_2 (35%), and CO_2 (5%) with 99.99% purity
Laser gas flow rate	: 10 liter/hour (for maximum power)
Assist gas (for cutting)	: Oxygen and nitrogen

Appendix B

Important specification of Profile projector

Make	: Optomech Engineers Pvt. Ltd.
Model	: PP 400 TE
Type	: Vertical axis-bench top projector with 10× telecentric lens
Least count	: 36 second (0.01°)

Appendix C

Dial indicator (Plunger type with magnetic base)

Make	: Mitutoyo
Model	: 2109S
Least count (µm)	: 1.0
Type	: Plunger type with magnetic base
Graduation	: 0.001 mm
Total Range	: 1 mm
Accuracy	: ±0.005 mm
Range per revolution	: 0.2 mm

Appendix D

Important specification of universal testing machine (UTS)

Make	: INSTRON
Model	: 8801
Capacity	: ±100 kN
Actuator stroke	: ±75 mm
Load cell height	: 97 mm
Actuator fully retracted	: 63 mm
Maximum daylight	: 1480 mm
Column spacing	: 652 mm
Column diameter	: 70 mm
Table height	: 890 mm
Overall width	: 920 mm
Overall depth	: 546 mm
Overall height (maximum)	: 2778 mm
Weight	: 625 kg

Appendix E

Important specification of Impact testing machine

Make	: FUEL INSTRUMENT AND ENGINEERING PVT. LTD.
Model	: IT-30
Energy range	: 0 to 300 Joules
Scale Graduation	: 2 J
Dimension	: 1.4 m × 0.5 m × 1.9 m
Net Weight (Approx.)	: 450 kg

Appendix F

Important specification of optical microscope

Make	: Carl Zeiss
Model	: Axiotech-100HD, 3D
Table movement	: Three-axis measuring system, reflect light measuring stage 75 mm × 55 mm × 50 mm
Tubes	: Binocular photo tube (siedentopf principle), 20°/23, 100 vis/100 doc
Camera	: Axio-Cam and Axiovision 4.8.2 software in built
Magnification range	: 500× to 5 k×

Appendix G

Important specification of scanning electron microscope (SEM)

Make	: Jeol
Model	: Jeol JSM 6390 LV
Resolution	: 3.0 nm (30kV)
Accelerating voltage	: 0.5 to 30 kV
Magnification	: ×5to ×300000
Filament	: Pre-centered W hairpin filament (with continuous auto bias)
Objective lens	: Super conical lens
Objective lens Apertures	: Three position, controllable in X and Y directions

Appendix H

Important specification of microhardness tester

Make	: Buehler
Model	: Micromet-2101
Indentation force	: 1, 10, 50, 100, 300, 500, 2000 g force
Dwell time	: 5 to 60 s at an interval of 5 s
Microscope Magnification	: 100× , 400×
Measurement of indentation	: Manual Filler eyepiece
Maximum measurement length	: 175 µm
Maximum height of specimen	: 65 mm
Maximum depth of specimen	: 85 mm
Stage dimension	: 100 mm × 100 mm
Video port	: For photography and computerization
Power Supply	: AC 230 V

Publications from This Thesis

Journal Papers

1. P. P. Dutta, U.S. Dixit and K. Kalita (2017), A strategy for achieving accurate bending by multi-pass laser line heating, Int. J. Mechatronics and Manufacturing Systems, Vol. 10, No.4, pp.277-298. https://doi.org/10.1504/IJMMS.2017.088912
2. P.P. Dutta, K. Kalita, U.S. Dixit and H. Liao (2018), Magnetic-force-assisted straightening of bent mild steel strip by laser irradiation, Lasers in Manufacturing and Materials Processing, Vol. 4, No. 4, pp.206–226, https://doi.org/10.1007/s40516-017-0047-x .
3. P.P. Dutta, K. Kalita and U.S. Dixit, 2018, Electromagnetic-force-assisted bending and straightening of AH 36 steel strip by laser irradiation, Lasers in Manufacturing and Materials Processing, Vol. 5, No. 3, pp.201–221, https://doi.org/10.1007/s40516-018-0062-6

Conference Papers

1. P. P. Dutta, K. Kalita and U. S. Dixit, Experimental investigation on laser bending of mild steel coated with black enamel paint, Proceedings of National Conference on Manufacturing : Vision for Future, October 12-13, 2013, IIT Guwahati, India.
2. B.N. Fetene, P.P. Dutta, K. Kalita and U.S. Dixit, Magnetic force assisted straightening of bent mild steel strips, 2nd National Conference on “Emerging Technologies” Contributions in Promoting Defence and Industry Capabilities (NCETCPDIC 2017), July 18-20, 2017, Defence University, College of Engineering, Bishoftu, Ethiopia.